HeavyMin: Utilizing heavy minerals in stream sediments as indicators for regional exploration potential in the Eastern Alps, Austria

F. Altenberger[1,2], J. Weilbold[3], T. Angerer[3], J. Krause[4], J. Berndt[5], A. Geringer[3], G. Schuberth-Hlavac[3], M. Werdenich[3], B. Neugschwentner[3], G. Feitzinger[2], J. G. Raith[1]

[1]Technical University of Leoben, Chair of Resource Mineralogy, Leoben Austria,
[2]ZT-Büro Dr. phil. Gerhard Feitzinger, Salzburger Straße 16, St. Gilgen, Austria
[3]GeoSphere Austria, Competence Unit of Mineral Resources, Vienna, Austria,
[4]Helmholtz-Zentrum Dresden-Rossendorf, Institute Freiberg for Resource Technology, Freiberg, Germany
[5]University of Münster, Institute for Mineralogy, Corrensstraße 24, Münster, Germany
e-mail: florian.altenberger@unileoben.ac.at, florian@geofeitzinger.at

Heavy minerals (density > 4.5 g/cm³) such as gold, scheelite, magnetite, zircon, rutile and apatite are concentrated in the alluvial sediments of rivers and mountain streams, where they may form economic placer deposits. Beyond their economic value, the mineralogical and geochemical composition of these heavy mineral fractions — particularly of so-called indicator minerals — provides valuable insights into the upstream geological environment and the potential presence of ore deposits (MCCLENAGHAN & HALL, 2011). Minerals such as magnetite, pyrite, scheelite and apatite have proven to be particularly robust indicators due to their resistance to weathering and their ability to incorporate diagnostic trace elements reflective of distinct ore-forming processes.

Among these, scheelite ($CaWO_4$) is especially significant in the Eastern Alps, where it occurs in various lithological units and mineralization styles and represents the principal tungsten ore (ALTENBERGER, 2025). Tungsten has been listed as a critical raw material by the European Union since 2011, and its strategic importance has been reaffirmed in the recently adopted Critical Raw Materials Act. While Austria maintains a degree of self-sufficiency through production from the Felbertal tungsten deposit, Europe's tungsten-processing industry remains highly import-dependent and vulnerable to supply chain disruptions — particularly from Asian markets.

The ongoing HeavyMin project evaluates the effectiveness of a novel exploration strategy by comparing trace element signatures of scheelite grains from stream sediment surveys in the Eastern Alps with those from globally important tungsten skarn deposits (e.g., Cantung, MacTung, Lened, King Island, Vostok). The integration of this dataset into a broader global geochemical framework will allow refinement of the proposed trace-element-based exploration tool and facilitate the early-stage detection of magmatic-hydrothermal tungsten mineralization with high economic potential. We will present the current status of systematic stream sediment campaigns in the Hohe Tauern region and outline future steps in Austria's critical raw materials exploration agenda.

ALTENBERGER, F. (2025): Evaluation of the tungsten potential in the Eastern Alps: New insights from geological, mineralogical and chemical (LA-ICP-MS) data on scheelite. Dissertation, Montanuniversität Leoben. https://doi.org/10.34901/mul.pub.2025.082.

MCCLENAGHAN, B. & HALL, G. (2011): Introduction to Indicator Mineral (IM) Special Issue. Geochemistry: Exploration, Environment, Analysis, 11(4), 249-249. https://doi.org/10.1144/1467-7873/11-IM-082.

On the geochemical analysis of graphite: how to do it and how to interpret the data

R. Arató[1], G. Obbágy[1], V. Dietrich[1], F. Melcher[1]

[1]Chair of Geology and Economic Geology, Technical University of Leoben, Leoben, Austria
e-mail: robert.arato@unileoben.ac.at

Graphite is a critical and strategic raw material in major economies worldwide. Given its fundamental role in energy storage, its responsible sourcing is particularly important. However, there is currently no routine methodology available to distinguish between different natural graphite deposits. In this contribution, we investigate the geochemical opportunities for graphite traceability. Due to its extraordinary chemical and physical properties, the chemical analysis of graphite is challenging. Complete dissolution of graphite is nearly impossible under standard laboratory conditions, and in-situ analyses are challenging due to its flaky/brittle structure. Accordingly, the knowledge of the chemical composition of graphite is currently limited.

In this study, we present results acquired by bulk analytical methods, such as inductively coupled plasma mass spectrometry (ICP-MS) and instrumental neutron activation analysis (INAA) as well as by in-situ methods on a comprehensive set of pressed graphite pellets. In-situ methods applied here include laser induced breakdown spectroscopy (LIBS) via benchtop and handheld instruments as well as laser ablation inductively coupled plasma mass spectrometry (LA-ICP-MS).

Solution ICP-MS analysis of graphite concentrates shows a wide range of detectable elements and very well reproducible results on different aliquots from the same concentrate. The results are in accordance with trace element concentrations obtained by INAA, however, certain elements are only detectable by either technique. To better understand the spatial distribution of elemental anomalies detected by bulk techniques, in-situ techniques were also applied. LIBS generates multi-elemental data at an unprecedented speed even from samples with non-ideal ablation characteristics, such as pressed graphite pellets. The generated data was used for constructing elemental maps to shed light on the chemical distribution of elements in the concentrates. Chemical inhomogeneities are ubiquitous in all studied concentrates. Based on the spatial relationship of the detected elements, it is also obvious that most chemical impurity elements stem from minerals, which are intermixed and/or intergrown with graphite flakes. The resulting chemical heterogeneity of the concentrates serves as a distinct fingerprint of individual deposits. On the other hand, the heterogeneity is also omnipresent between different samples of the same deposit and even within individual samples. This poses a significant challenge for LIBS and LA-ICP-MS analyses and raises the question if representative analysis of graphite concentrates via in-situ techniques is even possible. We test various approaches with both techniques and compare the outcome with the results obtained by bulk geochemical techniques.

For lithium-ion batteries, graphite concentrates are purified by alkali-autoclave leaching and/or hydrofluoric acid to reach a purity of at least 99.95%. We demonstrate that even though most of the above-described geochemical signature is removed by purification, the very low detection limit of the applied techniques also enables the traceability along the value chain to a certain extent.

This study was funded by the European Union under grant agreement no. 101091502, project MaDiTraCe – Material and Digital Traceability for the Certification of Critical Raw Materials, coordinated by the French Geological Survey (BRGM).

Hydrogen in fluid inclusions

R. J. Bakker[1*]

[1]*Chair of Resource Mineralogy, Technical University of Leoben, Austria*
e-mail: bakker@unileoben.ac.at

The interest in hydrogen is recently inflated due to its economic value for sustainable energy supply and mobility. Natural hydrogen is part of this interest. Although hydrogen is the most abundant element in the universe, it is relatively scarce on Earth. Hydrogen can be produced through industrial chemical processes, which, however, diminish the perceived cleanness of this energy source. The origin of H_2 in the earth crust and mantle is twofold: either primordial or produced by geological processes, and part of this hydrogen is preserved in fluid inclusions. Processes that produce hydrogen include serpentinization, radiolysis, and fluid-rock interactions under highly reduced conditions. There are only a few accessible scientific studies that document the presence of H_2 in fluid inclusions, directly related to these processes.

Mafic/ultramafic rocks in ophiolites are often affected by serpentinization, which is locally accompanied with rodingitization processes. The mineralogy of fine-grained serpentinites does not favour the trapping and preservation of fluid inclusions. As a result, H_2-rich fluids will primarily remain free in pore spaces, allowing them to escape the rock system through seeps. However, coeval rodingites (Ca-rich metasomatic alteration of mafic rock) may trap these fluids in coarse-grained diopside and garnet crystals, providing information about serpentinization and rodingitization. A preliminary study of rodingites from the ophiolitic complex of Troodos (Cyprus) reveals the presence of abundant hydrogen in fluid inclusions.

In addition, H_2 is detected in fluid inclusions in podiform chromitites, indicating that hydrogen was already present in the primary processes of ultramafic magma evolution. In a new project financed by the Austrian Science Fund (FWF, PAT5274524) the locality of hydrogen-rich fluid inclusions will be identified in a geological context to understand processes of hydrogen formation and trapping in natural rock. This study will be complemented with an experimental study about efficiency of hydrogen diffusion, that may cause post-entrapment modifications of fluid inclusions.

Glauconite as a paleo-environmental archive

A. Baldermann[1]

[1]Institute of Applied Geosciences, Graz University of Technology, Austria
e-mail: baldermann@tugraz.at

Up until the mid-1990s about 40% of all absolute ages used to constrain the geologic timescale of the last 250 Ma were derived from glauconite, $K(Fe^{3+/2+}AlMg)_2[AlSi]_4O_{10}(OH)_2$. However, apparent mismatches with chronostratigraphic constraints, yielding ages that are 'too young' or 'too old', mean that glauconite geochronology has been discarded. Erroneous ages have been attributed to the presence of detrital Rb- and K-bearing phases in single glauconite grains or post-depositional alteration, causing a resetting of e.g., the Rb-Sr system. Knowledge of the processes that potentially lead to an age resetting of glauconite is key to modern proxy applications, e.g., $\delta^{41}K$ isotope signatures recorded in glauconite to reconstruct paleo-seawater $\delta^{41}K$ compositions. In this study, four glauconite fractions were collected from the well-studied Langenstein section (Northern Germany) of Cretaceous (~96 Ma ago) age. High-resolution X-ray computed tomography (CT) was used to obtain 3-D images of each glauconite fraction, providing detailed visualization of cracks, microfabrics and porosity, core-rim transects and compositional ranges of glauconite. Following segmentation of the image data obtained on individual particles via mathematical procedures, the full range of compositional (maturity vs weathering intensity), substrate-inherited (sandstone vs limestone matrix) and microstructural (open vs dense fabrics, surface cracks) variability of the individual glauconite grains was explored. Surprisingly, all analysed glauconite fractions yielded an identical $\delta^{41}K$ isotopic composition of -0.67 ‰ ± 0.04 ‰, despite of significant differences in e.g., bulk porosity, composition and pore size distribution. These findings suggest that well-preserved glauconite deposits can potentially be used as a proxy for paleo-seawater $\delta^{41}K$, which opens the door for further studies that aim at testing other isotope proxies recorded in glauconite (e.g., $\delta^{56}Fe$, $\delta^{40}Ca$, $\delta^{26}Mg$ and $^{87}Sr/^{86}Sr$).

Timing of a brief regional igneous (and metamorphic) Late Cretaceous event in Croatia

D. Balen[1], D. Gallhofer[2], P. Schneider[1], E. Skrzypek[2], C. A. Hauzenberger[2]

[1]Department of Geology, University of Zagreb, Croatia
[2]Department of Earth Sciences, University of Graz, Austria
e-mail:drbalen@geol.pmf.unizg.hr

The Late Cretaceous magmatic event in the basement of the Pannonian Basin in Croatia is often associated with large-scale geological processes influenced by the closure of the Neotethys Ocean as a result of the collision between the African and European continental plates. This magmatism, triggered by tectonic convergence, is associated with arc-type subduction-related volcanism and produced a suite of highly diverse igneous rocks (high-K calc-alkaline magmas and isotopic data suggest contributions from both the mantle and the crust). On the other hand, the granitoid intrusions (S-type granite) in the broader research area were formed by partial melting of the crust during continental rifting in response to subduction and extension during tectonic interaction of the continental plates. Geochronological data indicate either a longer period of volcanic activity (related to a change in subduction geometry) or short, discrete pulses (magmatism mainly related to extensional tectonics, asthenospheric upwelling and partial melting of the mantle and overlying crust).

The magmatic activity took place in or near the contact zone of the continental plates during and after the final closure of the Neotethys Ocean. This contact zone is known as the Sava(-Vardar) Zone (PAMIĆ, 2002) or Sava Zone (SCHMID et al. 2020). In the area of Moslavačka Gora and the Slavonian Mountains (Papuk and Požeška Gora), magmatism occurred during time span of 85–79 Ma (zircon dating by LA-ICP-MS), measured on nine different samples from spatially distant locations along the Sava Zone. This high-temperature magmatic activity is accompanied with regional metamorphism dated by Ar-Ar cooling ages on hornblende of amphibolites (83 ± 2 and 81 ± 2 Ma) and Sm-Nd isochron on metamorphosed olivine gabbro (83 ± 9 Ma) from Moslavačka Gora (BALEN et al. 2001, 2003).

Age dating coupled with geochemical data indicates that magmatism was triggered by a brief pulse of mantle upwelling in the Late Cretaceous (~81 Ma) combined with tectonic interaction between continental plates, which caused partial melting of the lower crust. The newly formed magma interacted to some degree with the overlying, slightly thickened crust and underwent extensive fractional crystallisation and differentiation during its rapid ascent through the crust. An almost simultaneous regional metamorphism can be observed in the more refractory mafic lithologies.

BALEN, D., SCHUSTER, R., GARAŠIĆ, V. (2001): A new contribution to the geochronology of Mt. Moslavačka Gora (Croatia). – In: PANCARDI 2001, II. Abstracts, Ádam A., Szarka L., Szendrői J. (ed.), DP-2.

BALEN, D., SCHUSTER, R., GARAŠIĆ, V., MAJER, V. (2003): The Kamenjača olivine gabbro from Moslavačka Gora (South Tisia, Croatia). – Rad HAZU, 486, 27, 57-76.

PAMIĆ, J. (2002): The Sava-Vardar Zone of the Dinarides and Hellenides versus the Vardar Ocean. – Eclogae Geol Helv, 95, 99-113.

SCHMID, S.M., FÜGENSCHUH, B., KOUNOV, A., MATENCO, L., NIEVERGELT, P., OBERHÄNSLI, R., PLEUGER, J., SCHEFER, S., SCHUSTER, R., TOMLJENOVIĆ, B., USTASZEWSKI, K., VAN HINSBERGEN, D.J.J. (2020): Tectonic units of the Alpine collision zone between Eastern Alps and western Turkey. – Gondwana Res, 78, 308-374.

Hydrothermal alteration of cerussite, dolomite and rhodochrosite in oxygen-18 solution

L. Belohlavek[1], F. M. Stamm[1], M. Dietzel[1]

[1]Graz University of Technology, Institute of Applied Geosciences, Austria,
e-mail: l.belohlavek@tugraz.at

In this study, the kinetics and reaction mechanisms of hydrothermal transformation and oxygen isotope exchange are investigated for three carbonate minerals: cerussite ($PbCO_3$), rhodochrosite ($MnCO_3$), and dolomite ($CaMg(CO_3)_2$). For this purpose, well-controlled laboratory experiments were conducted with oxygen-18 solutions at 180 °C over a period of 5 months. Raman spectroscopy was employed to monitor and quantify the peak shift due to ^{18}O substitution for ^{16}O in the carbonate molecule. The results reveal progressive oxygen isotope exchange, accompanied by the formation of new mineral phases, indicating partial dissolution and reprecipitation during the alteration process.

These findings provide new insights into the mobility and redistribution of oxygen isotopes in carbonate systems under hydrothermal conditions. Moreover, the study highlights Raman spectroscopy as an excellent tool for understanding and tracing the oxygen isotope exchange behaviour between solid carbonate phases and reacting aqueous solutions.

Known, but overlooked: genetic insights and critical metal potential of sulfate-hosted sphalerite occurrences in the Northern Calcareous Alps of Austria

V. Bertrandsson Erlandsson[1], F. J. Hampl[1], F. Melcher[1], A. Šoster[2]

[1] Department Applied Geosciences and Geophysics, Technical University of Leoben, Leoben, Austria,
[2]Faculty of Natural Sciences and Engineering, University of Ljubljana, Ljubljana, Slovenia,
e-mail: viktor.erlandsson@unileoben.ac.at

Occurrences of Pb-Zn mineralizations in the Eastern Alps are well recognized and widespread, from Alpine-type carbonate-hosted (e.g., Bleiberg; MELCHER et al. 2023) to sedimentary exhalative (e.g., Arzberg). Sulfate-rock hosted Pb-Zn mineralizations, on the other hand, are underrepresented in the scientific literature, both in Austria and worldwide. Late Permian (Haselgebirge Formation) to Early Triassic (Gutenstein Formation) gypsum-anhydrite deposits are found throughout the Northern Calcareous Alps in the Eastern Alps. Sphalerite from the Tragöß (Bruck-Mürzzuschlag, Styria) and Moosegg (Hallein, Salzburg) sulfate deposits are only recognized by mineral collectors for their vibrant red and orange colors. The Zn-Pb mineralizations are predominantly comprised of sphalerite and galena with minor amounts of pyrite – native sulfur is readily found in the investigated samples. Sphalerite and galena occur as cm-large crystals, often intensely fractured with gypsum and celestine as fracture-filling minerals. Pyrite occurs as smaller, euhedral crystals both within the host rock and overgrowing the sphalerite.

Tragöß sphalerite has higher contents of Mn, Ga, Ge, Cd, Hg, Tl, and Pb, whilst Moosegg sphalerite has higher As, Sn, and Sb. Cu, Ag and In. Overall both sphalerite sets are significantly Fe-poor. Trace element analyses show elevated contents of both Ga, but foremost, Ge in the red and orange sphalerite from both mineralizations. Sphalerite from Tragöß has a median Ge content of 584 µg/g and 807 µg/g (red and orange, respectively). Element mapping of the red and orange sphalerite reveals irregular distribution patterns, seemingly unrelated to the color. Geothermometry using Ga, Ge, In, Mn, Fe, and Sb in sphalerite, yields temperatures of 120 – 155 °C, which is interpreted to be associated with tectonic and thermal overprinting caused by Eo-Alpine nappe-stacking that started in the Lower Cretaceous (115 Ma; SCHORN et al. 2013; KRENN et al. 2011). We propose a novel genetic model where the gypsum host rock itself was the source for the metals, sulfur, and fluids, responsible for the Pb-Zn mineralizations.

Additionally, the red- and orange-colored sphalerite show strong fluorescence color, when exposed to long-wave UV light ($\lambda = 365$ nm), corroborating newly suggested concepts of UV light as a cheap and easy-to-use prospecting tool for critical metal-rich (Ga and Ge) sphalerite.

KRENN, K., KURZ, W., FRITZ, H., HOINKES, G. (2011): Eoalpine tectonics of the Eastern Alps: implications from the evolution of monometamorphic Austroalpine units (Schneeberg and Radenthein Complex). - Swiss Journal of Geosciences 104: 471–491.

MELCHER, F., BERTRANDSSON ERANDSSON, V., et al. (2023): In: ANDREW, C.J., et al (eds), Irish Association for Economic Geology, Dublin, 443-478. DOI: https://doi.org/10.61153/NIWU8065

SCHORN, A., NEUBAUER, F., GENSER, J., BERBOIDER, M. (2013): The Haselgebirge evaporitic mélange in central Northern Calcareous Alps (Austria): Part of the Permian to Lower Triassic rift of the Meliata ocean? - Tectonophysics, 583, 28–48.

Monitoring staurolite growth and reaction progress in high-*P* high-*T* piston cylinder experiments using micro-computed tomography (µCT)

G. Degenhart[1], P. Tropper[2], L. Schröer[3], V. Cnudde[3,4]

[1]Core Facility MicroCT, Department for Radiology, Medical University of Innsbruck, Innsbruck, Austria
[2]Institute of Mineralogy and Petrography, University of Innsbruck, Innsbruck, Austria
[3]PProGRess-UGCT, Department of Geology, Ghent University, Ghent, Belgium
[4]Environmental Hydrogeology, Department of Earth Sciences, Utrecht University, Utrecht, the Netherlands
email: gerald.degenhart@i-med.ac.at

Experimental investigations using natural rocks are a forward modelling technique, which allow putting additional constraints on the mineralogical evolution of a rock under defined *P* and *T* conditions. In this study, experimental investigations of collision-related metamorphism of a natural muscovite-rich quartzphyllite sample (Grt + Ms + Chl + Bt + Rt + Qz) were done using a piston cylinder apparatus with an automated *P-T* control. For the *P-T* loop experiments, four different *P-T* conditions were chosen and run subsequently representing a clockwise *P-T* loop from a collisional setting. The *P-T* conditions were 400 °C, 0.8 GPa, 600 °C, 1.2 GPa, 700 °C, 0.8 GPa and 500 °C, 0.4 GPa. In the first *P-T* loop experiment (16 days) each *P-T* condition was run for 4 days before the *P-T* conditions were changed using the automated *P-T* control. Another experiment with a duration of 32 days was conducted (each *P-T* run for 8 days). Both *P-T* loop experiments yielded the same mineral assemblage: $Grt_{2,3}$ + Sta + Ms_2 + Bt_2 + Chl_2 + Ilm + Qz. Recent studies show that combining µCT datasets with threshold-based 3D segmentation enables the recognition of individual minerals within an assemblage, as well as the quantification of their modal abundances and grain size distributions in three dimensions. The investigations using µCT were performed at the Centre of X-ray Tomography (UGCT), Ghent University, Belgium, together with the EXCITE Network. For this investigation the Nanowood CT was used for the scanning of two samples with a diameter of about 1 mm resulting in a voxel size of 900 nm. The samples were prepared by extracting small volumes of run material from the Pt capsules using a diamond wire saw. Both samples were run along the *P-T* loop with different run times: sample W_001 was run for 16 days and 10% water, sample SJ-007 was run for 33 days and 20% water. In both samples mineral growth could be observed. The main goal of this investigation was to study the spatial 3-D distribution of newly formed phases as well as the documentation of changes in grain size and porosity of the samples. Contouring the scanned material including its porosity allowed establishing a threshold segmentation in the first step. Taking the measured mineral composition from the EPMA, six different mineral phases (staurolite + garnet, biotite, chlorite, muscovite, quartz, pores) could be identified and based on their mean atomic number their densities were transferred to the µCT measurements. Textural analysis was applied to each density segment individually. We evaluated on the one hand material properties like volume fraction (mineral volume (MV)/total volume (TV) [%]), mean mineral density (Lin Att.) and on the other hand the short axis diameter of the particles (particle thickness) of the minerals. For further separation between staurolite and garnet (both have similar densities), the different crystal shapes were used. The crystal shape of staurolite is prismatic whereas garnet shows a rounded habitus. The homogenous staurolite distribution throughout the capsules indicates no abnormal thermal gradients during the experiments. Further observations have shown increasing staurolite, garnet and quartz growth at the expense of muscovite, chlorite and biotite. This is also accompanied by an increase in grain size of experiment SJ-007 due to longer run time and elevated water content.

Stable isotopic constraints on low-temperature carbonate formation processes

A. Demény[1]

[1]*Institute for Geological and Geochemical Research, HUN-REN Research Centre for Astronomy and Earth Sciences, Hungary,*
e-mail: demeny@geochem.hu

Low-temperature carbonate formations are found everywhere in our environment; they are precipitating in lakes, creeks, caves, and even in our bathrooms. Animals and bacteria are also secreting carbonate minerals to produce their shields or just to get rid of 'toxic' calcium from their cells. We are building houses and monuments from limestones and travertines formed at low-temperature, eat carbonate shell protected creatures or use them to feed other domesticated animals, or just suffer from the presence of carbonate in hydrothermal well tubes. All these examples show how low-temperature carbonate formations affect our life; hence the knowledge of individual carbonate mineralization processes is logically needed. As carbonates are composed of metal and carbonate ions, and the latter is made of carbon and oxygen, these formations have been targets of stable isotope geochemical investigations for more than 70 years. Since the seminal paper by Harold Urey published in 1948, who first suggested that the $^{18}O/^{16}O$ fractionation between carbonates and water is temperature-dependent, temperature estimation of carbonate formation is one of the major application fields of stable isotope geochemistry. Numerous equations have been established to calculate carbonate formation temperatures from the oxygen isotope composition of carbonate and water based on laboratory experiments, theoretical calculations, and empirical observations. The former can be easily measured, but the latter has to be estimated (for example for past seawater) or can be determined by analyses of water trapped in fluid inclusions. Technical developments now allow us to directly measure the hydrogen and oxygen isotope compositions of inclusion-hosted water, which promotes the application of oxygen isotope thermometry. Additionally, the last two decades brought a new technique, clumped isotope analysis (briefly, the temperature dependence of preferential bonding – "clumping" – of the heavy C and O isotopes in the carbonate), that can be used to determine formation temperature without the knowledge of the composition of the carbonate-precipitating solution.

These together seemed to induce a revolution in paleotemperature investigations. However, as more studies are published, the problems, disadvantages, and drawbacks are also appearing. Uncontrolled kinetic fractionation, cryptic diagenetic effects, and 'hidden' mineral transformations affect the isotopic composition of carbonates, which precludes the use of these valuable methods in some cases. The present talk will show examples of successful and unsuccessful applications from near-freezing conditions (cryogenic carbonate formation) to mild environmental conditions (inorganic and bacterial carbonate precipitation in cave deposits, and biogenic calcite formation), and up to hydrothermal conditions (calcite vein formation from deep meteoric water migration at ~50 ºC). The problems encountered during paleotemperature analyses actually revealed new formation processes (e.g., bacterial carbonate precipitation on stalagmite surfaces), while the successful applications will demonstrate the power of combined use of oxygen isotope fractionation and clumped isotope measurements in paleothermometry and paleohydrology.

Multiple reaction microstructures in metagabbro from the Western Dharwar craton, India

A. Dey[1,2], T. Griffiths[1], R. Abart[1]

[1] Department of Lithospheric Research, University of Vienna, Althanstrasse 14, Vienna, Austria,
[2] Department of Geology, University of Delhi, North Campus, Chhatra Marg, Delhi, India,
e-mail: anindita.dey@univie.ac.at

A Precambrian metagabbro from the Western Dharwar craton of the Indian Peninsula exhibits relict igneous textures, metamorphic textures, and evidence of possible late-stage hydrothermal overprint. The igneous relics are represented by coarse grains of olivine (Ol), orthopyroxene (Opx), and clinopyroxene (Cpx), forming a cumulate texture with plagioclase (Pl) present as an intercumulus phase. These cumulates develop a variety of unique microstructural and compositional features as follows.

a) **Multi-layer corona:** The primary magmatic Ol grains are always separated from Pl by double-layer coronas showing the typical sequence of: relict magmatic Ol | Opx | Cpx + Opx + Al-spinel (Sp) symplectite | relict magmatic Pl. Locally amphibole (Am) may also be seen between the inner and outer corona, replacing the pyroxenes.

b) **Micro-inclusions hosted by plagioclase:** The intercumulus Pl of the meta-gabbro hosts ultra-fine µm to sub-µm sized micro-inclusions of green Al-Sp (X_{Al}=Al/(Cr+Al+Fe^{3+})>0.95; X_{Cr}=~0) and Am, exhibiting multiple well-defined shape-preferred orientations. The composition of the Pl shows a systematic change from anorthitic (X_{An} = 0.5-0.6) to more albitic composition (X_{An} = 0.35-0.40) in the micro-inclusion rich domains.

Pyroxenes with exsolution lamellae and micro-inclusions: The Opx and Cpx cumulate crystals show extensive lamellar exsolution within one another. Both pyroxenes also exhibit conspicuous clouding due to brown Cr-Sp micro inclusions (X_{Al}<0.90; X_{Cr}=0.1-0.25). The abundance of the micro-inclusions in pyroxene may vary randomly or systematically giving rise to patchy, oscillatory or hourglass-shaped clouded zones, possibly reflecting a primary igneous compositional zoning.

The inventory of reaction microstructures in the studied rock offers a unique possibility to explore to what extent other metamorphic mineral reactions, such as corona formation or the exsolution of ortho- and clinopyroxene, were involved in the precipitation of the micro inclusions. This study may also explain whether the common occurrences of Pl-hosted Al-Sp micro-inclusions in 'coronites' within the geological record reflect a possible genetic link between the corona formation and clouding of Pl.

Funded by the Austrian Science Fund (FWF)10.55776/ESP675.

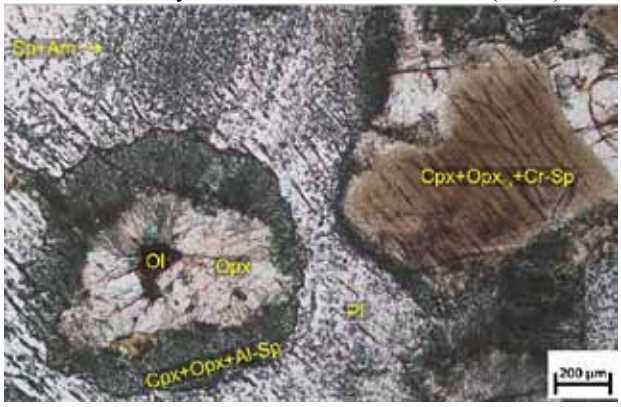

Figure 1. Microsctructures in the studied metagabbro.

Evaluating the economic potential and environmental impact of historic mine tailings – A case study from Spielberg, Styria

F. Dunkel[1], U. Moser[2], L. Wolf[2], S. Wagner[2], J. Irrgeher[2], P. Gopon[1]

[1]Department of Applied Geosciences and Geophysics, Technical University of Leoben, Leoben, Austria
[2]Department of General, Analytical and Physical Chemistry, Technical University of Leobe, Leoben, Austria
e-mail: frederik.dunkel@unileoben.ac.at

In order to meet current demand scenarios for the energy transition, the global output of Critical Raw Materials (CRM), such as copper (Cu), nickel (Ni), and cobalt (Co) must grow by 1.5 to 2.2 times until 2040 (IEA, 2024). Addressing this major challenge will require additional material production from non-traditional sources, including historic mine tailings. Throughout most of human history, significantly higher ore grades were mined than is common today. Moreover, past extraction techniques left behind up to 50 % of the target metals (GORDON, 2002) and did not recover elements which were then considered unimportant but are now classified as critical. Hence, historic mine tailings may be enriched in critical and precious metals and thus hold potential to contribute to future CRM supply.

Within the project SCIMIN-CRM (Sustainable & CIrcular Production of MINeral Critical Raw Materials), tailings at four different locations within Europe are analysed in detail for their CRM contents and possible recovery pathways. One of these pilot sites is a historic Cu-Au mining district near Spielberg (Styria, Austria). Mining activities in this area ceased around 1870, leaving behind more than 30 waste rock piles (tailings), which vary in size, age, and mineral/metal content.

A broad range of geochemical, mineralogical, and geophysical analysis techniques are applied to analyse the Spielberg tailings in detail. Whole-rock analysis and micro X-ray fluorescence (μXRF) mapping revealed significant concentrations of critical and precious metals (i.e., Cu, arsenic (As), gold (Au)) within the tailings. Additionally, a hydrological sampling campaign combined with inductively coupled plasma mass spectrometry (ICP-MS) analysis showed elevated As concentrations up to >500 $\mu g\ L^{-1}$ in local stream waters, indicating a substantial environmental risk. Therefore, the preliminary data highlights the importance of evaluating historic mine tailings with an integrated approach that considers both their economic potential and environmental impact. We will present our data on the tailings at Spielberg and discuss the potential contribution of the more than 4000 Cu-Au-As tailings found across Austria to a secure and sustainable European energy transition.

Project SCIMIN-CRM is funded by the European Union's Horizon Europe research and innovation programme under grant agreement No. 101177746.

GORDON, R.B., 2002. Production residues in copper technological cycles. – Resour. Conserv. Recycl. 36, 87–106.

IEA, 2024. Global Critical Minerals Outlook 2024. International Energy Agency, www.iea.org.

Zircons Forever?? The influence of acid diagenetic pore fluids on the U-Pb chronometer

I. Dunkl

Sedimentology and Environmental Geology, Georg-August-Universität Göttingen, Göttingen, Germany
e-mail: istvan.dunkl@geo.uni-goettingen.de

Zircon is the most commonly used mineral for U-Pb geochronology. The rapid development of the laser-ablation ICP-MS technique and its high throughput made this geochronometer very popular in the last decades. The zircon – U-Pb system is considered as an extremely reliable and robust geochronometer as accessory zircon crystals are able to preserve multiple ages in the core or in different growth zones. During weathering-erosion-transport-diagenesis-metamorphism-melting cycles the U-Pb system can remain intact and the chronometer can preserve ages of former igneous events. On the other hand, the presence of discordant U-Pb ages is a common phenomenon and it is typically linked to the loss of radiogenic lead.

The chemical instability - and thus the loss of Pb - depends on the density of the alpha-damages within the crystal. This phenomenon is used at the chemical abrasion procedure, when the high-U (=high alpha-dose, “more metamict”, more discordant) zones are dissolved by hydrofluoric acid, and thus the dating can be focused on the remaining low-dose parts of the crystals and they usually yield concordant U-Pb ages.

We studied the impact of weak acids on zircon crystals having different alpha-damage densities and different natural weathering conditions. On the contrary to the chemical abrasion procedure, we did not use HF that destroys the silicate lattice, but only weak sulfuric acid and other organic acids.

Two sets of samples were compared. (i) The pyrite-bearing metasandstone samples from an Archean formation of South Africa experienced surface weathering. They contain goethite, jarosite and the detrital rutile grains are etched. The oxidation of the originally detrital pyrite took place in the weathering zone and generated H_2SO_4. The majority of the zircon LA data is discordant, and we associate the Pb-loss to the acidic, telodiagenetic pore fluid. (ii) The other, Proterozoic sample set from the Fennoscandian Shield (Finland) is composed of unweathered paragneisses and granitoids, and the alpha-damage densities in these zircons are similar to the South African samples. 10 to 12 crystals were selected for the batches, their colour and transparency were similar within the batches.

The duration of the sulfuric acid treatment was 5 weeks, the 60 □C temperature and the pH = 2 acidity aimed to mimic the diagenetic conditions. The acidity matches well to the weathering zone of sulfide-rich ores. The etched, skeleton-like rutile grains and the high amount of diagenetic, pore-filling leucoxene gave hint also for Ti-mobilisation and thus for a pH around 2.

The amount of dissolved material was high in case of both sample sets, up to 5 wt%. The most characteristic difference was in the ratio of the dissolved uranium and lead. In case of the fresh Fennoscandian samples, the Pb/U ratio was high and it fits to the expectations. Namely, the radiogenic Pb ions experiencing 7 or 8 alpha-recoil events, “sit” in an interstitial position in a tiny volume having high degree of damage. Thus, these ions are well leachable. On the contrary, the weathered South African zircons emitted much more uranium than Pb in weak acid. This unusual ratio can be explained by the natural H_2SO_4 etching that took place in Mio-Pliocene time and mobilized already the lead and thus the laboratory treatment could dissolve more uranium than lead.

Colour and internal texture of synthetic blue star sapphire

J. Einzmann[1], W. Suwanmanee[1], M. Wildner[1], C. Chanmuang N.[1], B. Wanthanachaisaeng[2], C. A. Hauzenberger[3], L. Nasdala[1]

[1] Universität Wien, Vienna, Austria
[2]GIT – Gem and Jewelry Institute of Thailand, Bangkok, Thailand
[3]Karl-Franzens-Universität, Graz, Austria
e-mail: waratchanok.suwanmanee@univie.ac.at

There has been great progress in producing gem-quality corundum in almost all colours, including even multi-coloured stones (NASDALA et al. 2020), using the rather inexpensive flame-fusion (Verneuil) technique. As a virtual exception, manufacturing homogeneously body-coloured blue sapphire is still a challenge. Such Verneuil boules typically show a vivid cornflower-blue rim surrounding a nearly colourless centre (Fig. 1a), which is caused by preferential incorporation of Ti (≤0.07 wt%) and Fe (≤0.05 wt%) only in outer volume areas. The reason of such undesirable element-distribution pattern is still controversial.

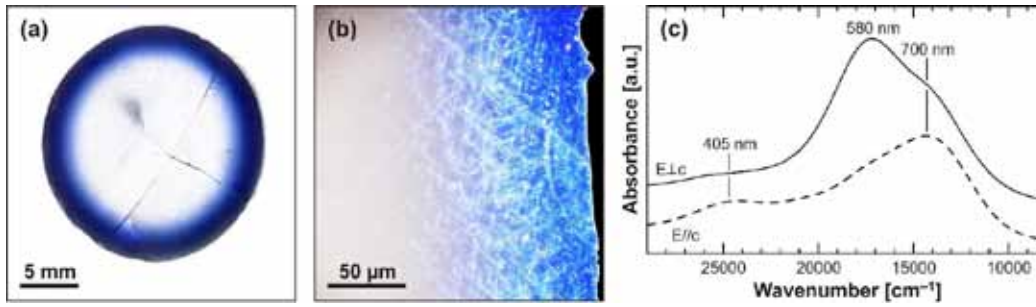

Figure 1: (a) Cross section (1 mm thickness) of a seemingly blue Verneuil boule. (b) Edge of a polished slab prepared from a cornflower-blue star sapphire that was produced by Ti- and Fe-diffusion treatment of a colourless cabochon. Oriented rutile needles and colouration are only present near the cabochon's outer surface. Image courtesy Sabine Stanek (Kunsthistorisches Museum Wien). (c) Optical absorption spectra.

The above problem affects the recently increased production of gem corundum with induced asterism (WANTHANACHAISAENG et al. 2022). Pre-shaped corundum cabochons are subjected to Ti diffusion followed by slow cooling that causes formation of oriented rutile needles. Such simple procedures work very well for red, yellow and colourless star corundum, whereas the analogous production of blue star sapphire is hampered by the unavailability of reasonably priced, homogeneously blue raw material. Therefore, colourless cabochons are subjected to combined Ti- and Fe-diffusion treatment. The resulting cornflower-blue cabochons are coloured only by a 50–100 µm skin (Fig. 1b) with ~0.14 wt% Ti and ~0.83 wt% Fe. Strong absorption in the orange-red range (Fig. 1c) is assigned to Fe^{2+}–Ti^{4+} charge transfer, whereas weak absorption in the violet range could point to minute amounts of O^- defects (KVAPIL et al. 1973). First results of chemical and spectroscopic analyses are presented and discussed.

KVAPIL, J., PERNER, B., SÚLOVSKÝ, J., KVAPIL, J. (1973): Colour centre formation in corundum doped with divalent ions. – Krist Tech, 8, 247-251.

NASDALA, L., CHANMUANG N., C., GIESTER, G., WANTHANACHAISAENG, B. (2020): Multi-coloured synthetic corundum and multicoloured glass doublets in the Thai gem market. – J Gemmol, 37, 18-20.

WANTHANACHAISAENG, B., NASDALA, L., CHANMUANG N., C., WILDNER, M. (2022): Synthetics and simulants in the Thai gemstone market: An update. – 7th International Gem & Jewelry Conference (GIT2021), Chanthaburi, Thailand, February 2022. GIT2021 Proceedings, pp 173-176.

Investigations on boron-rich tourmaline with the formula $NaAl_3Al_6(Si_3B_3O_{18})(BO_3)_3(OH)_3(OH)$

A. Ertl[1,2], A. Rosa[3], J. E. Post[4], R. Abart[5]

[1]*Mineralogisch-Petrographische Abt., Naturhistorisches Museum, Vienna, Austria*
[2]*Institut für Mineralogie und Kristallographie, Universität Wien, Vienna, Austria*
[3]*European Synchrotron Radiation Facility, Grenoble, France*
[4]*Department of Mineral Sciences, Smithsonian Institution, Washington, U.S.A.*
[5]*Department of Lithospheric Research, University of Vienna, Vienna, Austria*
e-mail: andreas.ertl@a1.net

Recently, ertlite, $NaAl_3Al_6(Si_4B_2O_{18})(BO_3)_3(OH)_3O$, a new mineral species of the tourmaline supergroup was described by CEMPÍREK et al. (2025). This is the first tourmaline in which boron (B) occurs in the endmember formula. Ertlite was described from two localities. The B-richest tourmaline sample exhibits lattice parameters of a = 15.590(2), c = 7.009(1) Å, and an empirical formula of ~$(Na_{0.74}Ca_{0.11}\square_{0.15})(Al_{2.84}Li_{0.15}Fe_{0.01})Al_{6.00}(Si_{4.05}B_{1.95}O_{18})(BO_3)_3(OH)_3[O_{0.72}(OH)_{0.24}F_{0.04}]$. Here, we describe an even more B-rich tourmaline with the approximate formula $NaAl_3Al_6(Si_3B_3O_{18})(BO_3)_3(OH)_3(OH)$. Tourmaline, synthesized from a reaction mixture of 0.625 Na_2O · 4.5 Al_2O_3 · 6 SiO_2 · 3 B_2O_3 + excess H_2O at 400 °C / 1500 MPa, was structurally analysed by Rietveld refinement. The synthetic product consists mainly of colourless tourmaline crystals, usually smaller than 1.5 µm × 300 nm (Fig. 1), and about 4 wt% quartz. Synchrotron X-ray data was recorded at the European Synchrotron Radiation Facility (ESRF). Structural parameters obtained from XRD patterns analysed by Rietveld refinement are a = 15.562(3), c = 7.001(1) Å. The refinement Si ↔ B resulted in an occupancy factor of 0.48(2) B. The microprobe data (8 analyses) of this tourmaline gave 20.79(68) wt% SiO_2, 50.02(18) wt% Al_2O_3, 0.11(3) wt% CaO, and 3.28(5) wt% Na_2O. Fluorine, Mg, Fe, Mn and Ti are below the detection limit. The values for B_2O_3 (22.11 wt%) and H_2O (3.75 wt%) were calculated for $Y + Z + T + B$ = 18 atoms per formula unit (apfu) and for Si + B = 6 apfu. The resulting formula is $(Na_{0.97}Ca_{0.02}\square_{0.01})Al_{3.00}$ $Al_{6.00}(Si_{3.17}B_{2.83}O_{18})(OH)_3[(OH)_{0.82}O_{0.18}]$. The T-site occupancy is in very good agreement with the result of the Rietveld refinement with $[Si_{3.12}B_{2.88(12)}]$. Therefore, this synthetic tourmaline comes close to a hypothetical tourmaline endmember with the formula $NaAl_3Al_6(Si_3B_3O_{18})(BO_3)_3(OH)_3(OH)$. Based on temperature-dependent correlations (ERTL et al. 2012) such a tourmaline is unlikely to form in hydrothermal to low pressure environments, because the expected temperature would be < 150°C. This study was funded in part by the Austrian Science Fund (FWF) project P 35585.

Figure 1: Synthetic B-rich tourmaline. Backscattered electron image, width: 6.5 µm.

ERTL, A., GIESTER, G., LUDWIG, T., MEYER, H.-P., ROSSMAN, G.R. (2012): Synthetic B-rich olenite: Correlations of single-crystal structural data. – Am Mineral, 97, 1591-1597.

CEMPÍREK, J., JONSSON, E., SKŘÁPKOVÁ, L., ŠKODA, R., KOLITSCH, U., ČOPJAKOVÁ, R., GROAT, L.A., KAMPF, A.R., LUSSIER, A.J., HAWTHORNE, F.C., HAIFLER, J., HOLÁ, M., ENDE, M. (2025): Ertlite, $NaAl_3Al_6(Si_4B_2O_{18})(BO_3)_3(OH)_3O$, a new mineral species of the tourmaline supergroup. – Am Mineral, 110, 12.

Limits and potentials in the automated characterization of excavated materials with Raman

M. J. Findl[1], A. Radinger[1], D. Schneider[2], R. Galler[2], E. Rückert[3], D. E. Sandu[4], K. P. Sedlazeck[1]

[1]Chair of Waste Processing Technology and Waste Management, Technical University of Leoben, Austria,
[2]Chair of Subsurface Engineering, Technical University of Leoben, Austria,
[3]Chair of Cyber-Physical-Systems, Technical University of Leoben, Austria,
[4]AiDEXA GmbH, Graz, Austria
e-mail: martin.findl@unileoben.ac.at

Excavated materials represent the largest waste stream in Austria by volume, accounting for approximately 59 % of total waste (BAWP 2023). At the same time, a significant portion of these materials is landfilled despite their potential for reuse (DepVO 2008, Galler 2015).

The NNATT project (long title: sustainable use of excavation materials with sensor-based technologies) aims to achieve a mineralogical-chemical characterization of excavated materials using sensor-based technologies, thereby laying the foundation for automated in-situ classification and enabling ecologically and economically optimized reuse of excavation. Representative excavated materials are characterized by Raman spectroscopy combined with hyperspectral imaging. These sensor data are systematically recorded in a database. Building on the logged data, geologically and mineralogically derived decision trees are developed to serve as the basis for an AI-supported rock classification system.

The goal is to systematically investigate the robustness and classification accuracy of the deployed sensor technology under standardized laboratory conditions and realistic operational scenarios. Initially, stationary Raman measurements are conducted on mono-mineralic materials as well as selected representative rock types to generate a high-quality data foundation in the central database system. The planned outcome includes spectral measurements of individual minerals as well as of sandstone, limestone, granite, and characteristic excavated materials such as molasse and sandy marlstone. A key methodological focus lies in data collection under dynamic conditions – especially on a continuously running conveyor belt – as well as in analyzing relevant interference factors such as dust adhesion, airborne dust, varying lighting conditions, surface contamination and mechanical vibrations in the construction site environment. The influence of dynamic factors is also studied in a controlled laboratory setting to comparatively evaluate differences in signal quality and classification accuracy between stationary and dynamic measurements.

A central objective is the quantitative determination of the minimum required measurement time or conveyor belt distance needed for reliable rock classification with statistical analysis of the spectral data playing a critical role. A target conveyor belt speed of 3 m s^{-1} is defined as the technical benchmark at which the sensor system should operate reliably. The scientific contribution lies in the methodological combination of mineralogical-chemical expertise with digital sensor technology to promote a circular economy.

BAWP (2023): Bundes-Abfallwirtschaftsplan. – Bundesministerium für Klimaschutz, Umwelt, Energie, Mobilität, Innovation und Technologie.

DEPVO (2008): Deponieverordnung vom 24.05.2008. – Österreichisches Rechtsinformationssystem.

GALLER, R. (2015): Development of resource-efficient tunnelling technologies – Results of the European research project DRAGON. – Geomechanics and Tunnelling, 8 (4), 302–309. DOI: 10.1002/geot.201500017.

The role of siderite ($FeCO_3$) in cementitious systems

I. Galan[1], M. Pons Pineyro[2], F. R. Steindl[1,2], A. C. M. Soares[1], J. Juhart[1], F. Mittermayr[3]

[1]Institute for Technology and Testing of Building Materials, Graz University of Technology, Austria
[2]Institute of Applied Geosciences, Graz University of Technology, Austria,
[3]Institute for Material Technology, University of Innsbruck, Austria
e-mail: igalangarcia@tugraz.at

The interplay between siderite and cement has been recently investigated. The iron carbonate mineral sourced from the Styrian Erzberg mine has been proved to significantly alter the setting, hardening, and deterioration mechanisms of cement-based materials.

In the past years, the replacement of cement clinker by so-called supplementary cementitious materials (SCMs) has become a common practice. Price reduction, valorization of waste and by-products, and reduction of the environmental footprint are among the most important benefits of incorporating these materials into cementitious binders. Additionally, SCMs help to improve the properties of mortar and concrete in the fresh and hardened state. However, the availability of some of the most commonly used SCMs, like ground granulated blast furnace slag and fly ash, is progressively decreasing, while the concrete demand keeps increasing. The need for new materials to replace cement in the binders while maintaining or even improving the performance of the resulting concrete is acute.

The potential use of siderite as SCM was recently assessed for the first time. While powdered siderite significantly retards early hydration reactions (MITTERMAYR et al. 2025), its presence seems to enhance several durability properties, such as the calcium leaching potential and resistance to sulfate attack (PONS PINEYRO et al. 2025). One of the reasons for this improvement is related to the consumption of portlandite formed during cement hydration, and the reduction of available calcium ions in the system. Despite this, other durability properties, such as carbonation resistance, do not seem to worsen due to the presence of siderite, as may have been expected due to the lowering of the CO_2 buffering capacity of the system.

In addition to the partial replacement of cement clinker in the binder, siderite can also be used as a fine aggregate in mortar and concrete mixes. This approach mitigates some of the challenges associated with the delay of the early hydration reactions and simplifies the grinding and preparation of the material. Additionally, the rapid oxidation of powdered siderite is partly inhibited with the reduction of the surface area when used as fine aggregate. The incorporation of siderite as sand in mortar and concrete leads to higher compressive strength values at later stages. This effect seems to be related to a densification of the interfacial zone between aggregates and matrix.

Our recent studies have demonstrated the high potential of siderite and iron carbonate-containing minerals to be used in concrete applications with enhanced mechanical and durability properties.

MITTERMAYR, F., STEINDL, F.R., PONS PINEYRO, M., BRIENDL, L., SAKOPARNIG, M., GALAN, I. (2025). Exploring Natural Siderite $FeCO_3$ as a Novel Supplementary Cementitious Material. – Cem Con Res, 197, 107975.

PONS PINEYRO, M., STEINDL, F.R., GALAN, I., SOARES, A.C.M., MITTERMAYR, F. (2025): How siderite ($FeCO_3$) enhances the sulfate resistance of cementitious systems. – Cem Con Res (under review).

Zircon survival during Carboniferous partial melting of Cambrian granitoid (Mt. Papuk, Croatia)

D. Gallhofer[1], E. Skrzypek[1], P. Schneider[2], D. Balen[2], C. A. Hauzenberger[1]

[1]Department of Earth Sciences, University of Graz, Austria,
[2]Department of Geology, University of Zagreb, Croatia,
e-mail: daniela.gallhofer@uni-graz.at

Partial melting is a ubiquitous process during the tectono-metamorphic evolution of collisional orogens. It is commonly recorded by migmatites or granitoids and particularly by their accessory phases such as zircon and monazite. While in many cases both minerals newly crystallise from partial melt, there are rare cases of nearly full preservation of precursor zircon. Here, we present an example of zircon preservation during partial melting of a peraluminous orthogneiss from Trešnjevica quarry, Mt. Papuk, Croatia. Mt. Papuk is located in the Slavonian Mountains, an Inselberg of (pre-)Variscan metamorphic rocks and granites in the southwestern part of the Pannonian Basin. We combine LA-ICPMS U-Pb zircon dating and trace element analysis, geochemical whole rock data and phase equilibria modelling to constrain pressure, temperature and water content during partial melting.

The peraluminous (aluminum saturation index 1.12) migmatitic orthogneiss is medium grained, well foliated and biotite-rich. It is cut by irregular veins and pockets of equigranular leucocratic granite. In the granite, monazite yields the age of partial melting (~350 Ma), while zircon remains largely unaffected by anatexis. The orthogneiss yields a protolith age of c. 499 Ma ($^{206}Pb/^{238}U$ zircon age). Zircon dates of the granite show the same range from 496-453 Ma and only two grains record young concordant dates of 390 and 397 Ma. Similar cathodoluminescence signals, trace element contents and element ratios (e.g., Th/U, U/Ce) in zircon from both samples indicate that the granite inherited the zircons from the orthogneiss.

Petrographic observations (stability of biotite, presence of muscovite, lack of sillimanite in the orthogneiss) and melt collection at, but without segregation from the site of formation indicate a low degree of partial melting in the orthogneiss probably associated with water influx at low melting temperatures (c. 710 °C from zircon and monazite saturation). This hypothesis is tested with phase equilibria modelling of the orthogneiss.

Our results are consistent with other studies of orthogneiss partial melting (e.g., COUZINIÉ et al. 2021) and corroborate that low-degree partial melting at low temperature (c. 710 °C) is not necessarily recorded by all accessory phases present.

COUZINIÉ, S., BOUILHOL, P., LAURENT, O., MARKO, L., MOYEN, J.F. (2021): When zircon drowns: Elusive geochronological record of water-fluxed orthogneiss melting in the Velay dome (Massif Central, France). – Lithos, 384-385, 105938.

Tracing stratiform Pb-Zn-Ag-Ba deposits in the Graz Paleozoic (Eastern Alps, Austria): geochemical and mineralogical vectors for ore proximity

A. Geringer[1], F. Melcher[2], R. Schuster[1], S. Rohrhofer[2]

[1]GeoSphere Austria, Division Geophysical and Applied Geological Services, Vienna, Austria
[2]Technical University of Leoben, Chair of Geology and Economic Geology, Leoben, Austria
e-mail: annika.geringer@geosphere.at

Geochemical and mineralogical vectors are commonly used for the exploration of various ore deposit types (e.g., volcanogenic massive sulfides (VMS), sedimentary-exhalative (SEDEX), porphyry copper deposits). We are generating such proximity vectors for the stratiform Pb-Zn-Ag-Ba deposits in the Graz Paleozoic (Eastern Alps, Austria), which are classified as SEDEX deposits. Mining of these deposits is documented for about 680 years until 1927 with the main mining sites Arzberg, Haufenreith, Kaltenberg-Burgstall, Deutschfeistritz, Rabenstein and Großstübing. These stratiform Pb-Zn-Ag-Ba occurrences are hosted by metasediments and metavolcanics of the Schönberg Formation (Schöckel nappe; Drauzug-Gurktal nappe system), which show a Permian and Cretaceous (Alpine) greenschist metamorphic overprint. Galena, sphalerite, barite, pyrite, pyrrhotite and magnetite are the dominating ore minerals, accompanied by chalcopyrite, arsenopyrite, fahlore, pyrargyrite, tetradymite, cobaltite, ullmannite, breithauptite, electrum, and others.

Whole rock geochemical data show a general increase of the elements Pb, Zn, Ag and Cu in host rocks samples towards the ore. Another trend is visible in the Nb content, which decreases towards the ore. This corresponds with Nb contents in rutile, also decreasing towards the ore. Increasing Fe/(Fe+Mg) towards the ore is observed in tourmaline as well as in chlorite. Further possible vectors are currently tested. To investigate the mineralogy and mineral chemistry scanning electron microscopy (SEM), electron probe micro-analysis (EPMA) and laser-ablation inductively coupled plasma mass spectrometry (LA-ICP-MS) are used.

In the hanging-wall and foot-wall of the ore horizons distinct hydrothermal alteration zones related to ore-forming processes are developed (ROHRHOFER et al. 2024). These zones are characterized by Fe and Mn rich carbonates (carbonatization), Fe rich chlorite (chloritization), K- and Ba-feldspars, Ba bearing white mica, fluorapatite, REE and HFSE minerals as well as disseminated ore minerals. Albitization is typical below sulfide rich horizons, whereas silicification is typical in the hanging-wall.

Our investigations will lead into a refined exploration model for the stratiform Pb-Zn-Ag-Ba deposits in the Graz Paleozoic and a revised understanding of their genesis.

ROHRHOFER, S., GERINGER, A., MELCHER, F., SCHUSTER, R. (2024): Alteration Zones as Exploration Parameters for Stratiform Pb-Zn-Ag-Ba Deposits in the Graz Paleozoic (Eastern Alps, Austria). Berg Huettenmaenn Monatsh., 169, 567–573.

Microstructural evaluation of carbon-based coatings deposited by atmospheric pressure plasma jet on 3D-printed polymers

J. Glettler[1], R. Kaindl[1], R. Elter[1], T. Prethaler[1], S. Chwatal[2], M. Stummer[2], C. Teichert[3], L. Major[4], J. M. Lackner[1], W. Waldhauser[1]

[1]JOANNEUM RESEARCH, MATERIALS – Institute for Sensors, Photonics and Manufacturing Technologies, Niklasdorf, Austria,
[2]INO GmbH, Attnang Puchheim, Austria,
[3]Chair of Physics, Department Physics, Mechanics and Electrical Engineering, Montanuniversität Leoben, Austria,
[4]Institute of Metallurgy and Materials Science, Polish Academy of Sciences, Kraków, Poland
e-mail: reinhard.kaindl@joanneum.at

The microstructures of coatings on polymer (Polyamide 12) substrates, deposited via atmospheric pressure plasma (APP) jet deposition from carbonized wood (CW) dust and carbon black (CB) powders were investigated. Both materials offer potential for the development of sustainable and environmentally friendly coating systems. Scanning and transmission electron microscopy (SEM/TEM), energy-dispersive X-ray spectroscopy (EDXS) and long-term tribological tests (pin-on-disc) provided detailed insights into the coatings' composition and microstructure. For CW dust coatings, the surface microstructure evolved from a homogeneous distribution of wood dust particles in an amorphous matrix to a near-surface zone with fewer particles and the formation of a ~680 nm thick nano-graphite rich tribofilm. This structural transformation was accompanied by a steady decrease in the coefficient of friction (CoF) with increasing load down to 0.21. CB coatings initially contained tubular-like nano-crystallites, non-catalytic oxidized soot, carbon nanotubes and various carbon black types (furnace, lamp, channel black), embedded in an amorphous matrix. Upon wear, these coatings structurally evolved from a porous to a densified two-layer structure, comprising a subsurface nano-graphite layer (maximum thickness approx. 600 nm) and an underlying amorphous matrix (BHOWMICK et al. 2015). The CoF initially increased before stabilized at approx. 0.34. These findings have essential implications for designing low-friction and wear-resistant surface treatments for tribological applications.

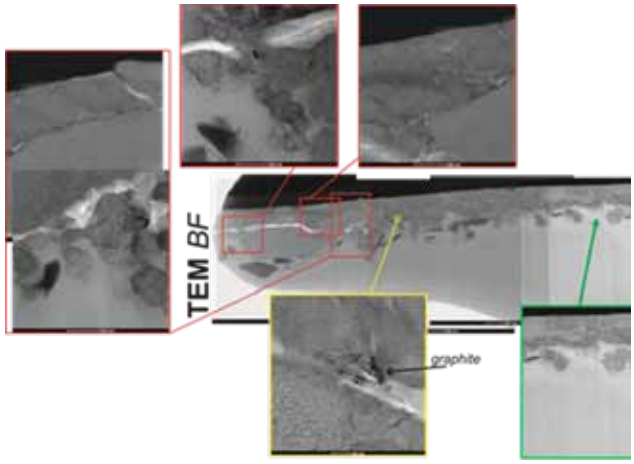

Figure 1: TEM bright-field cross-section of a wear track in APP carbonized wood dust coatings.

BHOWMICK, S., BANERJI, A., ALPAS, A.T. (2015): Role of humidity in reducing sliding friction of multilayered graphene. – Carbon, 87, 374-384.

Distribution of trace elements (Re, Mo, and Co) in the Kupferschiefer

S. Goldmann[1], H.-E. Gäbler[1], T. Graupner[1]

[1]*Bundesanstalt für Geowissenschaften und Rohstoffe, Hannover, Germany*
e-mail: simon.goldmann@bgr.de

The Kupferschiefer is an important ore deposit type for Cu, Zn, and Pb as well as Ag in Europe with active mining in southwestern Poland. The Kupferschiefer *sensu stricto* is a 40 to 90 cm thick organic-rich shale discordantly overlying the Middle Permian volcano-sedimentary rocks (so-called 'Rotliegend') and is covered by Upper Permian massive carbonates (so-called 'Zechstein'). The Kupferschiefer is stratified and composed of different horizons with varying contents of silicates, carbonates, organic matter, and sulphides (Fig. 1).

The studied polished sections originate from a drill core in the Sangerhausen district in Germany intersecting the Kupferschiefer succession from massive carbonates in the hanging wall through the Kupferschiefer *s.s.* into the footwall ores. The polished sections were investigated by scanning electron microscopy with Mineral Liberation Analysis (MLA) software for the mineral phase distribution and by laser ablation inductively coupled plasma time of flight mass spectrometry (LA-ICP-TOFMS) for the distribution of trace element concentrations.

In this study, the trace elements Re, Mo, and Co are taken as examples to show differences in their concentration and distribution along the Kupferschiefer profile; moreover, the hosts for the trace elements also change along the stratigraphy (Fig. 1). The trace element concentrations progressively increase from hanging wall carbonates towards the Kupferschiefer strata and abruptly drop reaching the footwall ores. The hosts for these trace elements also vary between the stratigraphic units and are represented either by organic matter (Fig. 1) or by sulphides. Furthermore, these trace elements either occur together (Fig. 1) or they partition into separate phases and even into different zones within a single host grain.

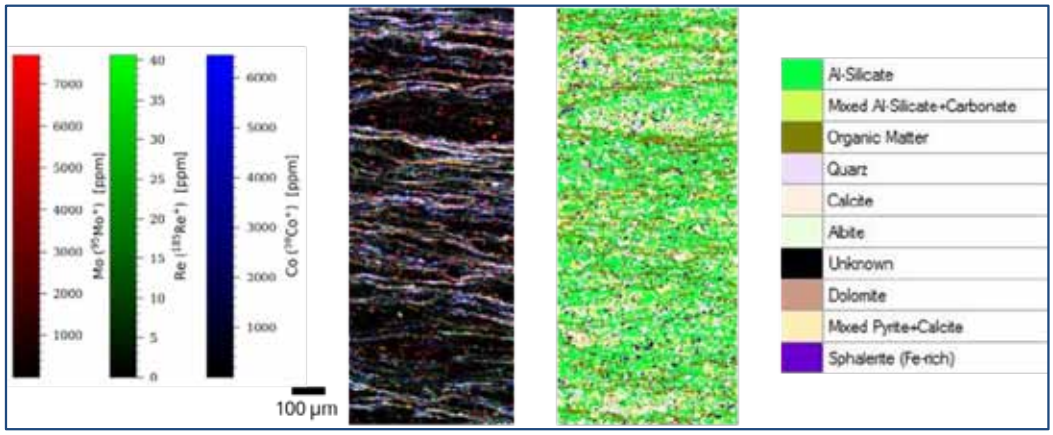

Figure 1: Distribution of trace elements (left) and of mineral phases (right) in Kupferschiefer from the Sangerhausen mining district, Germany. Left: Element distribution map of Mo (red), Re (green), and Co (blue) by LA-ICP-TOFMS. Explanatory note: Combination of red, green, and blue results in white colour, where all three elements occur together. Right: Mineral phase distribution by MLA of the same area as on the left.

Trace-metal enrichment in Wissenbach Shale from Bullars, Upper Harz

T. Graupner, G. Jacques, H.-E. Gäbler, S. Goldmann, J. Meima, W. Nikonow

Bundesanstalt für Geowissenschaften und Rohstoffe, Hannover, Germany,
e-mail: torsten.graupner@bgr.de

About 60 m of core from the drilling site Bullars (nearby Lautenthal, Upper Harz mining district) with moderate enrichment in base metals (Zn, ±Cu and Pb) were studied for bulk rock geochemistry, mineral chemistry, and Pb isotopic compositions. Two core scanners (LIBS 2D core scanner, µEDXRF 2D scanner) were used and the results verified using optical and scanning electron microscopy (32 polished sections). Quantitative ore mineral chemistry was determined using electron probe microanalysis (EPMA) and laser ablation-ICP-time-of-flight-MS. Lead isotope ratios were obtained via laser ablation-multicollector-ICP-MS.

Copper, Fe, and Zn sulfides occur in concordant lenses and phosphorite concretions, as well as in thin discordant carbonate-dominated veinlets of the Devonian Wissenbach Shale. Bulk rock trace element data (Ga/Al, Y/Ho, Zr/Hf) do not support intense hydrothermal overprint of the studied shale. However, a supply of hydrothermal ore-bearing fluids from greater depth and precipitation of ore minerals in numerous fissures without significant fluid-rock interaction cannot be ruled out.

Two sphalerite types from Bullars differ significantly in their trace element composition (Type I: moderate Ge and low In, Type II: low Ge and high In). These clear differences indicate the presence of more than one stage of ore mineral formation in this Devonian rock sequence. The In and Sn concentrations for the In-dominated sphalerite from Bullars (Fig. 1) are slightly lower than the values for high-In sphalerite 2b from the nearby Lautenthal deposit (GRAUPNER et al., 2024). Lead isotope ratios for sphalerite from Bullars suggest a different Pb source compared to the Rammelsberg Sedex deposit and vein-related ores of the Upper Harz (Lautenthal, Grund). This conference paper is a contribution to the DESMEX-REAL project.

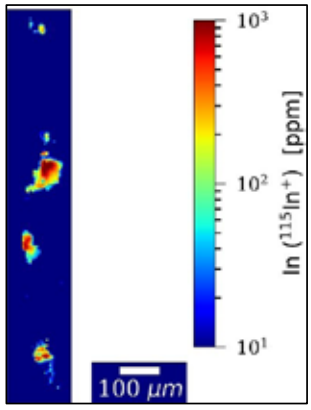

Figure 1: Indium-enriched sphalerite grains in a discordant carbonate-dominated veinlet from the Wissenbach Shale (Bullars drilling site)

GRAUPNER, T., HENNING, S., GOLDMANN, S., FUCHS, STEDINGK, K. LIESSMANN, W., BIRKENFELD, S. (2024). The In-Ga-Sb association of the post-Variscan Zn-Pb-Ag vein deposit at Lautenthal, Upper Harz Mountains, Germany: sphalerite mineral chemistry. Mineral. Deposita, 59, 1363-1386.

Evidence of (very-) low-grade metamorphism in Mesozoic carbonate rocks of the western part of Mt. Papuk, Croatia

Z. Gverić[1], D. Balen[1], P. Schneider[1], D. Tibljaš[1]

[1]University of Zagreb, Faculty of Science, Zagreb, Croatia
e-mail: zgveric@geol.pmf.unizg.hr

Two major tectonic units, ALCAPA (NW) and Tisia Mega-unit (SE), form the pre-Neogene basement of the Pannonian Basin. Tisia Mega-unit mainly consists of Variscan granites and very low-, low- and medium-grade metamorphic rocks (PAMIĆ & LANPHERE, 1991), which are overlain by post-Variscan sedimentary sequences. Tisia Mega-unit outcrops, found in several mountains of the area (Mt. Papuk being one of them), are geologically important study sites. Post-Variscan rocks in this area were considered to be unmetamorphosed, but in the meantime evidence has emerged that the metasediments have been metamorphosed to variable degree during Creteaceous period (BIŠEVAC et al. 2010; BALEN et al. 2018).

To better constrain the metamorphism affecting Mesozoic rocks in the area in the less investigated lithology that is poor in clay minerals, we sampled and studied carbonate rocks of Jurassic age (according to the geological map) and analyzed them in oriented thin sections using polarizing microscopy (microtectonic analyses) and X-ray diffraction (XRD). Mineral analyses involved detailed bulk rock and clay fraction investigations, including the measurement of Kübler (KI) and, where applicable, Árkai (ÁI) indices. KI and ÁI were measured according to the recommendations by KISCH (1991).

Samples of Jurassic carbonate rocks contain carbonate minerals (dominantly calcite, some dolomite), quartz, feldspars and occasional hematite in addition to around 10–30% of mica minerals and small amounts (2–7%) of chlorite in four of the nine samples. Oriented microscopic thin sections prepared from two representative samples revealed several features (calcite twinning type II and III, boudinage) that imply the influence of temperature on deformation, corresponding to temperatures of 200–300 °C. KI measured on illite 001 diffraction maxima placed all of the samples within the anchizone range (values from 0.254 to 0.384). ÁI (chlorite 002) was measured on three samples and confirmed KI results while one sample even yielded epizone values.

The changes on calcite observed in thin sections show a post-Jurassic deformation sequence and, alongside KI and ÁI results, provide strong evidence that the investigated Jurassic carbonate rocks represent a (meta)carbonate complex which records post-Jurassic very low- to low-grade metamorphism. This metamorphism can, most likely, be correlated with the Cretaceous metamorphism already recorded in clay rich Mesozoic lithologies. This study also underlines the potential of using KI and ÁI for studying the metamorphic evolution of low-grade metamorphism in carbonate rocks.

BALEN, D., MASSONE, H.-J., LIHTER, I. (2018): Alpine metamorphism of low-grade schists from the Slavonian Mountains (Croatia): new P-T and geochronological constraints. – Int. Geol. Rev., 60:3, 288-304.

BIŠEVAC, V., BALOGH, K., BALEN, D., TIBLJAŠ, D. (2010): Eoalpine (Cretaceous) very low- to low-grade metamorphism recorded on illite-muscovite-rich fraction of metasediments from South Tisia (eastern Mt Papuk, Croatia). – Geol. Carpath., 61, 469-481.

KISCH, H. J. (1991): Illite "crystallinity": recommendations on sample preparation, X-ray diffraction settings, and interlaboratory samples. – J. Metamorph. Geol., 9, 665-670.

PAMIĆ, J., LANPHERE, M (1991): Hercynian granites and metamorphic rocks from the Mts. Papuk, Psunj, Krndija, and the surrounding basement of the Pannonian Basin in Slavonija (Northern Croatia, Yugoslavia). – Geologija, Ljubljana, 34, 81-253.

Formation conditions of Veitsch-type sparry magnesite from the city of Leoben (Eastern Alps, Austria)

F. J. Hampl[1], V. Bertrandsson Erlandsson[2], R. J. Bakker[1], M. M. Feichter[1], G. Rantitsch[2], R. Arató[2], M. Werdenich[3]

[1]Chair of Resource Mineralogy, Technical University of Leoben, Leoben, Austria,
[2]Chair of Geology and Economic Geology, Technical University of Leoben, Leoben, Austria,
[3]Department Mineral Resources and Geoenergy, GeoSphere Austria, Vienna, Austria,
e-mail: ferdinand.hampl@unileoben.ac.at

Industrially vital carbonate-hosted sparry magnesite (Veitsch type) from the Eastern Alps has been investigated for over 100 years, but its formation is still unclear and debated. Two crucial parameters in this debate are the temperature and salinity of the mineralizing fluid, which are usually calculated based on fluid inclusion microthermometry. However, the majority of fluid inclusions in magnesites of the Eastern Alps is unsuitable for microthermometry due to their small size, resulting in scarce and uncertain temperature and salinity estimates. To shed light on the formation conditions of this commodity we investigated samples from an abandoned magnesite quarry on the mountain Häuselberg in the city of Leoben (Eastern Alps, Austria) where fluid inclusions of suitable size were found. In addition to Raman spectroscopy and microthermometry, we also used electron microprobe analysis and laser ablation inductively coupled plasma mass spectrometry to understand the formation of the sparry magnesite.

Preliminary results reveal two distinct fluid inclusion groups in the magnesite. Group 1 consists of fluid inclusions with gas bubbles occupying on average 11% of the fluid inclusions. Apart from trace amounts of CO_2 the gas bubbles mainly consist of H_2O vapor and the homogenization temperatures range between ~160 and ~220 °C. The salinity varies widely between ~4 and ~22 eq. mass% NaCl, indicating more than one generation of fluid inclusions. Fluid inclusions of group 2, on the other hand, are rarer and have bigger gas bubbles that occupy on average 27% of the fluid inclusion. Moreover, a different gas composition distinguishes them from group 1: on average, 96.1 mol% CO_2, 3.7 mol% N_2, 0.1 mol% H_2S and 0.1 mol% CH_4. Additionally, the homogenization temperatures are higher than in group 1 and range between ~270 and ~320 °C, whereas the salinity is more consistently at 4.5 eq. mass% NaCl on average. After the metasomatic magnesitization, the magnesite was overprinted by a peak regional metamorphism of 535 ± 30.5 °C as Raman spectroscopy on carbonaceous material in the magnesite rock discloses.

Our results do not only facilitate the reconstruction of the formation of sparry magnesite from Leoben but also provide a basis for a re-evaluation of formation models of sparry magnesite in the Eastern Alps and beyond.

On the reaction mechanisms of landfill mineral waste in alkali activated binders

A. Hassan[1], S. Radinger[1,2], O. Rudic[1,3], B. Ratz[1,4], F. R. Steindl[1,3], F. Mittermayr[5], A. Jodlbauer[6], M. Wilkening[6], C. Grengg[1]

[1]Christian Doppler Laboratory for Waste-based geopolymer construction materials in the CO_2-neutral circular economy, Institute of Applied Geosciences, Graz University of Technology, Austria
[2]Institute of Soil Mechanics, Foundation Engineering and Computational Geotechnics, Graz University of Technology, Austria
[3]Institute of Technology and Testing of Construction Materials, Graz University of Technology, Austria
[4]Chair of Waste Processing Technology and Waste Management, Montanuniversitaet Leoben, Austria
[5]Institute for Material Technology, University of Innsbruck, Austria
[6]Institute for Chemistry and Technology of Materials, Graz University of Technology (NAWI Graz), Austria
e-mail: amr.hassan@tugraz.at

The use of alkali-activated materials (AAMs) made from mineral wastes and/or secondary raw materials (WSRM) as primary binder components holds significant potential to enhance material circularity and reduce the environmental impact of material production. This study examines the performance of six Austrian WSRMs when used as major binder components in combination with metakaolin (MK) (45 wt.% WSRM/55 wt.% MK), activated with potassium waterglass. The WSRMs studied included two types of steel slags, three types of construction and demolition waste (including mineral stone wool), and glass waste.

All resulting binders exhibited high functionality, with 90-day strengths ranging from 71 to 106 MPa. However, the diverse setting behaviours, strength development, and microstructural features indicated that each WSRM contributed unique properties. Steel slags displayed relatively rapid setting times, high heat release, high strengths, and strong evidence of both C-A-S-H and K(C)-A-S-H gel phases as the primary binder phases. In contrast, the other WSRMs showed slower setting, lower early strengths, and slower strength gain rates, with a clear dominance of K(C)-A-S-H gel phases in the reaction products.

The findings highlight the promising potential of WSRMs as key binder components for AAMs and provide a foundation for further optimization and exploration of WSRM-based AAMs.

Influence of CaO on the hydration behavior of MgO

K. Hebenstreit[1], M. Pettauer[1], A. Baldermann[1]

[1]Institute of Applied Geosciences, Graz University of Technology, Austria
e-mail: kerstin.hebenstreit@student.tugraz.at

Magnesium oxide (i.e., periclase: MgO) is a potentially climate-friendly binder in the refractory industry, giving that the hydration process is complete and that the hydration products forming have proper characteristics, such as a self-organizing microstructure (PETTAUER et al., 2024). Calcium oxide (i.e., quicklime: CaO) is a main component in MgO-based materials, which is significantly more reactive than pure MgO, and after hydration, produces strongly alkaline conditions (pH ~13). In this study, we investigate the influence of the CaO content (0% up to 100% replacement) on the hydration behavior of MgO, and characterize the hydration products (i.e., portlandite: $Ca(OH)_2$; brucite: $Mg(OH)_2$), and the resulting microfabrics.

For this purpose, mixtures with different CaO/MgO ratios were prepared and hydrated at a solid/liquid ratio of 1:10 at 25°C over a period of seven days. During hydration, the pH and the electrical conductivity were measured regularly. Once hydration was complete, the solids were characterized by X-ray diffraction, Fourier transform infrared spectroscopy and scanning electron microscopy, while the reactive fluids were analyzed by optical emission spectrometry with inductively coupled plasma.

Our results show that the reaction behavior of MgO significantly changes depending on the initial CaO content. Differences in pH values and electric conductivity reflect the different solubilities of portlandite and brucite in the respective MgO-CaO mixtures, with higher initial CaO contents causing an almost complete Mg^{2+} removal from the solution at high pH, and thus massive and dense scale formation. Interestingly, Ca-Mg carbonates also formed upon ongoing MgO-CaO hydration, which implies that refractory products have to be cured and monitored carefully to avoid unwanted volume expansion, and thus crack formation during hydration. The knowledge gained may contribute to a better understanding of the hydration processes in MgO-CaO-H_2O systems.

PETTAUER, M., BALDERMANN, A., EDER, S., & DIETZEL, M. (2024). Hydration of MgO: Reaction kinetics and pH control on Brucite crystal morphology. – Cryst Growth Des, 24, 3544–3555.

From Mystery to Modulation: The Structural Story of $Rb_2Si_2O_5$

C. Hejny[1], H. Krüger[1], V. Kahlenberg[1]

[1] Mineralogy and Petrography, University of Innsbruck, Innrain52, 6020 Innsbruck
e-mail: clivia.hejny@uibk.ac.at

Alkali silicates have been extensively studied due to their range of applications, including their use in the glass industry, bioactive ceramics, and as host materials for rare-earth-element-based silicate phosphors. Despite their importance, the structural complexity of some alkali silicates remains a challenge.

The crystal structure of $Rb_2[Si_2O_5]$ has long posed difficulties, as even the original authors of the structure noted that "with such high *R* factor the structure on itself would not be publishable" (DEJONG et al., 1994). In a re-examination, a *C*-centred monoclinic cell, similar to the one previously reported was identified, but with additional reflections along the b^*-direction, which were interpreted as satellite reflections. Detailed analysis revealed satellite reflections up to the third order. In an average 3d crystal structure model, that does not account for the presence of these satellite reflections, most of the oxygen atom positions are split, and rubidium atoms are six-fold coordinated and strongly underbonded.

The crystal structure was solved as an incommensurately modulated phase in the (3+1)-dimensional superspace group $C2/c(0\beta0)s0$, with $\mathbf{q}$ = (0,0.377(1),0), a = 9.8695(6), b = 8.4012(1), c = 14.7701(1) Å, β = 90.113(1)°, and V = 1223.4(1) Å^3. The refinement converged to an *R*-value of 0.0370, significantly lower than the previously reported value of 0.12 (DE JONG et al., 1994). The $[SiO_4]$ tetrahedra adopt two distinct orientations, which were modelled using a crenel modulation function to describe the occupational modulation of atomic positions (PETRICEK et al., 2016). The structure consists of $[Si_2O_5]^{2-}$ - layers with intercalated rubidium atoms. The silicon layers are undulated, forming four- and eight-membered rings, a so-called 4.8^2 net (HAWTHORNE et al., 2019). Terminal oxygen atoms of the $[SiO_4]$ tetrahedra are pulled closer into the coordination sphere of rubidium, resulting in more balanced bond valence sums for rubidium. However, this adjustment induces strain in the silicon layer, particularly in the four-membered rings, which is alleviated by the switching of tetrahedra between two orientations.

A comparison with other silicate materials featuring 4.8^2 nets, such as $Cs_2Si_2O_5$ (DEJONG et al., 1994) and members of the mountainite mineral group (ZUBKOVA et al., 2010), reveals that larger interlayer cations or higher interlayer content relax the silicon layer, allowing for a larger unit mesh of the silicon layer without modulation.

HAWTHORNE, F.C., UVANOVA, Y.A., SOKOLOVA, E. (2019): A structure hierarchy for silicate minerals: sheet silicates. – Mineral. Mag., 83, 3-55.

DE JONG, B.H.W.S, SLAATS, P.G.G., SUPÈR, H.T.J., VELDMAN, N, SPEK, A.L. (1994): Extended structures in crystalline phyllosilicates. – J. Non-Crystalline Solids 176, 164-171.

PETRICEK, V., EIGNER, V., DUSEK, M., CEJCHAN, A. (2016): Discontinuous modulation functions and their application for analysis of modulated structures with the computing system JANA2006. – Z. Kristallogr. 231(5), 301-312.

ZUBKOVA, N.V., FILINCHUK, Y.E., PEKOV, I.V., PUSHCHAROVSKY, D.Y., GOBECHIYA, E.R. (2010): Crystal structures of shlykovite and cryptophyllite. – Eur. J. Mineral., 22, 547–555.

Orthorhombic $Ba_2Zr_2Si_3O_{12}$: A previously unrecognized polymorph or the true structure?

L. Herrero Schmidt[1], B. Krüger[1]

[1]University of Innsbruck, Innsbruck, Austria
e-mail: lars.herrero-schmidt@student.uibk.ac.at

$Ba_2Zr_2Si_3O_{12}$, commonly referred to as the 223-phase based on its $BaO:ZrO_2:SiO_2$ ratio, is a well-known compound within the ternary $BaO–ZrO_2–SiO_2$ system, which comprises several distinct crystalline phases. Although early studies by MASSE & DURIF (1973), later confirmed by LI et al. (2023), assigned this phase to the cubic space group $P2_13$, our experimental findings suggest that it crystallizes in an orthorhombic symmetry.

During a systematic investigation of the $BaO–ZrO_2–SiO_2$ system, solid-state reactions were carried out over a range of temperatures and starting compositions. In numerous experiments, the 223-phase crystallized preferentially over other phases, particularly in silica-rich conditions. Attempts to synthesize a pure 223-phase consistently required an excess of SiO_2 in the starting mixture. This surplus was necessary to obtain a powder diffraction pattern showing only the reflections of the 223-phase, with the excess SiO_2 remaining as a fine amorphous material. In the absence of this oversaturation with SiO_2, $BaZrO_3$ frequently formed as a secondary phase.

Rietveld refinements of powder X-ray diffraction data revealed a significantly improved fit when employing an orthorhombic space group ($P2_12_12_1$), opposing the previously assumed cubic symmetry. Closer inspection of the diffraction patterns showed that numerous reflections, initially interpreted as singular Bragg peaks under cubic symmetry, were in fact composed of multiple, closely spaced reflections. This observation is consistent with a lower-symmetry structure containing a greater number of distinct lattice planes. The best-fit refinement yielded lattice parameters of a = 10.23746(6) Å, b = 10.25058(6) Å, and c = 10.20352(5) Å and $\alpha = \beta = \gamma = 90°$, deviating slightly from the idealized cubic values of $a = b = c$ = 10.229 Å and $\alpha = \beta = \gamma = 90°$. All powder diagrams, including those containing multiple phases, consistently produced similar orthorhombic parameters. Moreover, the orthorhombic model consistently outperformed both the cubic and an alternatively tested trigonal refinement, being the only one to achieve a goodness-of-fit (GOF) value below 2. These results strongly indicate that the symmetry of the synthesized $Ba_2Zr_2Si_3O_{12}$ is orthorhombic. However, an important question remains: does this orthorhombic form represent a previously unreported polymorph stabilized by specific synthesis conditions, or does it in fact reflect the correct structure of $Ba_2Zr_2Si_3O_{12}$? Further studies involving single-crystal diffraction or in-situ phase formation analysis will be essential to resolve this structural ambiguity.

LI, Y., LIANG, D., ZHANG, X., XIONG, Z., TANG, B., SI, F., FANG, Z., Li, H., SHI, Z. CHEN, J. (2023). Crystal structure, sintering behavior, and microwave dielectric properties of low-permittivity $Ba_2Zr_2Si_3O_{12}$ ceramics. Journal of Electronic Materials, 52(11), 7164-7170. https://doi.org/10.1007/s11664-023-10651-z.

MASSE, R., DURIF, A. (1973), C. R. Seances Acad. Sci., Ser. C1973, 276, 1029-1031.

Influence of surface topography and microstructure on the ice nucleation activity of alkali feldspar

D. Heuser[1], M. Hagn[1], O. Ageeva[1], E. Petrishcheva[1], R. Abart[1]

[1]Department of Lithospheric Research, University of Vienna, Austria
e-mail: david.heuser@univie.ac.at

Ice formation on aerosol particles plays a crucial role for the properties of tropospheric clouds and in Earth's weather and climate. Some alkali feldspars have been identified as the most effective ice nucleating particles (INP) in airborne mineral dust (ATKINSON et al. 2013, HARRISON et al. 2016, PECKHAUS et al. 2016).

To identify possible causes for this phenomenon, we performed ice nucleation experiments with a variety of natural alkali feldspars, ranging from homogeneous and featureless gem-quality sanidine with disordered Al-Si in the tetrahedral framework to hydrothermally altered microcline with ordered Al-Si, several generations of exsolution lamellae and micropore-rich regions associated with domains of hydrothermal albitization. For each sample, (010) and (001) cleavage plates were mounted in a cold stage, and an array of 7 nl droplets of ultra-pure water was dispensed on the plates. In a second series of experiments, powder was produced from each sample, and a suspension was prepared from the 20–63 µm sieve fraction using ultra-pure water. Droplet arrays of the suspensions were placed on Si-wafers in the cold stage. For both series, a cooling rate of 2 K/min was applied, and droplet freezing was detected with an infrared camera.

Cleavage plate and suspension experiments show consistent results with the highest freezing temperatures for a hydrothermally altered and perthitic orthoclase and lowest for gem-quality sanidines. The (010) plates show higher freezing temperatures than the (001) plates, most pronounced in orthoclase (gem-quality as well as hydrothermally altered perthites). In our experiments, no correlation between ice nucleation activity and state of Al-Si-order was observed. The exceptionally good ice nucleation activity of alkali feldspars is mostly ascribed to pores along hydrothermally altered perthite lamellar interfaces.

ATKINSON, J.D., MURRAY, B.J., WOODHOUSE, M.T., WHALE, T.F., BAUSTIAN, K.J., CARSLAW, K.S., DOBBIE, S., O'SULLIVAN, D., MAKLIN, T.L. (2013): The importance of feldspar for ice nucleation by mineral dust in mixed-phase clouds. – Nature, 498, 355-358.

HARRISON, A.D., WHALE, T. F., CARPENTER, M.A., HOLDEN, M.A., NEVE, L., O'SULLIVAN, D., VERGARA TEMPRADO, J., MURRAY, B.J. (2016): Not all feldspars are equal: a survey of ice nucleating properties across the feldspar group of minerals – Atmos. Chem. Phys., 16, 10927–10940

PECKHAUS, A., KISELEV, A., HIRON, T., EBERT, M., LEISNER T. (2016): A comparative study of K-rich and Na/Ca-rich feldspar ice-nucleating particles in a nanoliter droplet freezing assay – Atmos. Chem. Phys., 16, 11477–11496.

REE mineralization at Koppamurra, South Australia: Insights into the transport, vertical and lateral distribution of REEs in a low-temperature environment

J. M. Hiller[1], S. Löhr[2], L. Morrissey[2], A. Baldermann[3], J. Payne[1], C. Doolette[1], C. Krapf[4], C. Spandler[2]

[1]University of South Australia, Australia
[2] University of Adelaide, Australia
[3]Graz University of Technology, Austria
[4]Geological Survey of South Australia, Australia
e-mail: jasmin.hiller@mymail.unisa.edu.au

The demand for rare earth elements (REE) is expected to increase in the near future, as new technologies develop and supply chain issues force countries to identify their own resources. Ion-absorption REE mineralisation is known from tropical weathering profiles developed on igneous rocks mainly in South China and Myanmar. Recent research by LÖHR et al. (2024) on the unusual ion-adsorption REE deposit at Koppamurra, South Australia, identified REE mineralization hosted in authigenic clays, secondarily formed carbonates, and cerianite, which acts as a Ce sink. This deposit has formed above a marine limestone unit and thus lacks an underlying REE-rich protolith, and it has not experienced tropical weathering conditions, which contrast common ion-adsorption REE deposits. Instead, the mineralization is proposed to have formed through rapid (< 2 Ma), pedogenic weathering-induced redistribution of REEs within lacustrine sedimentary material.

Our research provides new insights into the spatial and lateral distribution of REE in the Koppamurra deposit and their controlling factors in the low-temperature environment. In addition, we show that REE-rich horizons are predominantly associated with neo-formed smectitic clays (Fe-smectite or nontronite-like) and secondary carbonates. Steep pH gradients within the weathering profile exert a significant control on the immobilisation of REE. Our new data provides additional constraints on the availability and origin of REEs in Koppamurra.

LÖHR, S. C., SPANDLER, C., BALDERMANN, A. (2024): Controls on rapid rare earth element enrichment in sediments deposited by a continental-scale river system - Geochim Cosmochim Acta, 366, 48-64.

Allophanes in periglacial environments: A comparison of experimental and natural precipitation mechanisms

L. T. Huber[1], F. M. Stamm[1], P. J. Frings[2], A. Baldermann[1], M. Pettauer[1], C. Kohler[3], T. Wagner[3], G. Winkler[3], D. Hippler[1], M. Dietzel[1]

[1]Institute of Applied Geosciences, Graz University of Technology, Austria
[2]Earth Surface Geochemistry, GFZ German Research Centre for Geosciences, Germany
[3]Department of Earth Sciences, University of Graz, Austria
e-mail: laura.huber@tugraz.at

Active rock glaciers and permafrost ice in the Austrian Alps are increasingly affected by global climate warming. In recent years, enhanced acid rock drainage has been observed at springs and streams emerging from these systems, likely triggered by intensified bedrock weathering processes, such as sulfide oxidation and the hydrolysis of silicate minerals. The mixing of such acidic waters (pH < 5) with adjacent streams of near-neutral pH induces the formation of whitish precipitates within the streambeds. These precipitates have been identified as short range ordered hydroxy-aluminosilicates (SRO-HAS, i.e., allophane-like clay minerals). While their formation under ambient conditions has been addressed in recent literature (e.g., BALERDMANN et al. 2024), the mechanisms governing their development under low-temperature conditions (< 15 °C) remain insufficiently understood.

This study examines the formation of SRO-HAS, and the associated silicon isotope fractionation under low-temperature conditions by comparing batch experiment data with natural samples from two sites in the Austrian Alps. The experimental results reveal a three-stage precipitation process: (1) rapid formation of a proto-SRO-HAS phase, (2) near-complete re-dissolution of the proto-phase, and (3) subsequent slower re-precipitation of SRO-HAS. The kinetics were found to be markedly slower than those observed for comparable experiments conducted at 25 °C. Silicon isotope analyses of the reactive solutions indicate a pronounced silicon isotope fractionation, with $\Delta^{30}Si_{SRO\text{-}HAS\text{-}aq}$ values reaching as low as –2.82 ‰, consistent with preferential incorporation of the lighter isotope ^{28}Si into the solid phase. Field data from meltwater streams show the $\delta^{30}Si$ values are significantly heavier (i.e., $+0.91 \pm 0.10$ ‰ to $+1.88 \pm 0.16$ ‰) than those of the local bedrock ($\delta^{30}Si \approx -0.36 \pm 0.20$ ‰). This finding supports the interpretation that mineral precipitation processes, particularly the formation of SRO-HAS, are responsible for the removal of light ^{28}Si isotopes from the solution. We conclude that silicon isotope signatures of SRO-HAS may (1) serve as an effective tracer for ongoing mineral formation and (2) provide valuable insights into climate-driven changes in water–rock interaction in alpine permafrost environments.

BALDERMANN, A., STAMM, F.M., FARKAŠ, J., LÖHR, S., RATZ, B., LETOFSKY-PAPST, I., DIETZEL, M. (2024): Precipitation of short-range order hydroxy aluminosilicate (HAS) and hydrous ferric silicate (HFS) at ambient temperature: Insights into mineral formation pathways, crystal chemistry and solubility-stability relationships. – Chem Geol, 646, 121911.

Over 200 Myr of igneous history in the Eastern Tauern Window (Austria)

B. Huet[1], C. Költringer[1], C. Iglseder[1], D. A. Schneider[2]

[1]Division of Basic Geological Services, GeoSphere Austria, Vienna, Austria,
[2]Department of Earth and Environmental Sciences, University of Ottawa, Canada,
e-mail: benjamin.huet@geosphere.at

Two types of orthogneiss occur in the Tauern Window (Austria, Italy): (1) large intrusive bodies were emplaced during and shortly after the Variscan Orogeny, discordantly overlain by Permian and Mesozoic sediments and overprinted during the Alpine Orogeny. They are collectively termed "Zentralgneis" and occur in the Venediger Nappe System. (2) Relatively small bodies derived from intrusions or volcanic deposits of Ediacaran to Triassic age. These are often highly deformed and in contact with Permian to Cretaceous metasediments and occur in the Modereck Nappe System. Contrary to the Western Tauern Window where the age of orthogneisses is well constrained, robust modern data do not exist for the Eastern Tauern Window. In this contribution, we present preliminary LA-ICPMS U-Pb zircon age data of three "Zentralgneis" and two small orthogneiss bodies. These data were acquired in course of a mapping project at GeoSphere Austria.

The Sonnblick Orthogneiss is a fine- to coarse-grained and light grey "Zentralgneis" derived from granites. It is characterized by porphyritic structure and/or K-feldspar porphyroclasts, igneous biotite partly to fully replaced by metamorphic muscovite, abundant titanite and allanite rimed by metamorphic epidote. Two coarse-grained samples yielded ages of 363 ± 1 Ma (basis of the Sonnblick mountain) and 310 ± 1 Ma (Kleinfleiß valley). A fine-grained Sonnblick-Orthogneiss sample yielded an age of 308 ± 2 Ma (Hoher Sonnblick).

The Siglitz Orthogneiss is a fine-grained and medium grey "Zentralgneis" derived from granites and granodiorites. It is characterized by rounded albite porphyroblasts, igneous biotite partly to fully replaced by metamorphic muscovite and allanite rimed by metamorphic epidote. The analysed sample yielded an age of 333 ± 2 Ma, which is constrained by a few concordant analyses, while most of the measured U-Pb dates are strongly discordant.

The Romate Orthogneiss is a coarse grained and patchy "Zentralgneis", derived from monzonites and syenites. It is characterized by biotite-epidote aggregates pseudomorphing igneous hornblende in a K-feldspar matrix and aggregates of partly metamict zircon up to 500 µm. The analysed sample yielded only discordant ages with a poorly constrained Variscan to post-Variscan lower intercept.

The Trögereck Orthogneiss is fine-grained and (ultra)mylonitic. It appears as two lithologies: a white felsic orthogneiss with abundant large greenish white mica and a grey, biotite- and albite-rich mafic orthogneiss. Two samples from near the Trögereckalm yielded ages of 283 ± 1 Ma (felsic orthogneiss) and 318 ± 1 Ma (mafic orthogneiss).

The Edwein Orthogneiss is fine-grained, (ultra)mylonitic and derived from rhyolites and dacites. A dominant light greenish type with white mica, biotite, epidote and garnet contains dark layers of biotite-rich type. Two samples of the felsic orthogneiss from near the Edweinalm yielded ages of 496 ± 1 Ma and 497 ±1 Ma.

The preliminary age data provide correlations across the Tauern Window that confirm the existing classification based on field relationships and geochemistry. They also show that units like the Sonnblick Orthogneiss or the Trögereck Orthogneiss consist of different unmapped bodies separated by several 10's of million years. Finally, the similarity between ages of large orthogneiss from the Venediger Nappe System and small and highly deformed bodies from the Modereck Nappe System validates the hypothesis that the latter mostly derive from sheared parts of the former.

Bromine partitioning between olivine, orthopyroxene and silicate melt at MORB and OIB source conditions

B. Joachim-Mrosko[1], P.L. Clay[2], A. Pawley[3], R. Burgess[3], C. J. Ballentine[4], H. Busemann[5]

[1]Institute of Mineralogy and Petrography, University of Innsbruck
[2]Department of Earth & Environmental Sciences, University of Ottawa,
[3]Department of Earth and Environmental Sciences, The University of Manchester
[4]Department of Earth Sciences, University of Oxford
[5]Institute of Geochemistry and Petrology, ETH Z□rich
Email: bastian.joachim@uibk.ac.at

Heavy halogens, particularly bromine (Br) and iodine, are highly incompatible in mantle minerals, making them important tracers for understanding volatile transport processes within the Earth's mantle. However, their budget and distribution remain poorly constrained due to their extremely low concentrations in major upper mantle minerals and the absence of well-defined partition coefficients that describe their behavior during partial melting in mid-ocean ridge basalt (MORB) and ocean island basalt (OIB) source regions.

To address these uncertainties, we performed high-pressure, high-temperature experiments at 1.0 and 2.3 GPa and 1573□1873 K to simulate partial melting of an Fe-free peridotite analogue doped with Cl and Br. The experimental run products consisted of olivine and/or orthopyroxene embedded in quenched silicate melt. Since Br concentrations in these minerals are expected to be well below 1 ppm, conventional analytical techniques are insufficient for direct quantification. To overcome this limitation, we utilized neutron-irradiation noble gas mass spectrometry (NI-NGMS) combined with UV-laser ablation, enabling for the first time the precise measurement of trace Br in individual nominally anhydrous minerals.

Our results confirm the strong incompatibility of Br, with partition coefficients between olivine/orthopyroxene and silicate melt well below 10^{-3} at MORB and OIB source conditions. For example, we determined $D_{Br}^{fo/melt} = (4.5 \pm 1.6) \times 10^{-4}$ at 1773 K and 1 GPa, and $D_{Br}^{opx/melt} = (1.3 \pm 1.0) \times 10^{-5}$ at 1873 K and 2.3 GPa.

These findings, combined with additional consideration of modal abundances, suggest that olivine is potentially the primary Br carrier in the Earth's upper mantle, while orthopyroxene plays only a minor role. By combining our experimentally determined partition coefficients with existing Br bulk rock concentrations in MORBs and OIBs (KENDRICK et al. 2017), we can estimate Br concentrations in their respective mantle source regions. Our findings indicate that Br is significantly depleted in HIMU and high $^3He/^4He$ OIB sources compared to primitive mantle estimates. This depletion suggests that Earth's mantle experienced early and efficient heavy halogen loss to surface reservoirs. Consequently, the results of this study provide new insights into the geochemical evolution of halogens in the mantle and their role in volatile cycling between Earth's interior and surface.

KENDRICK, M. (2017): Seawater cycled throughout Earth□s mantle in partially serpentinized lithosphere. Nature Geoscience, 10, 222-228.

"Hopmannite" $Ba_2(Ti_5Fe)O_{13}$ – a potentially new mineral from the Bellerberg volcano, Germany

R. Juroszek[1], B. Krüger [2], G. Cametti[3], B. Marciniak-Maliszewska[4], Ch. Schäfer[5]

[1]Institute of Earth Sciences, University of Silesia, Katowice, Poland,
[2]Institute of Mineralogy and Petrography, University of Innsbruck, Innsbruck, Austria
[3]Institute of Geological Sciences, University of Bern, Bern, Switzerland
[4]Faculty of Geology, University of Warsaw, Poland
[5]Untereisesheim, Germany
e-mail: rafal.juroszek@us.edu.pl

A potentially new mineral "hopmannite", with the ideal formula $Ba_2(Ti_5Fe)O_{13}$, was discovered in a xenolith sample from an active quarry located in the southern lava flow of the Bellerberg volcano, Seekante district (50˚20'21"N; 7˚14'37"E), in the Eastern Eifel region, Germany. In the analysed xenolith, "hopmannite" occurs as crystals embedded among rock-forming minerals or within small fractures near low-temperature minerals. The mineral typically forms isolated, thin prismatic to platy crystals, up to 30 μm thick and 50 to 250 μm in length. "Hopmannite" is opaque in reflected light and exhibits a black colour with a submetallic lustre. The empirical formula, calculated based on 8 cations and 13 anions, is $(Ba_{1.00}K_{0.61}Na_{0.24}Sr_{0.08}Ca_{0.04})_{\Sigma 1.97}(Ti_{5.36}Fe^{2+}_{0.48}Fe^{3+}_{0.13}Mg_{0.06})_{\Sigma 6.03}O_{13}$.

The crystal structure of "hopmannite" was solved by direct methods using single-crystal X-ray diffraction data. It crystallizes in the monoclinic system (space group *C*2/*m*) with the following unit-cell parameters: a = 15.357(2) Å, b = 3.8500(7) Å, c = 9.129(2) Å, V = 533.03(17) Å^3, β = 99.030(10)°, Z = 2. The structure consists of linear units, which are composed of three distorted Ti-centred octahedra sharing edges in a single plane. These units repeat itself through edge-sharing along the *b*-axis, forming an infinite zig-zag band (Fig. 1). Adjacent bands are further connected via the corners of terminal Ti-octahedra, producing an open octahedral framework that encloses tunnels. These tunnels accommodate Ba/K/Na ions in eightfold coordination.

The presence of "hopmannite" alongside other Ba-bearing minerals identified in the analysed sample, such as fresnoite and batisite, suggests that they formed during the late crystallization sequence at temperatures below 1000˚C.

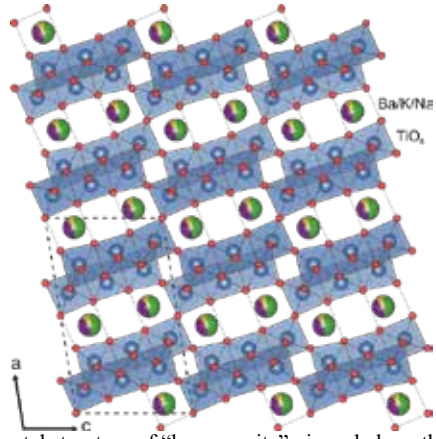

Figure 1: The crystal structure of "hopmannite" viewed along the b-axis.

The project is co-financed by the Polish National Agency for Academic Exchange BPN/BAT/2023/1/00019/U/00001 and OeAD Project: Scientific & Technological Cooperation Austria-Poland Project PL 11/2024.

Pre-Alpine evolution of Austroalpine basement units: new data from metapelites and metagranitoids from the Seckau Complex

K. Karner-Rühl[1], W. Kurz[1], C. A. Hauzenberger[1], H. Fritz[1]

[1]Department of Earth Sciences, NAWI Graz Geocenter, University of Graz, Graz, Austria, e-mail: kevin.karner-ruehl@uni-graz.at

Pre-Alpine basement units that originated along the northern margin of Gondwana were incorporated into the Austroalpine Nappe System during Alpine nappe stacking. While many of these units experienced substantial Alpine overprinting, others underwent only low-grade metamorphism, thereby preserving crucial records of their pre-Alpine evolution. The Seckau Complex, part of the Silvretta-Seckau Nappe System, was affected by greenschist-facies metamorphism during the Eo-Alpine event but retains mineral assemblages indicative of Variscan and possibly even pre-Variscan metamorphic processes. To better constrain the pre-Alpine metamorphic evolution of the Eastern Alps, this study integrates petrological, geochronological, geochemical, and geothermobarometric methods, with a particular focus on the metapelitic and magmatic sections of the Silvretta-Seckau Nappe System.

The Seckau Complex includes a variety of metagranitoids, notably the Late Cambrian to Early Ordovician Hochreichart Plutonic Suite and the Late Devonian to Early Carboniferous Hintertal Plutonic Suite. These intrusions are hosted by the Glaneck Metamorphic Suite, mainly composed of garnet-bearing paragneiss and micaschist but also amphibolite. U-Pb zircon dating reveals a detrital age spectrum, but one migmatized paragneiss yielded an age of 505 Ma, suggesting a pre-Variscan metamorphic event (MANDL et al. 2018). Several metapelitic samples exhibit a two-stage garnet growth, characterized by higher grossular content towards the rim, indicating a second metamorphic event. Geothermobarometry and thermodynamic modelling suggest initial garnet nucleation at ~550 °C and 0.4–0.5 GPa, with rim formation at 570–620 °C and 1.1–1.2 GPa, the latter representing typical conditions for Eo-alpine metamorphism. Zr-in-rutile thermometry yields consistent temperatures of approx. 600 °C. Monazite dating by EPMA of garnet-bearing micaschists from the Eisenpass area yields a young Eo-Alpine age, suggesting either that the basement was affected by Eo-Alpine metamorphism, or that the locality of Eisenpass is not a part of the Silvretta-Seckau-Nappe System but of the adjacent Koralpe-Wölz-Nappe System. U-Pb zircon dating of metagranitoids from the localities of Tremmelberg and Ortnerhof reveals Late Cambrian to Early Ordovician weighted mean ages of 491.6 ± 3 Ma and 485.1 ± 3 Ma, respectively, indicating an affiliation with the Hochreichart Plutonic Suite. However, an additional sample from the locality of Ortnerhof shows an Early Carboniferous mean age of 357.4 ± 1.2 Ma, corresponding to the Hintertal Plutonic Suite. One sample from the locality of St. Michael shows a Middle Ordovician mean age of 465.1 ± 4.6 Ma and a metagranitoid from the central part of the Gleinalpe region yields a Late Permian mean age of 256.9 ± 1.5 Ma.

Garnet-bearing amphibolites display homogeneous garnet compositions with minor spessartine enrichment towards the core, indicating prograde garnet growth. Peak metamorphic conditions derived from geothermobarometry and thermodynamic modelling reach ~620 °C and 0.7–0.8 GPa, again consistent with Zr-in-rutile temperatures of 600–620 °C. Geochemical analyses of these metabasites define a tholeiitic differentiation trend, derived from basaltic to andesitic protoliths. Trace element data indicate affinities to both, mid-ocean ridge basalts (MORB) and within-plate lava sources.

MANDL, M., KURZ, W., HAUZENBERGER, C., FRITZ, H., KLÖTZLI, U., SCHUSTER, R. (2018): Pre-Alpine evolution of the Seckau Complex (Austroalpine basement/Eastern Alps): Constraints from in-situ LA-ICP-MS U–Pb zircon geochronology. – Lithos, 296–299, 412–430.

Eclogite-facies metamorphism in the Speik Complex (Eastern Alps): tracing Early Devonian oceanic subduction in the Austroalpine domain

K. Karner-Rühl[1], C. A. Hauzenberger[1], W. Kurz[1], H. Fritz[1], D. Gallhofer[1], R. Schuster[2], H. Mali[3]

[1]Department of Earth Sciences, NAWI Graz Geocenter, University of Graz, Graz, Austria,
[2]GeoSphere Austria, Vienna, Austria,
[3]Chair of Geology and Economic Geology, Montanuniversität Leoben, Leoben, Austria,
e-mail: kevin.karner-ruehl@uni-graz.at

The Speik Complex, an ophiolitic unit predominantly exposed in the Gleinalpe region of the Eastern Alps, is part of the Austroalpine Silvretta-Seckau Nappe System. Comprising primarily basic and ultrabasic lithologies, the complex provides critical insights into the pre-Alpine evolution of the Eastern Alps. This study integrates petrological data, geothermobarometry, thermodynamic modelling and geochronological analyses to reconstruct the pressure-temperature-time (P-T-t) path of the Speik Complex and to constrain its tectono-metamorphic history.

Structurally, the Speik Complex forms an east–west trending belt within the Gleinalpe and Stubalpe area and a southeast-northwest trending zone along the southern border of the Seckauer Tauern. While isolated serpentinite bodies are also present east of the Mur Valley, the largest ultramafic exposures occur near the villages of Traföß and Kraubath and at Hochgrößen mountain. The Speik Complex comprises variably serpentinized ultrabasic rocks, (garnet-)amphibolite with rare eclogite and subordinate amounts of gneiss and marble. Eclogites from two localities in the Gleinalpe area exhibit characteristic mineral assemblages including garnet, clinopyroxene/omphacite, amphibole, zoisite, rutile, and quartz. Most of the garnets display homogeneous compositions with spessartine richer cores. However, some garnets show a two-stage growth pattern identified by increased grossular (Grs28–38) and almandine (Alm10–26) components at the rim. Geothermobarometric calculations and thermodynamic modelling indicate peak metamorphic conditions of approximately 600–620 °C at 1.5–1.7 GPa. Whole-rock geochemical analyses of eclogite and garnet-bearing amphibolite reveal a tholeiitic differentiation trend, derived from basaltic to andesitic protoliths. Trace element patterns indicate a mid-ocean ridge basalt (MORB) affinity, supporting an oceanic origin. U-Pb zircon dating of a coarse-grained amphibolite intruding massive serpentinite in the Preg quarry near the village of Kraubath yields Early Devonian weighted mean ages of 395 ± 1.5 Ma, 403 ± 3 Ma and 403.1 ± 2.5 Ma, respectively. These results align closely with the previously published $^{40}Ar/^{39}Ar$ amphibole cooling age of 397.3 ± 7.8 Ma from eclogitic relics at Hochgrößen (FARYAD et al. 2002). Additionally, Sm-Nd whole-rock-garnet isochron dating of garnet-bearing amphibolites in the vicinity of exposed eclogites yields ages of 406 ± 4 Ma and 413 ± 5 Ma. Metagranitoids from the same area provide Late Cambrian weighted mean zircon ages of 493.3 ± 2.8 Ma and 503.2 ± 1.6 Ma, likely associated with the emplacement of the Hochreichart Plutonic Suite (MANDL et al. 2018). Our data suggest, that the Speik Complex represents remnants of oceanic lithosphere and marks a suture zone that developed during the Early Devonian, preceding the Variscan continental collision.

FARYAD, S. W., MELCHER, F., HOINKES, G., PUHL, J., MEISEL, T., FRANK, W. (2002): Relics of eclogite facies metamorphism in the Austroalpine basement, Hochgrössen (Speik complex), Austria. – Mineral Petrol, 74(1), 49–73.

MANDL, M., KURZ, W., HAUZENBERGER, C., FRITZ, H., KLÖTZLI, U., SCHUSTER, R. (2018): Pre-Alpine evolution of the Seckau Complex (Austroalpine basement/Eastern Alps): Constraints from in-situ LA-ICP-MS U–Pb zircon geochronology. – Lithos, 296–299, 412–430.

Unravelling magmatic-hydrothermal processes by mineral micro-analysis

M. Keith[1]

[1]*Friedrich-Alexander-Universität Erlangen-Nürnberg (FAU), GeoZentrum Nordbayern, Erlangen, Germany*
e-mail: manuel.keith@fau.de

Critical metals are rare in the Earth's crust and positive anomalies of these elements only occur in geographically restricted areas. The wide economic application of these elements in electronics and renewable energies gives them a strategic importance, but the supply of these critical and energy critical elements is a growing challenge. Accumulations of critical metals in the form of ore deposits are the result of a complex interplay of magmatic and hydrothermal processes that occur from the nano- to the plate tectonic-scale, and which are often not well constrained (RICHARDS 2022; BÖRNER et al. 2023). Hence, it is important to develop new models with respect to metal sourcing, fractionation and precipitation to better define the magmatic-hydrothermal prerequisites that allow an enrichment of these rare commodities in the Earth's crust. Mineral micro-analysis is often used to study the elemental and isotopic composition of ore minerals to constrain the sources of metals, their fractionation behaviour during magmatic-hydrothermal processes and their final deposition and localized enrichment in ore deposits. It further represents an efficient tool to investigate the incorporation of trace metals into ore minerals, i.e., within the crystal lattice by solid solution or through mineral inclusions (KEITH et al., 2018), which is important for their recovery during ore the processing. The main challenge in using in-situ analytical techniques is to link micro-scale observations and data to processes that occur on the scale of ore deposits, metallogenic belts or even plate boundaries (FALKENBERG et al. 2024). In my contribution, I will introduce a scientific work flow that allows to achieve these research objectives. On this basis, I will present some of the recent advances in mineral micro-analysis that contribute to a better understanding of magmatic-hydrothermal processes in the Earth's crust. This will include active seafloor hydrothermal systems that provide the unique opportunity to sample hydrothermal fluids alongside their sulphide precipitates in a well constrained genetic context. This ultimately helps to better define the formation conditions of volcanogenic massive sulphide deposits in the geological record, which in combination allows to understand submarine ore-forming processes through space and time. I will also show that a continuum exists from submarine hydrothermal to subaerial epithermal systems that may be linked to deeper porphyry environments, where large ore deposits may form, if magmatic-hydrothermal activity occurs over longer time-scales. In summary, I will demonstrate how the geochemical signature of ore minerals may be used in exploration as a vectoring tool towards high-grade mineralisation, or to constrain fluid sources, fractionation processes or metallogenic trends in terranes with a complex geological history.

BÖRNER, F., KEITH, M., FOUGEROURSE, D., MACAULEY, C., FELFER, P., YOKOSAWA, T., APELEO ZUBIRI, B., SPIEKER, E. (2023): Between defects and inclusions: The fate of tellurium in pyrite. – Chem. Geol., 635, 121633.

FALKENBERG, J.J., KEITH, M., HAASE, K.M., KLEMD, R., KUTZSCHBACH, M., GROSCHE, A., SCICCHITANO, M.R., STRAUSS, H., KIM, J. (2024): Pyrite trace element proxies for magmatic volatile influx in submarine subduction-related hydrothermal systems. – Geochim. Cosmochim. Acta, 373, 52-67.

KEITH, M., SMITH, D.J., JENKIN, G.R.T., HOLWELL, D.A., DYE, M.D. (2018): A review of Te and Se systematics in hydrothermal pyrite from precious metal deposits: Insights into ore-forming processes. – Ore Geol. Rev., 96, 269-282.

RICHARDS, J.P. (2022): Porphyry copper deposit formation in arcs: What are the odds? – Geosphere, 18, 130-155.

Probing and engineering magnetism in phyllosilicates

M.Z. Khan[1], S. Leitner[1], D. Tizic Matković[1], A. Matković[1]

[1]Chair of Physics, Department Physics, Mechanics and Electrical Engineering, Montanuniversität Leoben, Leoben, Austria
[2]Chair of Resource Mineralogy, Montanuniversität Leoben, Leoben, Austria
email: muhammad.khan@unileoben.ac.at

The discovery of graphene (NOVOSELOV et al. 2004) sparked interest in two-dimensional van der Waals materials, including 2D magnetic materials which offer new avenues for studying low-dimensional magnetism and spintronic applications. Since the experimental observation of intrinsic magnetism in thin films, the catalogue of 2D magnetic materials has grown substantially. Various external strategies, such as chemical doping, defects, and strain engineering has been used to induce magnetic ordering. Although several 2D magnetic materials exhibit intrinsic magnetism at finite temperatures, their lack of ambient stability poses significant challenges for their incorporation into future devices. Naturally occurring 2D materials such as phyllosilicates provide stable, layered structures and high magnetic ion concentrations, making them attractive alternatives (MATKOVIĆ et al. 2021; KHAN et al. 2023).

We will provide an overview on both the intrinsic and engineered magnetism in phyllosilicates (Fig. 1). First, we investigate magnetic domain formation in monolayers of annite. Using scanning superconducting quantum interference device microscopy (SSM) with ~50 nm resolution, we directly visualize magnetic ordering and domain structure. Further, we extend our investigation to engineer magnetic order in non-magnetic phyllosilicates using broad-beam Fe ion implantation. We start from talc as a host matrix, and through ion implantation achieve substitution of Mg by Fe in octahedral sites. The modified talc exhibits room-temperature ferromagnetism, establishing a route toward the controlled synthesis of tunable 2D magnetic materials.

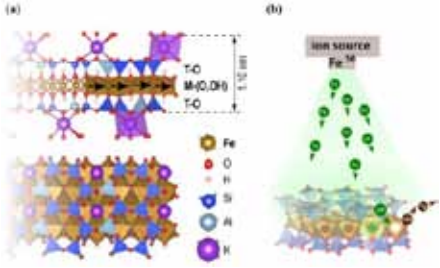

Figure 1: (a) Side and top views of the relaxed annite monolayer structure obtained from ab-initio calculations. Arrows represent the local magnetic moments of Fe atoms located at the central octahedral M–(O,OH) sites within the monolayer. (b) Schematic illustration of Fe ion-implantation in talc lattice

We acknowledge the supported by the Austrian Science Fund (FWF) under 2020 START programme (grant no. Y1298-N), and the support by the ERC Starting grant POL_2D_PHYSICS (101075821).

NOVOSELOV, K.S., GEIM, A.K., MOROZOV, S.V., JIANG, D.E., ZHANG, Y., DUBONOS, S.V., GRIGORIEVA, I.V., FIRSOV, A.A. (2004): Electric field effect in atomically thin carbon films. – Science, 306, 666-669.

MATKOVIĆ, A., LUDESCHER, L., PEIL, O.E., SHARMA, A., GRADWOHL, K.P., KRATZER, M., ZIMMERMANN, M., GENSER, J., KNEZ, D., FISSLTHALER, E., GAMMER, C. et al. (2021): Iron-rich talc as air-stable platform for magnetic two-dimensional materials. – npj 2D Material Appl, 5, 94.

KHAN, M.Z., PEIL, O.E., SHARMA, A., SELYSHCHEV, O., VALENCIA, S., KRONAST, F., ZIMMERMANN, M., ASLAM, M.A., RAITH, J.G., TEICHERT, C., ZAHN, D.R. (2023): Probing magnetic ordering in air stable iron-rich van der Waals minerals. – Adv Phys Res, 2, 2300070.

Phyllosilicates: naturally occurring 2D insulators

M. Z. Khan[1], S. Leitner[1], L. F. Almeida[1], D. Tizic Matkovic[2], O. E. Peil[3], A. Matkovic[1*]

[1]Chair of Physics, Department Physics, Mechanics and Electrical Engineering, Montanuniversität Leoben, Austria
[2]Chair of Resource Mineralogy, Montanuniversität Leoben, Austria,
[3]Group of computational materials design, Materials Center Leoben Forschung GmbH, Austria,
e-mail: Aleksandar.matkovic@unileoben.ac.at

In the past decade, two-dimensional (2D) materials have rapidly expanded, though research mostly focuses on synthetic single crystals from a few material classes. Naturally occurring van der Waals (vdW) crystals offer greater structural and chemical diversity but remain underexplored (FRISENDA et al. 2020). Using non-toxic, abundant surface minerals from soils and clays could enable sustainable and biodegradable electronics. Recently, the focus of 2D electronics has largely been on novel semiconductors and spontaneously polarized materials. However, the number of van der Waals (vdW) insulators is extremely disproportionate to both semiconductors and metals. The entire field almost exclusively relies on hexagonal boron nitride. This cannot surely be the only technologically relevant system; new members would also open new pathways in device design and functionality. In this talk, we will provide an overview of the opportunities that 2D phyllosilicates offer to nanoelectronics and discuss recent activities in this area by our group (VASIC et al. 2021, MATOVIC et al. 2021), KHAN et al. 2023). We will focus on three aspects: their performance as dielectrics in transistor applications; their inherent magnetic properties; and their potential use as charge trap layers for memory transistors and neuromorphic electronics.

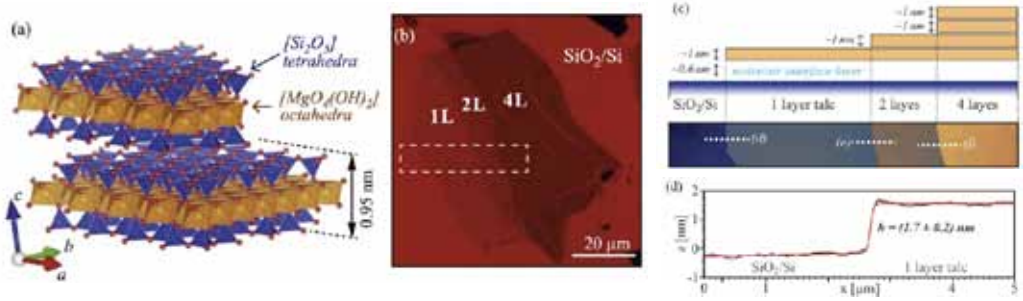

Figure 1**:** (a) Structure of talc (from ab initio calculations), (b) Optical micrograph of an exfoliated 2D talc crystal (L – number of monolayers), (c) Sketch of the cross-section and an atomic force microscopy (AFM) image of the area indicated by a dashed rectangle in (b), and (d) height profile (from the AFM image) of the mono-layer edge.

We acknowledge the supported by the Austrian Science Fund (FWF) under 2020 START programme (grant no. Y1298-N), and the support by the ERC Starting grant POL_2D_PHYSICS (101075821).

FRISENDA, R., NIU, Y., GANT, P., MUNOZ, M. and CASTELLANOS-GOMEZ, A. (2020): Naturally occurring van der Waals materials. npj 2D Materials and Applications, 4, 38.

VASIC, B., CZIBULA, C., KRATZER, M., NEVES, B.R., MATKOVIC, A., TEICHERT, C. (2021): Two-dimensional talc as a van der Waals material for solid lubrication at the nanoscale. Nanotechnology, 32, 265701.

MATKOVIC, A., LUDESCHER, L., PEIL, O.E., SHARMA, A., GRADWOHL, K.P., KRATZER, M., ZIMMERMANN, M., GENSER, J., KNEZ, D., FISSLTHALER, E., GAMMER, C., LUGSTEIN, A., BAKKER, R.J., ROMANER, L., ZAHN, D.R.T., HOFER, F., SALVAN, G., RAITH, J.G., TEICHERT, C. (2021): Iron-rich talc as air-stable platform for magnetic two-dimensional materials. npj 2D Materials and Applications, 5, 94.

KHAN, M.Z., PEIL, O.E., SHARMA, A., SELYSHCHEV, O., VALENCIA, S., KRONAST, F., ZIMMERMANN, M., ASLAM, M.A., RAITH, J.G., TEICHERT, C.ZAHN, D.R., SALVAN, G., MATKOVIC, A. (2023): Probing magnetic ordering in air stable iron-rich van der Waals minerals. Advanced Physics Research, 2, 2300070.

Petrology, textural evolution, mineral chemistry and CHIME U-Th-Pb dating of monazite along the Eoalpine metamorphic gradient in the Vinschgau Valley (Matsch Unit, Texel Unit, South Tyrol, Italy)

D. Klümper[1], P. Tropper[1], C. Morelli[2], V. Mair[2]

[1]Institute of Mineralogy and Petrography, University of Innsbruck, Innsbruck, Austria,
[2]Office of Geology and Materialtesting, Kardaun, Province Bozen, Italy,
e-mail: peter.tropper@uibk.ac.at

In this investigation, the petrology and mineral chemistry of monazite along the Eoalpine metamorphic gradient in the Vinschgau Valley (Matsch Unit, Texel Unit) were analyzed. In addition to the preparation of an analytical protocol for electron probe microanalysis (EPMA), Chemical Th-U-total Pb Isochron Method (CHIME) dating of monazite, the petrographic and mineral chemical investigation of monazite based on thin sections from the Matsch- and the Texel-Units is carried out, along with its correlation to the polymetamorphic history of the rocks along the increasing Eoalpine metamorphic gradient in the Vinschgau. The work aims to refine the tectonometamorphic history of the region by applying and optimizing advanced CHIME Th-U-Pb monazite dating techniques using EPMA, which allow a more precise temporal resolution of metamorphic events. A set of elements was chosen and their specific spectral interferences considered under the operating conditions of 20 kV accelerating voltage, 100 nA beam current and 5 µm beam diameter. Precise overlap corrections of interferences were evaluated. To improve the precision of age determination, efforts were being made to enhance the detection limit (D.L.) for lead. By extending the counting time from 80 to 600 seconds a 69.3 % reduction in the 2σ error was observed. The D.L. was improved by 63.4% with a counting time of 600 seconds compared to 100 seconds, and in contrast to the standard deviation (S.D.), the D.L. follows a negative exponential function rather than a linear one, indicating that the D.L. improvement slows as counting time increases. This finding shows that further D.L. optimization is analytically limited. Petrographic observations show increasing monazite breakdown to apatite and allanite within the Matsch Unit from the western sample AM81 to the more eastern sample LM112. In the easternmost sample of the Texel Unit SZ532, texturally older monazite is completely replaced by apatite and allanite, while tiny newly-grown monazites grew. The EPMA age dating of the monazites from the Matsch Unit samples resulted in two age groups: Variscan and Permian. The results indicate that younger Permo-Triassic ages dominate, particularly in cases where larger monazite grains allowed multiple individual measurements or appeared as inclusions within minerals such as staurolite. In contrast, older Variscan ages are sporadically observed in matrix-embedded grains or in monazites with identifiable reaction textures. Unfortunately, it was not possible to date the tiny newly-grown monazites in the Texel Unit sample due to their small grain size. The age values indicate a partial rejuvenation of the monazites during the Permian, indicating a possible thermal influence. Although the Variscan and Permian ages differ significantly, the chemical compositions of the two groups are remarkably similar. However, the Permian monazites show a slightly reduced concentration of rare-earth-elements (REE), especially Ce, Nd, Sm and La. The observation of U-Th exchange substitutions suggests a predominance of cheralite substitution over huttonite substitution. The increase of huttonite substitution from west (AM81) to east (LM112) could possibly indicate a prograde Permian metamorphic overprint within the Matsch Unit. This research demonstrates the utility of monazite as a reliable chronometer for tracing intricate metamorphic histories.

Rutile inclusions in garnet: simultaneous formation of host and inclusions

V. Kohn[1], T.A. Griffiths[2], R. Abart[2], G. Habler[3]

[1] Natural History Museum Vienna, Mineralogisch - Petrographische Abteilung, Vienna, Austria
[2] Department of Lithospheric Research, University of Vienna, Vienna, Austria
e-mail: victoriakohn@nhm.at

Since the pioneering work by GRIFFIN et al. (1971), the presence of needle-shaped rutile inclusions in garnet host crystals is often interpreted as a result of the precipitation from Ti-bearing garnet. However, further mechanisms of inclusion formation have been discussed. These include overgrowth of pre-existing rutile by garnet, and simultaneous growth of host and inclusion phases. As the interpretation of the relationships between the host and its inclusions will have a significant impact on the inferred history of the rock or lithological unit, it is of major importance to unequivocally determine the origin of the inclusions.

The investigated rutile-bearing almandine-spessartine garnet from the Moldanubian Zone from the Bohemian Massif, Austria, formed in three distinct growth stages during the fractional crystallization of a pegmatoid melt (KOHN et al., 2024b). During the first growth stage, the garnet core and an inner rim domain formed without significant changes in pressure and temperature conditions, as reflected by a gradual change of the major element composition across the core-rim boundary. In contrast, the microstructural change (size and habit) of rutile inclusions is significant: while the coloured garnet core bears equant rutile inclusions (80 - 200 nm), the uncoloured rim is dominated by needle-shaped rutile (<150 µm length, c. 200 nm width) with clear shape preferred orientations (SPOs).

These rutile needles are elongated along the four Grt⟨111⟩, the three Grt⟨100⟩ directions and one particular Grt⟨112⟩ direction. On the basis of a statistical dataset of the SPOs of elongated rutile inclusions in the uncoloured rim, and the geometrical relationship of individual SPOs with the particular garnet growth facet in which they occur, it was found that the most abundant rutile needles are those with an SPO closest to the garnet growth direction, whereas rutile inclusions with an SPO parallel to the garnet growth facet are absent. Therefore, we conclude that the growth direction of garnet has a selective effect on SPO frequencies and that the host and the rutile inclusions formed simultaneously (KOHN et al., 2024a).

Furthermore, the changes of the rutile inclusion habit from equant to acicular signals changes in the relative growth rates of garnet and rutile, as well as the nucleation rate of rutile, resulting from compositional changes (Na_2O and OH) during the fractional crystallization of the pegmatoid melt and according changes in the melt viscosity.

Consequently, inclusion microstructures, which have formed simultaneously with the host phase, have the capacity to document and preserve information regarding parameters to which the major garnet elements are not sensitive.

Funded by Austrian Science Fund (FWF): I4285-N37.

GRIFFIN et al (1971) Anomalously elongated rutile in eclogite-facies pyroxene garnet. Norsk Geologisk Tidsskrift, 51:177–185, 1971.

KONH, V. et al. (2024a) Variations in orientation relationships between rutile inclusions and garnet host relate to magmatic growth zoning. Contributions to Mineralogy and Petrology, 179, 69

KOHN, V. et al (2024b) Directed growth of a sector-zoned garnet in a pegmatoid from the Bohemian Massif, Austria. Lithos, 466–467, 107461

Introducing G.O.Joe: A new online tool for LA-ICP-MS data reduction

J. Krause[1], F. Altenberger[2], T. Auer[3], A. Auer[3], J. Berndt[4]

[1]Helmholtz Institute Freiberg for Resource Technology, Helmholtz-Zentrum Dresden-Rossendorf, Freiberg, Germany,
[2]Department of Applied Geosciences and Geophysics, Technical University of Leoben, Leoben, Austria
[3]Moonshot Pioneers GmbH, Dorfbeuern/Salzburg, Austria,
[4]Institute for Mineralogy, University of Münster, Münster, Germany,
e-mail: joachim.krause@hzdr.de

The coupling of laser ablation systems with inductively coupled plasma-mass spectrometers (LA-ICP-MS) was introduced in the 1980s. Since then, this technique has become indispensable for rapid in-situ trace element and isotopic analysis of both natural and synthetic solid samples. Its applications extend across various fields, including chemistry, materials science, geosciences, biological and environmental analysis, bio-imaging and forensic investigations. However, analytical advances are still needed to address challenges in trace element analysis using LA-ICP-MS, such as those caused by interferences.

The novel, non-commercial software tool G.O.Joe is designed to facilitate the calculation of trace element mass fractions in solid samples obtained by LA-ICP-MS analysis. It is written in the Dart programming language using the Flutter framework and operates entirely as a web-based application (i.e., no installation required). Since the data processing is performed on the user's computer, there is no need to upload data to the G.O.Joe-server, maximizing data security. In addition to enabling the quick and efficient processing of large datasets, G.O.Joe includes various optional interference corrections methods.

G.O.Joe's intuitive user interface simplifies the workflow during data evaluation, allowing for straightforward selections of peak- and background signals, importation of instrument settings, reference material compositions, and mass fractions of the internal standard to convert the measured raw signals into element mass fractions. Ensuring transparency in data processing, the results file (.xlsx) includes the calculated element mass fractions, associated statistical parameters as well as input data alongside instrument settings. Additionally, users can download a more comprehensive file containing the intermediate results of each calculation step. The software´s key advantages include implemented corrections for isobaric interferences and abundance sensitivity.

The capabilities of G.O.Joe are demonstrated through the processing of two case studies, including trace element analyses of tungstates (e.g., scheelite) and silicates (e.g., garnet). In conclusion, G.O.Joe is a time-efficient, transparent and easy-to-use software tool that appeals to both experienced LA-ICP-MS users as well as newcomers to LA-ICP-MS data analysis. More details and the latest version of G.O.Joe are available at the following link: https://www.gojoe.software.

Spinel-type crystals in municipal solid waste incineration bottom ashes

T. Kremlicka[1], P. Demschar[1], K. P. Sedlazeck[1]

[1]Chair of Waste Processing Technology and Waste Management, University of Leoben, Austria
e-mail: thomas.kremlicka@unileoben.ac.at

In Austria, wastes with an organic carbon content exceeding 5 wt.% must undergo pretreatment – such as incineration – prior to landfilling (BMLFUW, 2008). During grate incineration processes, temperatures can reach up to 1200 °C (GOHLKE & BUSCH, 2001). One of the residues of municipal solid waste incineration (MSWI) is bottom ash, which predominantly consists of glass, ceramics, slag, and both ferrous and non-ferrous metals (WILES, 1996). The crystalline phases present in MSWI bottom ash have been the subject of several studies, for example by EGGENBERGER et al. (2004). Spinel-type phases are among the most consistently identified phases, typically detected through powder X-ray diffraction.

In this study, MSWI bottom ashes from an Austrian incineration facility were subjected to chemical and mineralogical characterization. Total digestion followed by analysis using ICP-MS and ICP-OES revealed the presence of numerous elements known to be compatible with incorporation into spinel-type structures (BOSI, 2019). X-ray diffraction confirmed the presence of magnetite. Electron probe micro analysis revealed a noteworthy abundance of grains containing euhedral crystals of spinel-type phases (Fig. 1).

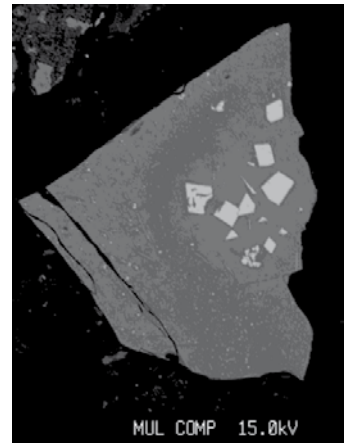

Figure 1: Backscattered electron image of a bottom ash grain containing large spinel-type crystals.

Chemical analysis was performed on 140 individual crystals using wavelength dispersive X-ray spectroscopy. Iron concentrations ranged from 53 to 96 wt.%. Aluminum and chromium contents reached approximately 30 wt.% each. Magnesium concentrations were as high as 11 wt.%, while titanium a maximum of about 6 wt.%. The concentrations of titanium, chromium, magnesium, and aluminum were all below the detection limits. Manganese was essentially absent, with a maximum concentration of 0.76 wt.%.

While bulk chemical analysis by ICP-MS revealed comparable concentrations of iron and aluminum at approximately 7 wt.%, the markedly higher iron content observed in EPMA measurements suggest that many of the analyzed crystals are likely magnetite or other iron bearing spine-type phases like hercynite and chromite.

BMLFUW (2008). Verordnung des Bundesministers für Land- und Forstwirtschaft, Umwelt und Wasserwirtschaft über Deponien: Deponieverordnung: DVO 2008.

BOSI, F. (2019). Chemical and structural variability in cubic spinel oxides. – Acta Cryst B, 75, 279–285.

EGGENBERGER, U., SCHENK, K., MÄDER, U. (2004). Chemistry and mineralogy of municipal solid waste incinerator bottom ash. – Geol Soc Lond, Spec Publ, 236, 411–422.

GOHLKE, O., BUSCH, M. (2001). Reduction of combustion by-products in WTE plants: O_2 enrichment of underfire air in the MARTIN SYNCOM process. – Chemosphere, 42, 545–550.

WILES, C. C. (1996). Municipal solid waste combustion ash: State-of-the-knowledge. – J Hazard Mater, 47, 325–344.

Golden fruits and blue-spotted panthers: first pigment investigations on the Roman "Amor and Psyche" sarcophagus in Vienna

R. Krickl[1], R. Linke[2], V. Pitthard[3], M. Mozdyniewicz[3], G. Kremer[1], G. Plattner[3]

[1]Österreichisches Archäologisches Institut / Österreichische Akademie der Wissenschaften, Vienna, Austria
[2]Bundesdenkmalamt, Vienna, Austria
[3]Kunsthistorisches Museum, Vienna, Austria
e-mail: robert.krickl@oeaw.ac.at

The very first historical object that people encounter when entering the *Kunsthistorisches Museum Vienna* through the side entrance facing the Vienna Ringstraße, is a Roman sarcophagus located to their left (*KHM* inv. no. I 162, Collection of Greek and Roman Antiquities). Found 1865 in the former Roman city of Sirmium (today Sremska Mitrovica, Serbia) it received its modern appellation after the prominent depictions of Amor and Psyche in two frontal panels. Though it was on display since the installation of the museum, we report the first material investigations that primarily focussed on the pigment application on the marble artefact (performed within the *Austrian Academy of Sciences Heritage Science Austria* project *PolychroMon* – cf. KRICKL et al. 2024). Non-invasive (multiband spectral imaging, digital microscopy, portable X-ray fluorescence analysis) and micro-invasive techniques (cross section analysis with optical and scanning electron microscopy, including gas chromatography – mass spectrometry for the identification of organic binders) provided evidence for a typical Roman colour palette comprising the pigments carbon black, Egyptian blue, yellow and red ochre and red lead. Furthermore, remnants of gold leaf were detected on yellow and red base layers at several iconographic features, most of all the hair of Amor and Psyche and the fruits associated to the leafed head in the pediment. Subtle traces of former polychromy that are not accessible to the naked eye, enable insights not only into the spatial allocation of colours to the iconographic elements but also into information only given by painting and not by sculpturing. The sarcophagus is identified as an outstanding example of preserved Roman provincial polychromy on stone objects, enriching our understanding of technical, aesthetic and socio-cultural dimensions of sarcophagi production in the former province of Pannonia.

Figure 1: Eye region of the leafed head in the pediment of the sarcophagus, as an example for knowledge gain on spatial pigment phase distributions – a) visible reflected light image, b) applied red ochre enhanced in deconvolution stretched lre-colourspace image, c) CoRL image showing the distribution of Egyptian blue as whitish areas (white scale bar = 1 cm).

KRICKL, R., KREMER, G., LINKE, R., PLATTNER, G., POLLHAMMER, E., SILNOVIC, N., BRZAKOVIC, M., STOSS, S. (2024): PolychroMon – Ein interdisziplinäres Projekt zur Polychromie römerzeitlicher Monumente der Donauprovinzen. – Mitt Österr Mineral Ges, 170, in print.

Two new djerfisherite-group minerals with charge-unbalanced formulas

B. Krüger[1*], I. O. Galuskina[2], E. V. Galuskin[2], H. Krüger[1], Ye. Vapnik[3]

[1]Institute of Mineralogy and Petrography, University of Innsbruck, Austria,
[2]Institute of Earth Sciences, Faculty of Natural Sciences, University of Silesia, Poland,
[3]Department of Geological and Environmental Sciences, Ben-Gurion University of the Negev, Israel,
e-mail: biljana.krueger@uibk.ac.at

Minerals of the djerfisherite group commonly display charge-imbalanced empirical formulas, often with a surplus of positive charge. This characteristic is exemplified by djerfisherite ($K_6Fe_{25}S_{26}Cl$), which shows a calculated charge imbalance of 56+ to 53−. We report the discovery of two new sulfide minerals in this group: zoharite, $(Ba,K)_6(Fe,Cu,Ni)_{25}S_{27}$, and gmalimite, $K_6\square Fe^{2+}_{24}S_{27}$, both exhibiting similar charge discrepancies (GALUSKINA et al. 2025).

These minerals were found in a gehlenite–wollastonite paralava with pyrrhotite nodules within the Hatrurim pyrometamorphic complex, Negev Desert, Israel. The occurrence and associated minerals suggest they formed at temperatures below 800 °C, where sulfides interacted with residual Ba- and K-enriched silicate melt (PATTEN et al. 2013)

Zoharite and gmalimite are isostructural with owensite, crystallizing in the cubic space group Pm-3m, with unit-cell parameters of a = 10.3137(1) Å and a = 10.3486(1) Å, respectively. Their structures are built from M_8S_{14} clusters, consisting of MS_4 tetrahedra surrounding central MS_6 octahedra (M = $Fe^{2+,3+}$, $Cu^{2+,1+}$, Ni), forming a dense cubic framework. The channels within this framework are occupied by anion-centered polyhedra: SBa_9 in zoharite and SK_9 in gmalimite. The close spacing of transition metals within M_8S_{14} clusters facilitates d-orbital overlap and metal–metal bonding, akin to the bonding environments in pentlandite.

Given the recurring presence of charge-imbalanced formulas and metal–metal interactions, we propose that members of the djerfisherite group, along with bartonite and pentlandite, represent a distinct class of sulfide minerals where the standard rules of electroneutrality may not apply when using formal valences in empirical formula calculations.

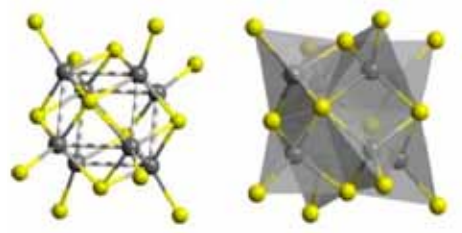

Figure 1: Clusters M_8S_{14}, with S atoms in yellow, and M atoms (M = $Fe^{2+,3+}$, $Cu^{2+,1+}$, Ni) in grey

GALUSKINA, I.O., KRÜGER, B., GALUSKIN, E.V., KRÜGER, H., VAPNIK, Y., MURASHKO, M., BANASIK, K., AGAKHANOV, A.A. (2025): Zoharite, $(Ba,K)_6(Fe,Cu,Ni)_{25}S_{27}$, and gmalimite, $K_6\square Fe^{2+}_{24}S_{27}$ – new djerfisherite group minerals from gehlenite-wollastonite paralava, Hatrurim Complex, Israel. Minerals, 15*(6)*, 564.

PATTEN, C., BARNES, S.-J., MATHEZ, E.A., JENNER, F.E. (2013): Partition coefficients of chalcophile elements between sulfide and silicate melts and the early crystallization history of sulfide liquid: LA-ICP-MS analysis of MORB sulfide droplets. Chem Geol, 358,170–188

The mineralogy and weathering of thallium-rich waste dumps of Crven Dol locality, Allchar deposit

N. Lammer[1], E. Libowitzky[1], T. Đorđević[1,2]

[1]Department of Mineralogy and Crystallography, University of Vienna, Vienna, Austria
[2]E057-02 USTEM, TU Wien, Vienna, Austria
e-mail: tamara.djordjevic@univie.ac.at

The Crven Dol area of the former Sb–As–Tl–Au Allchar mine (North Macedonia) contains large quantities of abandoned mine waste that is extremely rich in thallium (Tl) and arsenic (As). According to ĐORĐEVIĆ et al. (2021), these wastes often contain up to 142 g/kg of As and up to 18 g/kg of Tl, both of which are retained in primary sulfides and in newly formed secondary minerals resulting from the oxidative weathering of Tl-bearing metal sulfides. In addition to well-known secondary Tl minerals, many poorly- or nano-crystalline phases lack appropriate chemical and structural characterization. Therefore, we are working extensively to characterize various specimens containing these two pollutants. As part of the current study, we mineralogically characterized two weathered hand specimens (Allchar 1 and 2) using secondary electron microscopy with energy dispersive X-ray spectrometry (SEM-EDS), powder X-ray diffraction (PXRD), and Raman spectroscopy.

Macroscopically, Allchar 1 is a solidified technosol sediment ranging from dark grey to red in color, with yellow and white spots on the surface. It is brittle and porous, and the mineral phases are not distinguishable visually. It mainly contains clusters of realgar (As_4S_4) and pararealgar (As_4S_4); the latter is a product of weathering by sunlight and was also found inside the rock, not just on the surface. These clusters are found in a matrix of iron arsenates (mostly scorodite, $FeAsO_4{\cdot}2H_2O$), gypsum ($CaSO_4{\cdot}2H_2O$) and hydrogen iron oxides (HFOs), which have undergone zoned alteration of their main constituents due to oxidation, followed by adsorption and co-precipitation with iron minerals, organic matter and clays. In addition to realgar and pararealgar, the primary sulfides present include pyrite (FeS_2), marcasite (FeS_2), and Tl-sulfosalts such as lorándite ($TlAsS_2$), fangite (Tl_3AsS_4), ranguinite ($TlFeS_2$), and picotpaulite ($TlFe_2S_3$). Tl that is dissolved during weathering is predominantly precipitated as thallium pharmacosiderite ($TlFe_4[AsO_4(OH)_4]{\cdot}4H_2O$), which is either poorly crystalline or nano-crystalline.

Allchar 2 is a waste rock sample that exhibits clearer macroscopic features and simpler mineralogy. It has a white, glassy matrix with large yellow veins and scattered fine black veins. The dominant mineral is dolomite, the fractures of which were subsequently filled with orpiment (As_2S_3) and, to a lesser extent, pyrite and marcasite. Minor fangite grains have been observed as inclusions in the orpiment. The main weathering phase is arseniosiderite ($Ca_2Fe^{3+}{}_3(AsO_4)_3O_2{\cdot}3H_2O$), with minor amounts of gypsum present. Within the orpiment veins, ellisite (Tl_3AsS_3), a Tl mineral not previously reported in the deposit, crystallized.

The fate of the pharmacosiderite-group minerals with respect to their long-term stability, and thus the bioavailability of Tl at Allchar, is the subject of further investigation.

Financial support of the Austrian Science Fund (FWF) [P 36828-N] to T. Đorđević is gratefully acknowledged.

ĐORĐEVIĆ, T., DRAHOTA, P., KOLITSCH, U., MAJZLAN, ..., BOEV, B. (2021). Synergetic Tl and As retention in secondary minerals: An example of extreme arsenic and thallium pollution. – Appl Geochem, 135, 105114-150130.

Air-stable 2D magnets harvested from iron-rich talc minerals

A. Matković[1], M. Z. Khan[1], L. Ludescher[1], O. E. Peil[2], K-P. Gradwohl[1], M. Kratzer[1], M. Zimmermann[3], J. Genser[1], D. Knez[4], E. Fisslthaler[5], C. Gammer[6], R. J. Bakker[3], L. Romaner[2,7], F. Hofer[4,5], J. G. Raith[3], C. Teichert[1*]

[1]Chair of Physics, Montanuniversität Leoben, Austria,
[2]Materials Center Leoben Forschung GmbH (MCL), Austria,
[3]Chair of Resource Mineralogy, Montanuniversität Leoben, Austria,
[4]Institute of Electron Microscopy and Nanoanalysis (FELMI), Graz University of Technology, Austria,
[5]Graz Centre for Electron Microscopy (ZFE), Austria,
[6]Erich Schmid Institute of Materials Science, Austrian Academy of Sciences, Austria,
[7]Department of Materials Science, Montanuniversität Leoben, Austria,
e-mail: teichert@unileoben.ac.at

Since the first reports on intrinsically magnetic two-dimensional (2D) materials in 2017 (GONG et al. 2017; HUANG et al. 2017), the price-to-pay for accessing their monolayers is the lack of ambient stability and that magnetic ordering persists only at cryogenic temperatures.

We discovered in a mineral aggregate – mainly composed of hematite, magnetite, and chalcopyrite – soft layers of which macroscopic flakes easily could be peeled off that stuck to a permanent magnet. Employing mechanical exfoliation, we succeeded in thinning and transferring micrometer sized – mainly pseudohexagonally shaped – flakes to SiO_2 substrates. Energy dispersive x-ray spectroscopy (EDS) revealed magnesium and silica as major components of the flakes. Raman spectroscopy indicated the presence of hydroxide groups, pointing towards talc, a hydrated magnesium phyllosilicate mineral. Long-term EDS and Raman revealed that in the flakes about 10 % of the Mg atoms are substituted by Fe. With atomic force microscopy, a minimum flake thickness of 1 nm was determined indicating cleavage down to a talc monolayer. Combined magnetic force microscopy and superconducting quantum interference device magnetometry measurements imply that this 2D Fe-rich talc exhibits weak ferromagnetic behaviour at room temperature (MATKOVIĆ et al. 2021).

As convincingly demonstrated by electron diffraction, the Fe-rich flakes are also showing long-term stability under ambient conditions in contrast to the 2D magnets reported so far. Meanwhile, we also explored further 2D flakes from iron-rich phyllosilicates like minnesotaite, biotite, and annite (KHAN et al. 2023) with respect to their magnetic ordering.

GONG, C., et al., (2017): Discovery of intrinsic romagnetism in two-dimensional van der Waals crystals. – Nature, 546, 265–269.

HUANG, B., et al., (2017): Layer-dependent ferromagnetism in a van der Waals crystal down to the monolayer limit. – Nature, 546, 270–273.

MATKOVIĆ, A. et al., (2021): Iron-rich talc as air-stable platform for magnetic two-dimensional materials. – npj 2D Mat Appl, 5, 94-1-9.

KHAN, M.Z., et al., (2023): Probing magnetic ordering in air stable iron-rich van der Waals minerals. – Adv Physics Rev, 2, 2300070-1-13.

Lithium (Li) mineral characterization of drill cores and hand specimens: supporting exploration with rapid mineralogy mapping

A. H. Menzies[1], J. Ferreira[2], P. Avila[2], N. M. Kelly[3]

[1] Bruker Nano Analytics GmbH, Berlin, Germany
[2] Laboratório Nacional de Energia e Geologia, Porto, Portugal
[3] Bruker Nano Analytics, Denver, CO, USA
e-mail: andrew.menzies@bruker.com

Batteries are a key part of the energy transition. Lithium(Li)-ion batteries, due to their energy density, are currently the main source of compact energy storage in the market and will likely remain so for the foreseeable future. Lithium is currently regarded as a "critical mineral" both for central role in rapidly developing electric technologies and a predicted shortfall in production versus expected demand. Therefore, identification of new resources is both economically and strategically important, driving a boom in Li exploration.

Like other metals, exploration for hard-rock lithium resources faces the challenge of how to bridge scales and dimensions of observations, from field-scale (in 3D-4D) down to laboratory-based imaging and analysis (3D-2D). Moreover, the ability to identify and accurately characterize Li mineralogy is critical to evaluate the potential economics of a deposit, including the required mineral processing to extract the Li resource. Combined micro-XRF and Automated Mineralogy (AMICS) is capable of high-speed analysis at the micrometer scale that can identify a wide range of Li mineralogy non-destructively in minimally prepared drill core samples, providing valuable, rapid turn-around information early in exploration. This case study will present mineral characterization from potential lithium resources in Portugal. Preliminary results suggest significant added value of the micro-XRF approach, where a much-improved mineral-textural understanding aids exploration, future processing needs, and ongoing evaluation of deposit potential.

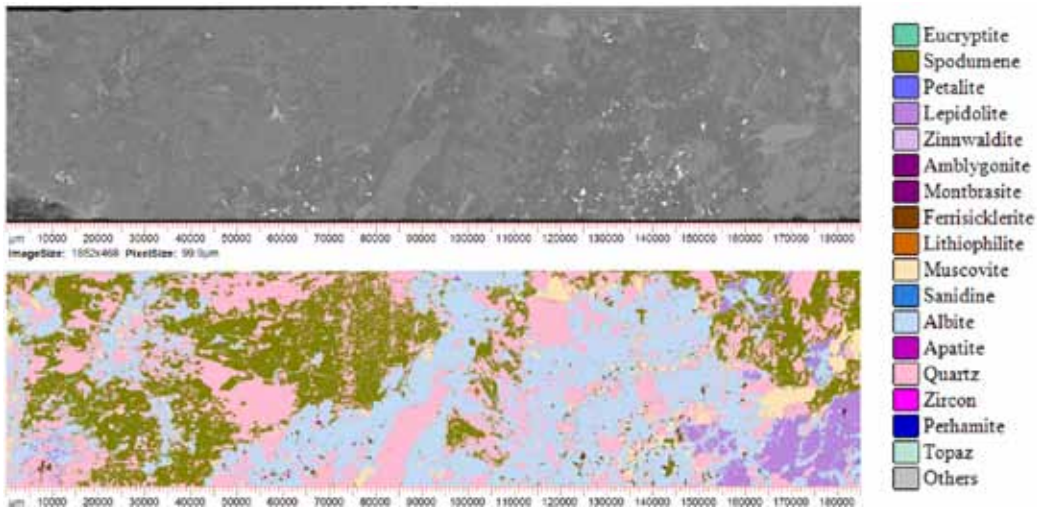

Figure 1: Example of the analysis of a lithium bearing pegmatite drill core from Portugal. Top Image: Total X-ray Intensity Map that highlights the potential different mineral phases in the sample. Bottom Image: AMICS Mineralogical classification that clearly identifies the lithium bearing minerals from other silicate phases in the drill core.

Fluid inclusion study of the Høydal volcanogenic massive sulphide deposit (Norwegian Caledonides)

M. M. Mina[1, 3*], H-K. Paulsen[2], G. B. Kiss[1]

[1] Department of Mineralogy, ELTE Eötvös Loránd University, Hungary,
[2]Norwegian Geological Survey, Norway,
[3]Department of Earth Sciences, Faculty of Science, University of Gezira, Sudan,
e-mail: minamusa@student.elte.hu

The Høydal volcanogenic massive sulphide (VMS) deposit is associated with thick basaltic flows, which are parts of the Løkken ophiolitic sequence of Lower Ordovician age, in the Central Norwegian Caledonides. It is found, together with some other smaller prospects, in the close vicinity of the world-famous VMS orebody at Løkken. Høydal is one of the very few Scandinavian Caledonian VMS deposits that only suffered minimal effects of Caledonian deformation and metamorphism (only very low to low grade metamorphism occurred) and therefore the original textural features are quite well preserved. Also preserved is the spatial relationship between the layered massive sulphide and the adjacent feeder zone with its characteristic host rock alteration, as well as to extensive jasperoid layers and fault-scarp talus deposits (see e.g., GRENNE & VOKES 1990).

Modern fluid inclusions study with a system-based approach has not previously been performed in the area, though it would be crucial to better understand the ore forming processes at Høydal, as well as it would improve our understanding on the Caledonian, (slightly) metamorphosed VMS deposits. This study presents the results of the first detailed microthermometric study on fluid inclusions within sulphide-associated quartz from Høydal, with the objective to reconstruct the formation conditions as well as the development of the ore-forming fluids.

Two generations of quartz are observed within the massive sulphide samples; the first is an earlier one, which occurs as fine-grained aggregate closely associated with sulphide ore minerals (pyrite, sphalerite, and chalcopyrite), while the second is later and occurs as micro-brecciating veins, crosscutting throughout the samples. In the stockwork feeder zone, only one quartz generation was identified. In both cases, quartz formed together or after the ore minerals formed.

Petrographic and microthermometric analyses of primary fluid inclusions in quartz from massive sulphide and stockwork feeder zones reveal homogenisation temperatures (T_h) of 139–211°C and salinities of 5.8–9.1 wt.% NaCl equivalent, with eutectic temperatures (T_e) about −20.8°C. These results indicate a NaCl-H_2O-dominated fluid system, while the textural characteristics suggest entrapment from a homogeneous parent fluid. Although in this case T_h is interpreted as minimum formation temperature, we do not expect significant pressure correction, as the relatively low temperature range is also supported by sphalerite thermometry.

A general positive correlation between salinity and T_h is observed, with higher values characteristic in the stockwork feeder zone. This points to the dilution effect of ambient seawater as the fluid is reaching the seafloor. Formation of the second quartz generation is the result of the fluid evolution, based on its microthermometry data, it represents a later phase of the submarine hydrothermal process.

GRENNE, T., VOKES, F. (1990). Sea-floor sulfide at the Høydal volcanogenic deposit, central Norwegian Caledonides – Econ Geol, 85, 344-359.

Applied mineralogy in construction: Toward greener building materials

F. Mittermayr[1], I. Galan[2], F. R. Steindl[2,3], C. Grengg[3]

[1]Institute for Material Technology, University of Innsbruck, Austria,
[2]Institute for Technology and Testing of Building Materials, Graz University of Technology, Austria,
[3]Institute of Applied Geosciences, Graz University of Technology, Austria
e-mail: florian.mittermayr@uibk.ac.at

The global construction industry faces significant sustainability challenges, particularly due to the high environmental impact of cement production, responsible for approximately 8% of anthropogenic CO_2 emissions worldwide. Concrete, the second-most consumed material globally after water, intensifies this issue due to vast production volumes combined with notably low recycling rates. Applied mineralogy presents a pivotal tool toward developing greener and more sustainable building materials, directly addressing these environmental concerns. Improving the efficiency of ordinary Portland cement (OPC) through innovative supplementary cementitious materials (SCMs) is a primary strategy. SCMs such as fly ash and calcined clays enhance OPC performance, reducing clinker content and associated emissions. Our study has identified natural siderite ($FeCO_3$) from Erzberg as a promising new SCM (MITTERMAYR et al. 2025). Investigations indicate that freshly ground siderite temporarily retards early cement hydration by forming iron hydroxide phases; however, this retardation diminishes over time, ultimately improving durability and strength due to the newly discovered "ferrolanic" reaction. Notably, siderite incorporation effectively reduces calcium leaching and enhances sulfate resistance, providing both environmental and performance benefits without requiring thermal activation. Beyond OPC systems, alkali-activated materials (AAMs), also known as geopolymers, represent another critical advance toward greener construction. High durability is one key aspect, complemented by the possibility to incorporate industrial wastes and secondary raw materials. Specifically, recent research highlights the effectiveness of steel slags – basic oxygen furnace (BOF) and open-hearth furnace (OHF) – in AAM formulations (GRENGG et al. 2024). These slags, typically underutilized and disposed of in landfills, have demonstrated substantial potential as reactive binder components, achieving high mechanical strengths and significantly lowering global warming potential by approximately 52%. Incorporating waste cooking oil (WCO) into steel slag AAMs enhances material durability and further decreases their carbon footprint by up to 74%, primarily through forming insoluble metal soap phases within the microstructure. Moreover, the utilization of construction and demolition waste (CDW) in AAM systems exemplifies a circular economy approach, reducing natural resource consumption and enabling substantial carbon sequestration. Pretreatment of CDW aggregates with WCO notably improves the performance of these materials, countering typical drawbacks such as high water absorption and reduced workability. This innovative strategy not only boosts mechanical properties but also achieves considerable negative global warming potentials, underscoring significant carbon sequestration capacities (up to -670 kg CO_2eq/m³). Such WCO-modified CDW-based AAMs represent a transformative step toward carbon-negative concrete materials.

MITTERMAYR, F., STEINDL, F., PONS PINEYRO, M., BRIENDL, L., SAKOPARNIG, M., GALAN, I. (2025): Exploring natural siderite ($FeCO_3$) as a novel supplementary cementitious material. – Cem Concr Res, 197, 107975.

GRENGG, C., RUDIC, O., SAADE, M.R.M., STEINDL, F., WILKENING, M., JODLBAUER, A., ZOEGL, I., WOHLMUTH D., MITTERMAYR, F. (2024): Alkali activated steel slag – oil composites: Towards resource efficiency and CO_2 neutrality. – Cem Concr Res, 186, 107678.

From lakebed to structure: Evaluating dredged sediment for sustainable 3D-printing

B. Nader[1], H. Vašatko[1], J. Jauk[1], M. Taibon[2], D. Hippler[2], M. Stavric[1]

[1]Institute of Architecture and Media, Graz University of Technology, Austria
[2]Institute of Applied Geosciences, Graz University of Technology, Austria
e-mail: b.nader@tugraz.at

The construction industry is under growing pressure to adopt sustainable practices and materials to reduce its environmental impact. In order to address these issues, we explore an innovative approach to utilize dredged mud from Lake Neusiedl in Austria, a resource that is both abundant and largely untapped, transforming it into a 3D-printable material for building applications within a natural heritage site. The central research questions address (1) how this natural material can be characterized in terms of its textural, mineralogical, and geochemical composition, (2) which adjustments are necessary to make 3D-printing technology compatible with it and (3) what performance characteristics, such as strength and durability, can be achieved in the resulting 3D-printed objects. Therefore, the project employs an integrated research approach, including primal material analyses, such as X-ray diffraction and fluorescence, scanning electron microscopy, grain size analysis and BET. Moreover, optimization of the 3D-printing processes and mechanical testing of the printed components are conducted to complement our approach. Facing the dual challenges of climate change and high CO_2 emissions from construction, this work demonstrates the potential of repurposing dredged sediment as a sustainable material for temporary structures, offering a compelling solution for the Lake Neusiedl region and beyond.

Figure 1: 3D-printed structure from dredged sediment of Lake Neusiedl
Photo: B. Nader

Mineralogical study of industrially polluted sediments in Campania, Italy

M. Nahlik[1], L. Plakolm[2], T. Đorđević[3,1]

[1]Department of Mineralogy and Crystallography, University of Vienna, Austria
[2]Department of Paleontology, University of Vienna, Vienna, Austria
[3]E057-02 USTEM, TU Wien, Vienna, Austria
e-mail: tamara.djordjevic@univie.ac.at

The Campania region of Italy has long been a center for a wide range of anthropogenic and industrial activities, resulting in high levels of pollution in local ecosystems. Although there is extensive data on sediments (ROMANO et al. 2018) and water quality (ARIENZO et al. 2001), detailed research on mineralogy and mineral-water interactions is lacking. Therefore, we characterized both marine and fluvial sediments using a combination of powder X-ray diffraction (PXRD), secondary electron microscopy with energy-dispersive X-ray spectroscopy (SEM-EDS) and Raman spectroscopy, in order to draw conclusions regarding the stability and retention of pollutant elements, with the special focus on the retention of iron (Fe) in minerals.

Bulk mineralogical composition of the samples was determined by PXRD. Marine sediments were dominated by sanidine, muscovite, quartz, and anorthite, with smaller amounts of hematite, clay minerals, scorodite, magnetite, and chabazite. The sediments from the Sarno river have a broader mineral diversity, consisting mainly of clinopyroxenes, sanidine, anorthite, leucite, orthoclase, phlogopite, analcime, scorodite, and magnetite. In contrast, the Irno River sediments displayed the simplest composition, comprising mainly dolomite, clinopyroxenes, calcite, and quartz.

A combination of SEM-EDS analyses and Raman spectroscopy (of polished aliquots) was used to characterize the Fe-retention in sediments. Fe is trapped mostly in iron-oxides (hematite, Fe_2O_3, magnetite, $Fe^{2+}Fe^{3+}{}_2O_4$ and magnesioferrite, $MgFe^{3+}{}_2O_4$) and iron silicates (ferrosilite/clinoferrosilite, $Fe^{2+}{}_2Si_2O_6$) and occasionally in pyrite, FeS_2. Fe-oxides can show slightly elevated concentrations of Mn, Co and Zn (up to 1 at. % each) and Fe-silicates showed elevated concentrations of Al (up to 4 at. %), Mg (up to 4 at. %) and Zn (up to 1 at. %). Secondary Fe-minerals are associated with amorphous hydroxy iron oxides (HFOs).

Our findings closely align with the mineralogical composition of soils that were previously used to store raw materials at the former ILVA plant (ADAMO et al. 2002). This suggests that solid metallurgical waste products, such as slags and fly ash from the ILVA plant, have significantly influenced the mineralogical composition of marine and river sediments in the Bagnoli area.

We would like to thank Sergio Balzano and Michael Lintner for letting us use their samples.

ADAMO, P., ARIENZO, M., BIANCO, M.R., TERRIBLE, F., VIOLANTE, P. (2002): Heavy metal contamination of the soils used for stocking raw materials in the former ILVA iron–steel industrial plant of Bagnoli (southern Italy). – Sci Total Environ, 295, 17-34.

ARIENZO, M., ADAMO, P., ROSARIA BIANCO, M., VIOLANTE, P. (2001): Impact of land use and urban runoff on the contamination of the Sarno river basin in Southwestern Italy. – Water Air Soil Poll, 131, 349-366.

ROMANO, E., BERGAMIN, L., CELIA MAGNO, M., PIERFRANCESCHI, G., AUSILIS, A. (2018): Temporal changes of metal and trace element contamination in marine sediments due to a steel plant: The case study of Bagnoli (Naples, Italy). – App Geochem, 88, 85-94.

Baddeleyite and “ordered srilankite” from Sri Lanka

L. Nasdala[1], G. Giester[1], C. Chanmuang N.[1], C. A. Hauzenberger[2], G.W.A.R. Fernando[3], K.A.G. Sameera[1,4], M. Ende[5], G. Habler[1]

[1]Universität Wien, Vienna, Austria
[2]Karl-Franzens-Universität, Graz, Austria
[3]The Open University of Sri Lanka, Nugegoda, Sri Lanka
[4]Geological Survey and Mines Bureau, Pitakotte, Sri Lanka
[5]Martin-Luther-Universität Halle-Wittenberg, Halle (Saale), Germany
e-mail: lutz.nasdala@univie.ac.at

Baddeleyite (monoclinic ZrO_2) crystals up to 2 cm size were found in a carbonatite near Eppawala, northwestern Sri Lanka (for the geological background see WANG et al., 2021). The material shows multiple, polysynthetic twinning that is typical of this mineral. In addition to subordinate primary, compositional growth zoning, there are indications of intense secondary, probably fluid-driven alteration emanating from the outer surface and internal fractures (Fig. 1). The latter seems to contradict the potential use of this baddeleyite as an analytical reference material, at least until detailed, spatially-resolved isotopic studies have been undertaken.

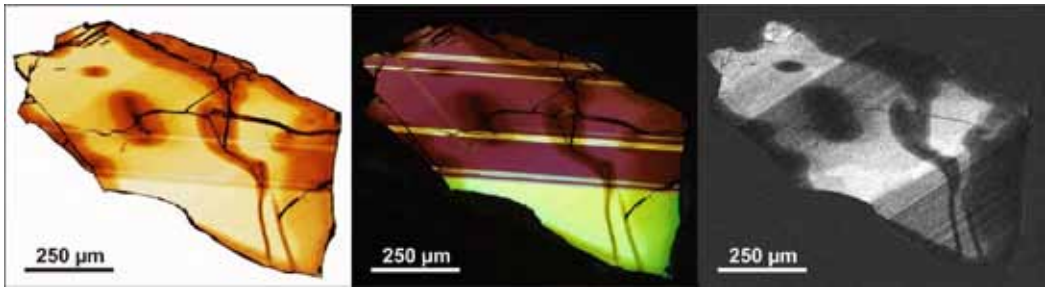

Figure 1: Series of plane- (left) and cross-polarised transmitted light (centre) and cathodoluminescence (CL; right) photomicrographs of a polished baddeleyite from Eppawala, Sri Lanka (25 µm thin section). Note secondary alteration indicated by darkened colouration and depleted CL intensity.

It is most interesting that inside the baddeleyite $ZrTi_2O_6$ lamellae were discovered. This compound, however, with random (disordered) occupation of the six-coordinated cation site by Zr^{4+} and Ti^{4+}, is known as the mineral srilankite (space group *Pbcn*; WILLGALLIS & HARTL, 1983). In the Eppawala $ZrTi_2O_6$ (also *Pbcn*; a = 14.198 Å, b = 5.326 Å, c = 5.002 Å, Z = 4), in contrast, the cation distribution is ordered, as Ti and Zr occupy different atomic positions: Ti^{4+} is six-coordinated (Ti–O = 1.85–2.09 Å) whereas Zr^{4+} is eight-coordinated (Zr–O = 2.11–2.47 Å). The conjecture that the Eppawala $ZrTi_2O_6$ phase may represent a hitherto undiscovered polymorph, is supported by the observation that srilankite (KONZETT et al., 2013) and the studied $ZrTi_2O_6$ yield vastly different Raman spectra. We present a description of the structure of “ordered srilankite” along with results of chemical and spectroscopic analyses.

KONZETT, J., WIRTH, R., HAUZENBERGER, C., WHITEHOUSE, M. (2013): Two episodes of fluid migration in the Kaapvaal Craton lithospheric mantle associated with Cretaceous kimberlite activity: evidence from a harzburgite containing a unique assemblage of metasomatic zirconium-phases. – Lithos, 182, 165–184.

WANG, J., SU, B.X., CHEN, C., FERRERO, S., MALAVIARACHCHI, S.P.K., SAKYI, P.A., YANG, Y.-H., DHARMAPRIYA, P.L. (2021): Crustal derivation of the ca. 475 Ma Eppawala carbonatites in Sri Lanka. – J Petrol, 62, 1–18.

WILLGALLIS, A., HARTL, H. (1983): $(Zr_{0,33}Ti_{0,67})O_2$ – ein natürliches Zirkonium-Titanoxid mit α-PbO_2-Struktur. – Z Krist, 164, 59–66.

Mineral impurities and their traceability along the graphite value chain

G. Obbágy[1]*, R. Arató[1], Z. Dallos[1], F. Melcher[1]

[1]Chair of Geology and Economic Geology, Technical University of Leoben, Leoben, Austria, e-mail: gabriella.obbagy-arato@unileoben.ac.at

Graphite is a critical raw material essential for the energy transition, most commonly used as an anode material in lithium-ion batteries. In the Critical Raw Materials Act, the European Union seeks to diversify raw material imports and aims for at least 10% of its annual consumption to originate from domestic mines by 2030. However, there is currently no standardized method to trace or differentiate between sources of natural graphite.

Graphite ore is extracted from diverse geological environments. The ore is crushed and floatated onsite, resulting in concentrates with approximately 95% purity that are traded globally. Our goal is to develop a fingerprinting method for major natural graphite deposits by identifying material characteristics that remain traceable along at least part of the value chain. In-situ analytical techniques (e.g., LA-ICP-MS and LIBS) reveal a wide range of detectable elements in spatially restricted areas, indicating separate phases as the source of chemical differences between samples (ARATÓ et al. 2025). However, it remains unclear what these phases are and whether they stay traceable throughout the value chain.

In this study, a sedimentary provenance analysis approach was applied to identify the source region of graphite concentrates. Phases with a density higher than that of graphite were separated using heavy liquid (ρ = 2.46 g/cm³) to enhance the mineralogical signal of each locality. These mineral impurities were embedded in epoxy for easier measurement. For morphological and chemical analysis, an SEM-EDS system (Carl Zeiss SmartPI™) was used. Each phase type was verified using Raman spectroscopy, and a database was created for automatic phase identification. The most common mineral impurities in the graphite concentrates include quartz, mica, plagioclase, and iron oxides; at some localities, amphiboles, pyroxenes, talc, apatite, titanite, and sulfides are also found. The main phases detected align well with X-ray diffraction results from bulk graphite concentrates. Additionally, high-resolution transmission electron microscopy revealed the size and nature of the mineral impurities. Most minerals are adsorbed on the surface of graphite flakes, while sheet silicates are often intergrown with graphite. The mineral sizes range from a few nanometers to millimeters.

For battery-specific applications, graphite concentrates are purified using alkali-autoclave leaching and/or hydrofluoric acid treatment to achieve a minimum purity of 99.95%. These purified samples were also subjected to the density separation and analytical protocol described above. As a result of chemical purification, some mineral phases are completely removed, reducing the relative mineral impurity ratio. Conversely, the more resistant mineral phases (e.g., titanite, rutile, zircon) become enriched in the “heavy” fraction, allowing traceability along the value chain.

This study was funded by the European Union under grant agreement no. 101091502, project MaDiTraCe – Material and Digital Traceability for the Certification of Critical Raw Materials, coordinated by the French Geological Survey (BRGM).

ARATÓ, R., QUARLES, Jr. D., OBBÁGY, G., DALLOS, Z., ARATÓ, M., GOPON, P., MELCHER, F. (under review): Towards a chemical fingerprint of graphite by Laser-induced Breakdown Spectroscopy. Journal of Analytical Atomic Spectrometry (submitted).

Crystal chemical studies on transition metal-bearing solid solution systems with kieserite-type crystal structures

N. Omer[1], D. Talla[1], M. Wildner[1]

[1]Institut für Mineralogie und Kristallographie, Universität Wien, Vienna, Austria
e-mail: manfred.wildner@univie.ac.at

The abundant presence of low-hydrated sulfates, e.g. kieserite ($MgSO_4 \cdot H_2O$), on the surface of Mars and probably also on icy moons of Jupiter and Saturn has gained much attention during the past 40 years. While solid solutions between kieserite and cosmochemically relevant isotypic 3*d* transition metal (*Me*) compounds, (Mg,*Me*)$SO_4 \cdot H_2O$ (Me^{2+} = Mn, Fe, Co, Ni, and Zn), have been extensively investigated by our group within the last few years and found to form continuous systems without mixing gaps (e.g. BECHTOLD & WILDNER, 2016; TALLA & WILDNER, 2019; WILDNER & TALLA, 2019; TALLA et al. 2023 and references therein), solid solutions between the various Me^{2+} endmembers themselves have not been studied so far.

Therefore we performed low-hydrothermal synthesis experiments, up to now on the binary systems Mn–Ni (with the largest difference in their octahedral Me^{2+} ionic radii (SHANNON, 1976), Δ_r = 0.14 Å), Fe–Ni (Δ_r = 0.09 Å), and Co–Zn (Δ_r = 0.005 Å), and investigated suitable products by single-crystal X-ray diffraction and respective crystal structure refinements using the program SHELXL (SHELDRICK, 2015).

The results obtained up to now indicate the existence of quite large miscibility gaps in the Mn–Ni and Fe–Ni systems (albeit in the latter case based on a very small dataset so far), in contrast to an obviously continuous Co–Zn solid-solution system, as to be expected judging from their practically identical Me^{2+} ionic radii. Vice versa, the miscibility gap in the Mn–Ni system might be attributed to the striking Me^{2+} size mismatch of Δ_r = 0.14 Å (cf. for Mn–Mg Δ_r = 0.11 Å). For the Fe–Ni system, however, the distinctly different octahedral distortion in the endmembers – i.e. a clear-cut, 'kieserite-typical' octahedral [4+2]-elongation for Ni, Mg, and all the other Me^{2+} cations, vs. a tendency towards a [2+2+2] coordination in $FeSO_4 \cdot H_2O$, in turn presumably related to the specific $3d^6$ electron configuration of Fe^{2+} – might play a decisive role in preventing continuous mixing.

Anyway, along their respective regions of miscibility, all three systems seem to obey linear Vegard-type behaviour for the unit-cell parameters as well as for most crystal chemical features. Besides, no structural ordering effects have been observed in our studies so far.

BECHTOLD, A., WILDNER, M. (2016): Crystal chemistry of the kieserite-cobaltkieserite solid solution, $Mg_{1-x}Co_x(SO_4) \cdot H_2O$: well-behaved oddities. – Eur J Mineral, 28, 43-52.

SHANNON, R.D. (1976): Revised effective ionic radii and systematic studies of interatomic distances in halides and chalcogenides. – Acta Cryst, A32, 751-767.

SHELDRICK, G.M. (2015): Crystal structure refinement with SHELXL. – Acta Cryst, C71, 3-8.

TALLA, D., WILDNER, M. (2019): Investigation of the kieserite–szomolnokite solid solution series, (Mg,Fe)$SO_4 \cdot H_2O$, with relevance to Mars: Crystal chemistry, FTIR, and Raman spectroscopy under ambient and Martian temperature conditions. – Amer Mineral, 104, 1732–1749

TALLA, D., GIESTER, G., WILDNER, M. (2023): Structural and spectroscopic study of the kieserite-type (Mg,Mn)$SO_4 \cdot H_2O$ solid solution at ambient and low temperatures relevant to Mars. – Icarus, 401, 115583.

WILDNER, M., TALLA, D. (2019): Comparative crystal chemistry of the solid solution systems between kieserite ($MgSO_4 \cdot H_2O$) and transition metal kieserite-type compounds ($M^{2+}SO_4 \cdot H_2O$, M^{2+} = Mn, Fe, Co, Ni, Zn). – ECM32, Book of Abstracts, 201.

The “rapid blood test” approach to volcanic eruption monitoring using micro-XRF

M. Pankhurst[1], A. Butcher[2], E. Jolis[3], A. H. Menzies[4]

[1] Gaiaxiom Pty Ltd, Denmark,
[2] Hafren Scientific Ltd, Welshpool, UK,
[3] Geological Survey of Finland, Espoo, Finland,
[4] Bruker Nano Analytics GmbH, Berlin, Germany,
e-mail: mjp@gaiaxiom-geoscience.com

A comprehensive time-series of integrated chemical and textural data from products of the 2021 eruption on La Palma, Canary Islands, using scanning micro-XRF are presented. Within our data we observe critical changes in plumbing system dynamics, including a progressive shutting-down of deep magma supply, weeks before the eruption concluded. These data and our workflow demonstrate how near-real-time volcano petrology can now be delivered. Answering “what is happening now?” has long been the highest priority for volcanic observatories, and approaches with rapid and data-rich returns like geophysics, and less so gas geochemistry, are favoured. This is like listening to the heartbeat or smelling the breath of volcanoes respectively, which can indicate changes are occurring deep within the plumbing system. Yet with approximately 20% of the world’s increasing and interconnected population now living within a 100 km of an active volcano, answers to new questions are being urgently demanded. To understand the driving mechanisms of melting, storage, crystallisation, volatile charging, ascent, and eruption of magma, comprehensive “blood tests” are needed which can help answer “what will happen next?” and “how long will it continue?”. This is shown to be possible with scanning micro-XRF. Moreover, geophysics and gas geochemistry cannot be used to look back into the past of a volcano, and so are faced with an unaddressable lack of empirical historical comparisons. Our study disproves the traditional view that petrology is too slow, too expensive, and too specialized to deploy in many volcano monitoring settings.

Figure 1: Example of the analysis of samples from La Palma volcanic eruptions in 2023. From left to right: (a) Total X-ray intensity map that highlights the potential different mineral phases in the sample; (b) AMICS Mineralogical classification that clearly identifies the phenocryst phases from the matrix; (c) size distribution of clinopyroxene phenocrysts; (d) size distribution of olivine phenocrysts.

Methane- and hydrogen-rich fluid inclusions in hydrothermally altered felsic granulite

A. Pengg[1*], R. J. Bakker[2], D. Misch[1]

[1]Chair of Energy Geosciences, Technical University of Leoben, Austria,
[2]Chair of Resource Mineralogy, Technical University of Leoben, Austria,
e-mail: alexander.pengg@unileoben.ac.at

Natural hydrogen harbours great potential to support a future carbon-neutral energy system and therefore, moved into the focus of recent research in geosciences and energy geosciences, in particular. This contribution presents the preliminary results of fluid inclusion studies that were carried out on serpentinized ultramafic rocks and felsic granulites from the Bohemian Massif (Austria) to investigate different processes of natural hydrogen formation, to characterize the rocks regarding their overall hydrogen-generative potential, and to ultimately, assess the natural hydrogen potential of the study area. The samples were taken from outcrops in an active quarry where the investigated lithologies occur spatially associated with each other, separated by a tectonic contact that is characterized by strong deformation and hydrothermal alteration. The fluid inclusion studies comprise Raman spectroscopy, microthermometry, and thermodynamic calculations.

Fluid inclusions were generally scarce in the serpentinized ultramafic rocks as well as in the unaltered granulitic rocks and the few detected inclusions contained mainly water. The hydrothermally altered granulite, however, contains large amounts of fluid inclusions (Fig. 1) mainly hosted by quartz, in which CH_4 ($\pm$ H_2O) was the main component. Molecular H_2 (up to 25 mol%), H_2S, N_2, and C_2H_6 occur as minor components (Fig. 1). CO_2 was never detected. As this fluid composition, reduced gas species on the one side and the absence of CO_2 on the other side, is uncommon for felsic granulites, the question of the fluid's origin arises. The adjacent serpentinite represents a potential source for CH_4 and H_2, which would imply a later hydrothermal origin of the fluid inclusions. The fault zone potentially provided enhanced permeability for fluid migration. Alternatively, H_2 could be related to Fe^{2+}-oxidation or mantle exhalation.

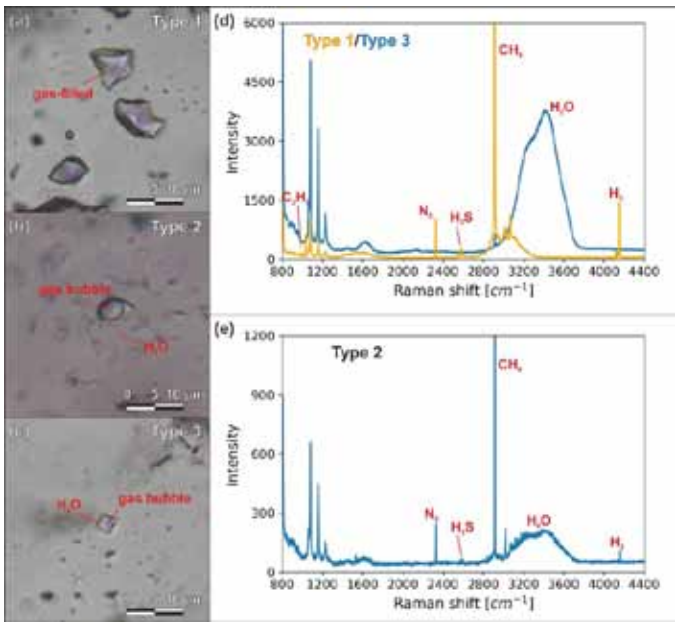

Figure 1: Fluid inclusions hosted by quartz found in the hydrothermally altered granulitic rocks (a-c) and the corresponding Raman spectra (d, e). Photos A. Pengg

Characterisation and technological procedures for recycling and reuse of flotation tailings from the Rudnik Mine in Serbia

S. Petrović[1*], V. Simić[1], F. Arnaut[2], D. Radulović[3], J. Stojanović[3], N. Nikolić[4], J. Senćanski[5]

[1]Faculty of Mining and Geology, University of Belgrade, Serbia,
[2]Institute of Physics, Belgrade, Serbia,
[3] Institute for Technology of Nuclear and Other Mineral Raw Materials, Serbia,
[4]Institute for Multidisciplinary Research, Serbia,
[5]Institute of General and Physical Chemistry, Serbia,
e-mail: stefan.petrovic@rgf.bg.ac.rs

The project titled "Characterisation and Technological Procedures for Recycling and Reuse of Flotation Tailings from the 'Rudnik' Mine" (acronym: REASONING) is multidisciplinary research focused on the comprehensive investigation of mine tailings through geological, mineralogical, geochemical, geophysical, and metallurgical methods. The project team comprises researchers from six Serbian institutions, as well as RWTH Aachen University (IME – Institute for Process Metallurgy and Metal Recycling) from Germany. The project addresses environmental challenges associated with mining waste and explores opportunities to integrate circular economy principles into mining operations.

Funded by the PRIZMA programme of the Science Fund of the Republic of Serbia, REASONING investigates tailings generated over decades of exploitation and flotation processing of Pb-Zn-Cu-Ag ores from the Rudnik mine in central Serbia. To date, approximately 11 million tonnes of fine-grained tailings have been produced and deposited in an oval-shaped area up to 40 metres deep, covering more than 30 hectares. The main objectives of the project include the comprehensive characterisation of the tailings, the development of efficient technological methods for extracting valuable metals and elements, and the evaluation of the potential for using the tailings as a secondary raw material. The research will include: monitoring physico-chemical changes in the tailings with depth; correlating magnetic susceptibility with heavy metal content to identify enrichment zones; determining the distribution of mineral assemblages and associated elements; analysing pore water chemistry and geochemical trends with depth; modelling stable mineral associations and element distribution using theoretical geochemical approaches; exploring optimal extraction pathways through theoretical modelling and electrochemical separation from synthetic and leached solutions; and developing technological procedures for the valorisation of useful components from the tailings.

The REASONING project is expected to set a benchmark for future research and complex valorisation of mine tailings in Serbia. Through case studies and proposed applications, the project seeks to demonstrate how circular economy strategies can support environmental protection, enhance resource efficiency, and promote sustainable economic development.

Inhibition of $CaCO_3$ nucleation - mobile fluorescence spectroscopy for in-situ analysis of polyaspartate

M. Pettauer[1], A. Leis[2], W. Gotschy[3], R. Boch[1], L. Hasenhüttl[1], M. Dietzel[1]

[1] Institute of Applied Geosciences, Graz University of Technology, Austria,
[2]JR-AquaConSol GmbH, Graz, Austria,
[3]Dr. Walter Gotschy, Ingenieur- und Sachverständigenbüro für Optik, Physik und Tracertechnik, Adnet, Austria
e-mail: michael.pettauer@tugraz.at

The nucleation and growth of calcium carbonate ($CaCO_3$) minerals in aqueous environments are influenced by a wide range of organic and inorganic compounds. Among these, the amino acid aspartate has the ability to modify the nucleation and crystallization pathways of $CaCO_3$. Aspartate can stabilize amorphous calcium carbonate (ACC) phases and influence the selection of specific polymorphs, such as calcite and vaterite. Furthermore, it is known to alter crystal morphology and reduce particle aggregation and the adhesion of crystals to substrate surfaces. Aspartate plays a key role in the biomineralization processes of marine organisms, particularly in the shell formation of mollusks. Accordingly, the synthetic polymer polyaspartate (PASP) has been developed as a biomimetic analogue. PASP is a biodegradable, environmentally friendly antiscalant widely used to inhibit scale formation in various industrial systems, including membrane filtration units, geothermal energy facilities, and tunnel drainage networks (LEIS et al. 2022). Accurate, real-time monitoring of PASP is essential for effective dosing, especially at low concentrations (2–10 mg/L). However, conventional analytical methods—though precise—are typically lab-based, time-consuming, and impractical for *in-situ* use. To address this, we developed the ***F****luorescence-based* ***I****n-situ* ***P****olya****s****partate* ***A****nalysis (FIPSA)*, a portable fluorescence spectroscopy system equipped with optical fiber sensors for on-site PASP quantification. *FIPSA* utilizes the intrinsic fluorescence of thermally synthesized PASP (excitation at ~336 nm, emission at ~411 nm), enabling real-time measurements with a detection limit of ~1 mg/L and a working range up to 5,000 mg/L. The method has been tested across various PASP products and water matrices, accounting for key variables such as pH, temperature, ionic strength, and turbidity. On-site calibration ensures robust performance under field conditions. *FIPSA* enables continuous monitoring and adaptive dosing control, improving operational efficiency and reducing dependency on delayed laboratory analyses in applications such as tunnel drainage, wells, and pipelines.

LEIS, A., WAGNER, H., EICHINGER, S., DOMBERGER, G., WEDENIG, M., DIETZEL, M., BOCH, R. (2022): Use of green inhibitors for hardness stabilisation of tunnel drainage systems. – Geomechanics and Tunnelling, 15(4), 402-413. https://doi.org/10.1002/geot.202200018

Hydration of periclase and the influence of pH on brucite crystal morphology

M. Pettauer[1], L. Lang[1], M. Dietzel[1]

[1]Institute of Applied Geosciences, Graz University of Technology, Austria
e-mail: michael.pettauer@tugraz.at

The transformation of periclase [MgO] to brucite [$Mg(OH)_2$] via hydration is known as an important reaction due to the increase in solid volume by H_2O consumption, and energy transfer. Despite extensive research on the conversion of MgO to $Mg(OH)_2$, the key factors governing its kinetics, reaction mechanisms, and the size, shape, and orientation of individual brucite crystals remain only partially understood. The self-regulating pH during hydration is strongly influenced by impurities in the raw material, such as CaO or $MgCl_2$. Furthermore, pH plays an important role in controlling the hydration rate and the morphology of newly formed brucite crystals (PETTAUER et al. 2024). In this study, laboratory experiments were conducted using highly pure synthesized MgO (≈99.9%) to investigate its transformation into $Mg(OH)_2$ while eliminating the influence of foreign components. By maintaining pH levels between 11 and 13, it appears that the surface charge of both MgO and the newly formed $Mg(OH)_2$, along with their respective precipitation rates, governs the availability of dissolved Mg^{2+} and, consequently, the resulting brucite crystal morphology. Below the point of zero charge ($pH_{PZC} \approx 11.5 \pm 0.5$) of MgO and $Mg(OH)_2$, subhedral flaky hexagonal brucite crystals dominate at pH ≈ 10.0. At pH ≈ 11.5, brucite develops euhedral forms, exhibiting pyramidal to tabular morphologies with smooth crystal surfaces. At pH ≈ 13.0, brucite also exhibits tabular shapes but with a preferred growth along the c-axis. By advancing our understanding of hydration kinetics and crystal growth mechanisms, brucite can be optimized for specialized applications and tailored product engineering.

PETTAUER, M., BALDERMANN, A., EDER, S., DIETZEL, M. (2024): Hydration of MgO: reaction kinetics and pH control on brucite crystal morphology. Cryst Growth Des, 24(7), 3085-3092. https://doi.org/10.1021/acs.cgd.4c00243

Cosmic dust in Tyrol and the search for urban micrometeorites: mineralogical-chemical analysis of metallic spherules

A. Pflügler[1], P. Tropper[1*], S. Wagner[1], T. Gatt[1]

[1]Institute of Mineralogy and Petrography, University of Innsbruck, Innsbruck, Austria,
e-mail: peter.tropper@uibk.ac.at

Micrometeorites contain information about our solar system and its formation. They are for example collected in the Antarctic, the Sahara desert, the deep sea, but also in urban areas. In this investigation, a total of 250g of sediment was collected from roofs in Innsbruck (Audioversum, Wilhelm Greil Strasse) and from a family home in Zirl and searched for micrometeorites. The samples were sieved, magnetically separated and manually sifted for spherules. In addition to optical microscopy (reflected light binocular), micro-XRF, the scanning electron microscope and the electron microprobe were used for micro-chemical analysis. Numerous metallic spherules could be identified. According to literature studies, these spherules are most likely of terrestrial origin and they are compositionally Fe-Cr-Ni metals and are thus most probably from anthropogenic origin.

During further investigation and by looking at the mineralogy and comparing with literature data, three micrometeorites of the types: barred olivine, cryptocrystalline turtleback and cryptocrystalline microcrystalline could be identified. They all show characteristic structures such as cusp structures of olivine or barred olivine, which allow them to be categorized into these groups. The micrometeorites are two cryptocrystalline micrometeorites of the subspecies Turtleback (ZC-1) and Microcrystalline (ZAB-10). The third micrometeorite was identified as Barred-Olivine (ZC-2). They all consist of olivine phenocrystals in a silicate matrix. The cryptocrystalline turtleback exhibits typical “knoppy” structures due to the shape of the olivine crystals. All three types of these barred-olivine micrometeorites consist of olivine bars that extend across the surface. In addition. large dendritic magnetite crystals also occur.

The terrestrial spherules probably originate from industrial processes and traffic (Wilhelm Greil Strasse is close to the railway station), as some of them have been characterized as Fe-Cr-Ni spherules and may be, for example, car austenitic steels. The anthropogenic influence of the surrounding city can be recognized by the fact that only terrestrial spherules were found in Innsbruck, while the three micrometeorites were found on a rooftop in Zirl.

From the universal-stage to TEM-based electron diffraction: studies on shock metamorphism

L. Pittarello[1,2], T. Griffiths[2], G. Giuli[3], M. Gemmi[4], P. Parlanti[4]

[1]Mineralogich-Petrographische Abteilung, Naturhistorisches Museum, Vienna, Austria
[2]Departement für Lithosphärenforschung, Universität Wien, Vienna, Austria
[3]School of Science and Technology, Geology div., University of Camerino, Camerino, Italy
[4]Istituto Italiano di Tecnologia, Electron Crystallography, Pontedera, Italy
e-mail: lidia.pittarello@nhm.at

Shock metamorphic effects recorded in rock-forming minerals in terrestrial impact craters and in meteorites provide important information on the pressure and temperature conditions that the host rock has experienced (e.g., STÖFFLER et al. 2018). Therefore, choosing the most effective analytical method for the identification and quantification of shock metamorphic effects is fundamental. Here, we present a broad spectrum of analytical methods to investigate shock metamorphic effects in silicate minerals, which have not yet been applied or only limitedly applied for this purpose. For the identification and indexing (i.e., the attribution to a specific crystallographic orientation) of shock-induced planar microstructures in quartz and feldspar, we propose the combined use of the universal-stage (U-stage, a tool applied to a petrographic optical microscope, which allows the tilting of thin section in all directions), scanning electron microscopy back scattered (BSE) imaging, and electron backscatter diffraction (EBSD). The data are processed through specifically written MTEX/MATLAB codes. This method enables to overcome the limits posed by deformed or altered crystals (e.g., strong undulatory extinction of quartz or extensive alteration of feldspar) and facilitates the indexing of amorphous planar features (e.g., planar deformation features – PDFs- or amorphized feldspar twins). The application of these methods has allowed the indexing of two generations of amorphized twins in plagioclase from the Manicouagan impact structure, Canada (PITTARELLO et al. 2020) and the indexing of PDFs in strongly deformed quartz and in plagioclase from the El'gygytgyn impact structure, Russia (PITTARELLO & GRIFFITHS, in prep.). Extremely fine-grained shock-generated microstructures, such as the transformation of olivine into the high-pressure polymorphs ringwoodite and wadsleyite along lamellae or at the margin of crystals, can generally be only observed by transmission electron microscopy (TEM). The advancement of technology allows now TEM-based electron diffraction phase and orientation mapping at the nanoscale, producing maps, which show the mutual crystallographic relationship between host and polymorphs, and between polymorphs, contributing to discriminating their origin and constraining the shock process (e.g., CAMPANALE et al. 2024). This method enabled to constrain the formation by fractional crystallization from impact melts rather than solid-state transformation for coexisting ringwoodite and wadsleyite aggregated in the Alfianello meteorite (PITTARELLO et al. in subm.). **Acknowledgments**: V. De Santis, L. Carone, A. Steiger-Thirsfeld, A. Di Michele, C. Burlet, G. Habler, L. Daly, L. Ferrière, R. Kilian, and C. Koeberl.

CAMPANALE, F., MUGNAIOLI, E., FOLCO, L., PARLANTI, P., GEMMI, M. (2024): TiO_2 II: The high-pressure Zr-free srilankite endmember in impact rocks. – Meteoritics & Planetary Science 59, 529-543.

PITTARELLO, L., GRIFFITHS, T. (in prep.): Combining universal-stage, electron microscopy and electron backscatter diffraction for better indexing of planar microstructures in quartz and plagioclase.

PITTARELLO, L., DALY, L., PICKERSGILL, A.E., FERRIÈRE, L., LEE, M. (2020): Shock metamorphism in plagioclase and selective amorphization. – Meteoritics & Planetary Science 55, 1103-1115.

PITTARELLO, L., DE SANTIS, V., CARONE, L., PRATESI, G., GEMMI, M., PARLANTI, P., STEIGER-THIRSFELD, A., DI MICHELE, A., GIULI, G. (submitted): Coexisting wadsleyite and ringwoodite in the Alfianello L6 ordinary chondrite. – Meteoritics & Planetary Science.

STÖFFLER, D., HAMANN, C., METZLER, K. (2018): Shock metamorphism of planetary silicate rocks and sediments: Proposal for an updated classification system. – Meteoritics & Planetary Science 53, 5-49.

A mineralogical perspective on foraminiferal architecture: insights into a unique biosphere-geosphere interaction

L. Plakolm[1], N. Lammer[2], M. Nahlik[2], M. Nagy[1], S. Balzano[3], M. Lintner[4], T. Đorđević[2,5], P. Heinz[1]

[1]Department of Palaeontology, University of Vienna, Vienna, Austria
[2]Department of Mineralogy and Crystallography, University of Vienna, Vienna, Austria
[3]Department of Ecosustainable Marine Biotechnology, Stazione Zoologica Anton Dohrn Napoli, Naples, Italy
[4]ING PAN – Institute of Geological Sciences, Polish Academy of Sciences, Research Centre in Kraków, Poland
[5]E057-02 USTEM, TU Wien, Vienna, Austria
e-mail: leonp01@unet.univie.ac.at

Foraminifera – microscopic single-celled marine eukaryotes – are among the most productive and important biomineralizing organisms in modern oceans and play a crucial role for global carbon and nitrogen cycles. Certain types of foraminifera are capable of assembling and cementing together surrounding sediment particles to form intricate shell structures. By doing so, these so-called agglutinated foraminifera effectively create an archive of ambient mineralogical composition, which has the potential to be preserved as microfossils and endure for hundreds of millions of years. In order to evaluate the mineral grain incorporation into agglutinated foraminiferal shells and previously observed mineral selectivity, sediment samples from different locations in the Mediterranean Sea (Gulf of Naples and Haifa Bay) were analysed using powder X-ray diffraction (PXRD) and X-ray fluorescence (XRF). Additionally, the element distribution and mineral composition of agglutinated foraminifera occurring within the investigated sediments was analysed via energy dispersive X-ray spectroscopy (EDX) and Raman spectroscopy. Preliminary EDX results reveal that the mineral phases constituting foraminiferal shells contain an abundance of relatively rare metals; one particular individual of the species *Textularia bocki* demonstrates elevated levels of indium, molybdenum, and titanium within its shell (Fig. 1a), whereas other investigated foraminifera contain relatively high amounts of iron (Fig. 1b), manganese and silver. PXRD and Raman spectroscopy indicate that certain foraminifera incorporated minerals (e.g. brookite (TiO_2)) in quantities higher than the surrounding sediments, implying an underlying selectivity mechanism.

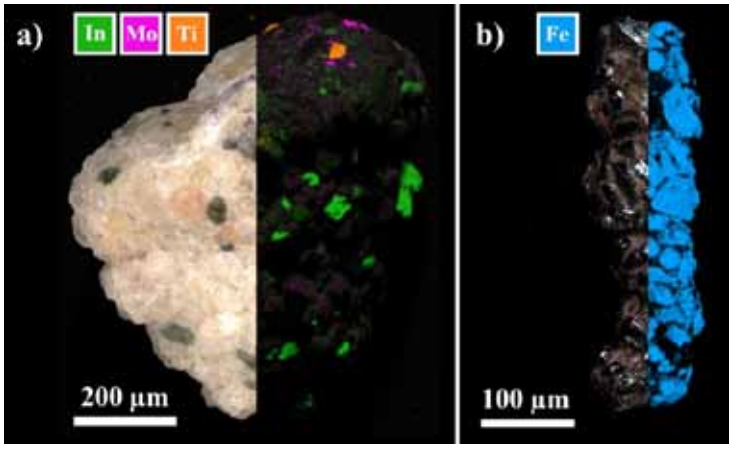

Figure 1: combined photomicroscope image/EDX map of *Textularia bocki* (a) and *Reophax* sp. (b) with highlighted element distributions (a: indium, molybdenum, titanium. b: iron)

Mössbauer spectroscopy for identification of Fe-phases in siderite ($FeCO_3$)-cement systems

M. Pons Pineyro[1], I. Kupenko[2], D. Bessas[2], F. R. Steindl[1], F. Mittermayr[3], A. C. Maciel Soares[4], I. Galan[4]

[1]Institute of Applied Geosciences, Graz University of Technology, Graz, Austria
[2]ESRF-The European Synchrotron, Grenoble, France
[3]Institute for Material Technology, University of Innsbruck, Innsbruck, Austria
[4]Institute for Technology and Testing of Building Materials, Graz University of Technology, Graz, Austria
e-mail: mponspineyro@tugraz.at

Identifying new supplementary cementitious materials (SCMs) is crucial for developing more environmentally friendly future cement, as traditional sources are becoming increasingly scarce. Siderite ($FeCO_3$) shows great potential as a future SCM, having been proven to significantly impact cement hydration while greatly enhancing important durability properties of concrete and shotcrete (MITTERMAYR et al. 2025, PONS PINEYRO et al. 2025).

There is limited understanding of the formation of Fe-rich phases occurring in these systems. Furthermore, conventional analysis techniques such as X-ray diffraction analysis (XRD) do not suffice to identify amorphous Fe-rich phases or differentiate between oxidation states. ^{57}Fe Mössbauer spectroscopy is a powerful technique capable of differentiating between Fe^{2+} and Fe^{3+} compounds, regardless of their crystallinity. With this method, we analyzed siderite-cement pastes from 4 hours up until 180 days of hydration, using both conventional and Fe-free cements. With the latter, it was possible to observe Fe-bearing phases that precipitate solely due to the influence of siderite (Fig. 1). Additionally, XRD measurements were carried out to obtain a more complete picture of the hydration mechanisms of these systems.

The combination of these techniques helps us to get a more complete understanding of the hydration mechanisms of siderite-cement systems. We see how, over time, the Fe^{2+}/Fe^{3+} ratio changes, as Fe^{2+}-bearing phases partially dissolve and subsequently oxidize to Fe^{3+}. Additionally, it was possible to observe that crystalline phases decreased as amorphous phases took more prominence.

Our main objective is to get a more complete understanding of the hydration mechanisms of siderite-cement systems. This would allow us to get a deeper understanding and better design and optimize sustainable composite iron-carbonate containing binders.

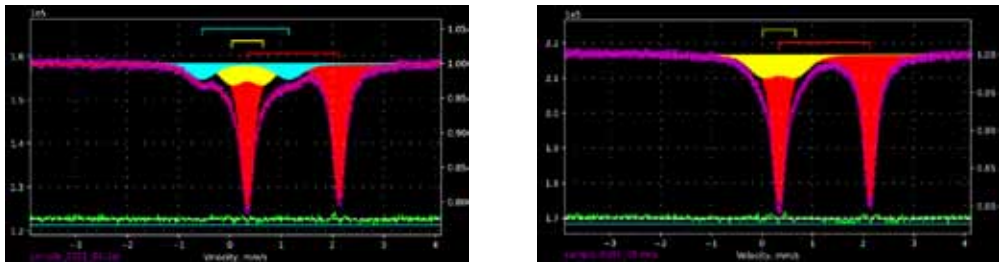

Figure 1: Mössbauer spectroscopy of hydration-stopped cement-siderite (left) and white cement-siderite (right) samples after 1 day of hydration.

MITTERMAYR, F., STEINDL, F.R., PONS PINEYRO, M., BRIENDL, L., SAKOPARNIG, M., GALAN, I. (2025). Exploring natural siderite $FeCO_3$ as a novel supplementary cementitious material. - Cem Con Res, 197, 107975.

PONS PINEYRO, M., STEINDL, F.R., GALAN, I., SOARES, A.C.M., MITTERMAYR, F. (2025): How siderite ($FeCO_3$) enhances the sulfate resistance of cementitious systems. – Cem Con Res (under review).

Long-term quiescent-flow incubation experiment: deciphering metal mobilization from slags

A. Potysz[1], T. Đorđević[2,3], A. Pędziwiatr[4], W. Wegner[5]

[1]Institute of Geological Sciences, Faculty of Earth Sciences and Environmental Management, University of Wrocław, Poland
[2]E057-02 USTEM, TU Wien, Vienna, Austria
[3]Department of Mineralogy and Crystallography, University of Vienna, Austria
[4]Institute of Agriculture, Department of Soil Science, Warsaw University of Life Sciences, Warsaw, Poland
[5]Naturhistorisches Museum Wien, Central Research Laboratories, Vienna, Austria
e-mail: anna.potysz@uwr.edu.pl

Laterite nickel-smelting operations at Vozarci in the Republic of North Macedonia have produced large quantities of smelting waste, much of which has been dumped close to the smelter. As a part of our previous study (ĐORĐEVIĆ et al. 2024) we have mineralogically and chemically characterized various groups of slags from this area. To stimulate natural weathering conditions, we conducted long-term quiescent-flow leaching experiments. This case study refers to a real-life environmental scenario in which metallurgical slags originating from nickel processing were disposed of, leaving the slag boulders continuously exposed to rainwater during the rainy season. Our objective was to decipher the mobilization of contaminants from metal-bearing slags and to predict their potential environmental impact. The experimental conditions involved immersing the slags in the aqueous solutions adjusted to pH 2.9 and 4.8 for a period of 18 months. The result of the solution chemistry combined with a direct surface observation, indicated the potential for dissolution of individual group of slags and delineated the weathering sequence of phases under specific weathering conditions. The results revealed a pronounced variability in the leaching potential of the studied slags, with the release of nickel (Ni) and cobalt (Co) ranging from <0.01 % to 90 %. The 20-year-old electric furnace slag (IS-A), which used ore imported from Indonesia, emerged as the most effective source of Ni, due to the dissolution of pentlandite and micro- to nano-sized ferronickel grains. Magnesium (Mg) release (up to 1.9–2.1 %) from the IS-A slag also indicated the breakdown of major silicate phases, particularly forsterite. Slags containing magnesiochromite, (IS-C and IS-B) exhibited significant chromium (Cr) mobilization, ranging from 0.3 % to 0.6 %. Additionally, the dissolution of larnite in MS- and CS-samples was confirmed by substantial calcium (Ca) release (at least 13 %) in contrast to other slags lacking this phase. Comparisons between short-term and long-term leaching revealed that the concentration of some elements in the leachate may deplete over time, proving that the precipitation of secondary phases in stagnant conditions is more significant than that observed in a dynamic system. In conclusion, the long-term exposure of metallurgical slags to weathering conditions affects the stability of metal-bearing phases, resulting in the release of contaminants. The materials studied are promising candidates for metal recovery using a (bio)hydrometallurgical approach.

This research was funded by the Wissenschaftlich-Technische Zusammenarbeit (WTZ) of the OeAD [PL 14/2024] and the Polish National Agency for Academic Exchange (NAWA) [BPN/BAT/2023/1/00021]. The analytical research was financed within the framework of the research project OPUS 2023/49/B/ST10/01227 and by the Own Science Development Fund of the Warsaw University of Life Sciences.

ĐORĐEVIĆ, T., TASEV, G., AICHER, C., POTYSZ, A., NAGL, P., LENGAUER, C.L., PEDZIWIATR, A., SERAFIMOVSKI, T., BOEV, I., BOEV, B. (2024): Mineralogy and environmental stability of metallurgical slags from the Euronickel smelter, Vozarci, North Macedonia.–J Appl Geochem, 170, 106068-106081.

Effects of synthesis parameters on the mineralogy and transformation kinetics of waste-derived sodium silicates

S. Raič[1], F. R. Steindl[1,2], M. Dietzel[1], C. Grengg[1]

[1]Christian Doppler Laboratory for Waste-based geopolymer construction materials in the CO_2-neutral circular economy, Institute of Applied Geosciences, Graz University of Technology, Austria
[2]Institute of Technology and Testing of Construction Materials, Graz University of Technology, Austria
e-mail: cyrill.grengg@tugraz.at

The use of soluble silicates in the production of mineral-based construction materials has gathered increasing interest in recent years, particularly in the alkaline activation of aluminosilicate binders. To address environmental and economic challenges, future production of soluble silicates for construction applications should prioritize (i) the valorization of mineral wastes and secondary raw materials, and (ii) the development of low-energy synthesis pathways. This study aims to advance these objectives by systematically investigating sodium silicates synthesized from two silicon-rich waste materials – glass wool (MW) and glass waste (GW) – via thermochemical reactions conducted at 200°C for 3 hours.

A series of experimental design spaces was established to evaluate the influence of key parameters, including waste type, SiO_2/Na_2O molar ratio (modulus, M_s), reaction temperature, and heating duration, on the reactivity of the resulting products. Furthermore, the dissolution behavior of the synthesized products was examined to assess their reactivity.

X-ray diffraction and Fourier-transform infrared spectroscopy analyses revealed that the M_s plays a central role in governing the extent of reaction and the nature of crystalline phases formed. The highest conversion efficiencies (i.e. how much SiO_2 was transformed into a soluble form), 95 wt.% for GW and 78 wt.% for MW, were achieved at M_s values exceeding 0.79 and 0.78, respectively, with Na-metasilicates (e.g. disodium silicate, sodium silicate) and Na-carbonates (e.g. natrite, thermonatrite) identified as the primary crystalline phases. Notably, at lower M_s values (<0.78), the MW system exhibited a noticeable/significant increase in amorphous phase content (up to 70 wt.% at M_s = 0.34), whereas the GW system maintained high crystallinity, predominantly forming natrite.

The greatest degree of silica dissolution was observed at elevated M_s values of 0.89 (GW) and 0.87 (MW), corresponding to mineralogical compositions with 44 wt.% and 37 wt.% Na-metasilicates, 14 wt.% and 12 wt.% Na-carbonates, and residual amorphous fractions of 40 wt.% and 51 wt.% for GW and MW systems, respectively.

Using mineralogical and chemical analysis for evaluating the application potential of Austrian mineral wastes in alkali-activated materials

B. Ratz[1,2], K. P. Sedlazeck[2], A. Hassan[1,3], S. Radinger[1,3], S. Raič[1,3], F. R. Steindl[1,3,4], C. Grengg[1,3]

[1]Christian Doppler Laboratory for Waste based geopolymer construction materials in the CO_2 neutral circular economy ($GECCO_2$),
[2]Chair of Waste Processing Technology and Waste Management, Technical University of Leoben, Austria,
[3]Institute of Applied Geosciences, Graz University of Technology, Austria,
[4]Institute of Technology and Testing of Construction Materials, Graz University of Technology, Austria,
e-mail: bettina.ratz@unileoben.ac.at

Mineral waste is the largest waste stream in Austria, comprising 76% of the total waste arisings, with the majority still being landfilled. The generation of mineral waste has significantly increased over the last decades, also in part due to the building and construction industry, which is simultaneously responsible for considerable amounts of CO_2 emissions and the consumption of primary resources. To support circular economy goals, this contribution explores the potential of utilizing mineral wastes in geopolymers – also known as alkali-activated materials (AAM) – which are sustainable inorganic binders formed by activating aluminosilicate precursors with alkaline solutions, resulting in performance properties comparable to conventional cement. Relevant Austrian mineral wastes and secondary raw materials (WSRM) were identified and evaluated for their suitability as reactive precursors for AAM production. Their chemical and mineralogical properties, including amorphous content and reactive phase composition, were characterized using X-ray fluorescence (XRF) and X-ray diffraction (XRD). The XRD results were used to determine the amorphous content of the materials, applying Rietveld refinement. The fundamental reactivity was further assessed through systematic paste mixtures with varying formulations with Si/Al ratios ranging from 1.5 to 2.5. The resulting AAM pastes were analyzed for workability, visual setting behavior, and 7-day compressive strength.

The resulting dataset represents a comprehensive mineralogical and chemical characterization of various WSRM streams, as well as insights into their contribution mechanisms, such as chemical and physical effects, in the AAM system.

Cambrian arc magmatism and Variscan metamorphic overprint in the Ötztal-Stubai Complex: Insights from U–Pb zircon dating and geochemical data

M. Reiser[1], C. Iglseder[1], B. Huet[1], C. Költringer[1], M. Linner[1]

[1]GeoSphere Austria, Wien, Österreich,
e-mail: martin.reiser@geosphere.at

New U-Pb zircon ages and geochemical analyses from the Stubai Alps (Eastern Alps) offer insights into the early Paleozoic evolution of the Ötztal-Stubai Complex and its subsequent overprint during the Variscan orogeny. Our study targets an assemblage of metasedimentary rocks, amphibolite, and small tonalitic bodies in the upper Stubai Valley. The rocks are exposed in the hinge zone of a kilometer-scale, eastward plunging antiform near the locality Ranalt (Tyrol).

Geochemical signatures from the different lithologies are all consistent with a volcanic island arc setting with magmatic activity from both mafic and felsic sources. Metasediment analyses show trace element ratios (high La/Yb, low Nb/Y and Th/Sc) as well as high Ba and Sr values that clearly indicate a volcanic island arc or active magmatic arc setting. Amphibolite geochemistry reveals low-Ti, subalkaline compositions with LREE enrichment, strong Nb–Ta depletion, and elevated Ba/Th and Ba/Nb ratios – typical of arc tholeiites derived from a subduction-modified mantle source.

Coarse-grained tonalite, featuring garnet, zoned epidote, and deformed K-feldspar, displays a peraluminous composition with high LREE concentrations (La = 75.5 ppm, Ce = 150 ppm), elevated Ba (1049 ppm), and pronounced Nb-Ta depletion. This geochemical fingerprint indicates a fluid-enriched, evolved crustal melt, likely sourced from partial melting of metasedimentary rocks in water-undersaturated conditions.

U–Pb LA-ICP-MS zircon dating of several orthogneiss samples provides new information on the Cambrian to Ordovician genesis. The new data constrain the crystallization of the tonalite to the Cambrian (506 Ma). Non-zoned metamorphic overgrowth rims from the same sample yield an age of 345 Ma potentially documenting metamorphism during Early Variscan continental collision. Additional microstructural evidence from the metasediments and amphibolites, such as rutile inclusions in centimeter-sized garnet porphyroblasts and ilmenite exsolution lamellae, supports a metamorphic overprint at rather high pressure in the amphibolite facies.

Together, the petrological, geochemical, and geochronological data document the presence of a remnant Cambrian volcanic arc, subsequently overprinted by Variscan metamorphism. These findings refine the pre-Alpine tectonometamorphic history of the Ötztal-Stubai Complex and provide new constraints on its lithodemic succssion, one of the objectives of the ongoing EAGLe Project at GeoSphere Austria.

Impact of mineral composition on CO_2 sequestration efficiency in Ca-rich steel slags

S. Reiter[1], M. Lehner[1]

[1]*Chair of Process Technology and Environmental Protection, Technical University of Leoben, Austria*
e-mail: sarah.reiter@unileoben.ac.at

Carbonation of primary and secondary minerals is a promising pathway for long term CO_2 storage. During direct, aqueous carbonation, a mineral powder rich in Ca- or Mg-bearing minerals is suspended in water, where CO_2 is subsequently introduced to under elevated pressures and temperatures. This study investigates the CO_2 uptake of blast furnace (BF) and basic oxygen furnace (BOF) slag during direct aqueous carbonation under four distinct experimental conditions. Based on their chemical compositions, the theoretical maximum CO_2 uptakes are 216.3 kg t^{-1} and 387.8 kg t^{-1} for the BF and the BOF slag sample, respectively. The slags differ significantly in their mineralogical composition: BF slag contains gehlenite ($Ca_2Al_2SiO_7$) and β-belite (Ca_2SiO_4 polymorph) as primary Ca-bearing minerals, while the BOF slag is dominated by β-belite and brownmillerite ($Ca_2(Al,Fe)_2O_5$), as identified by semi-quantitative X-ray diffraction (XRD) analysis (Fig. 1). Carbonation experiments are conducted under varying temperature (20 and 100 °C) and CO_2 pressure (5 and 20 bar) conditions, with additional tests incorporating $NaHCO_3$ and NaCl to the aqueous phase. The CO_2 uptake is then determined via thermogravimetric analysis (TGA). The LD slag consistently exhibits higher CO_2 uptakes and carbonation efficiency than the BF slag, achieving a maximum of 150 kg CO_2 t^{-1} at 20°C and 20 bar. The β-belite phase is identified as the most reactive carbonate-forming mineral. In contrast, gehlenite in BF slag shows poor reactivity, limiting the CO_2 uptakes to below 35 kg t^{-1} across all conditions. Elevated temperatures slightly improved carbonation in BF slag via enhanced Ca-silicate dissolution, while BOF slag performance declined marginally at 100 °C, likely due to reduced CO_2 solubility and pH effects. Overall, the results demonstrate that carbonation potential is strongly governed by mineralogical composition, highlighting the need for targeted dissolution of reactive phases to optimize CO_2 sequestration.

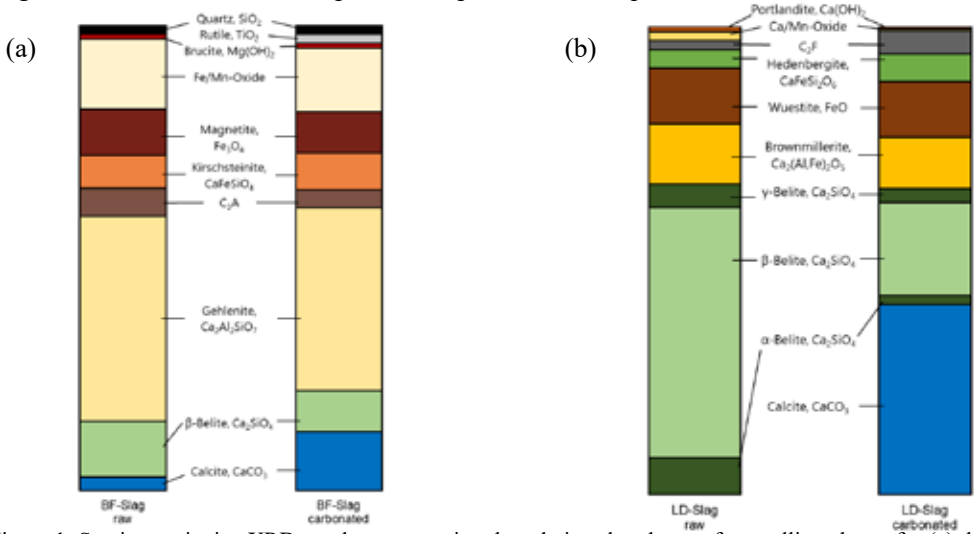

Figure 1: Semi-quantitative XRD-results representing the relative abundance of crystalline phases for (a) the raw BF-slag and the carbonated sample at 20 bar, 100 °C and (b) the raw LD-slag and the carbonated sample at 20 bar, 20°C

Is there radiation damage in baddeleyite (ZrO_2)?

K.A.G. Sameera[1,2], A. Brazzoli[1,3], C. Chanmuang N.[1], L. Nasdala[1]

[1]Universität Wien, Vienna, Austria
[2]Geological Survey and Mines Bureau, Pitakotte, Sri Lanka
[3]Università degli Studi di Milano Statale, Milan, Italy
e-mail: lutz.nasdala@univie.ac.at

It has long been discussed controversially as to which degree the mineral baddeleyite (ZrO_2; monoclinic space group $P2_1/c$) is prone to the long-term accumulation of self-irradiation damage that arises from the decay of incorporated radioactive elements. Such information is, among others, of interest in interpreting results of U-Pb dating or O-isotope analyses (DAVIES et al. 2018). LUMPKIN (1999) found that baddeleyite remains basically un-damaged whereas DAVIES et al. (2018) assigned increased Raman-band widths of the Phalaborwa baddeleyite, compared to that of synthetic ZrO_2, to initial stages of "metamictisation".

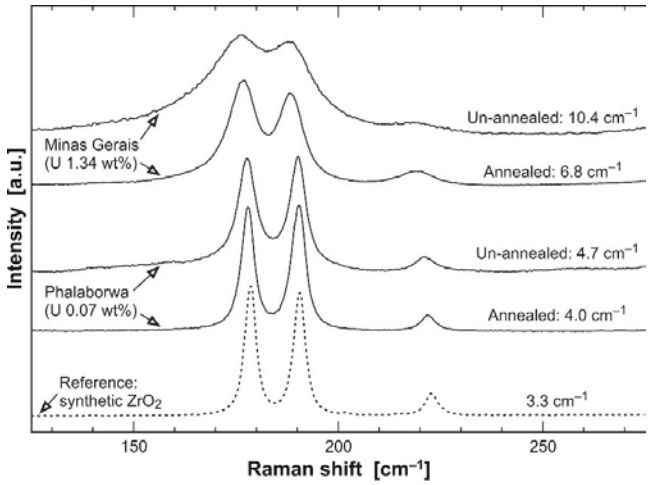

Figure 1: Raman spectra (633-nm excitation) of un-annealed and annealed aliquots of baddeleyite samples from Minas Gerais, Brazil, and Phalaborwa, RSA, in comparison with the spectrum of synthetic monoclinic ZrO_2. Spectra are labelled with the full width at half maximum (FWHM) of the Raman band at ~190 cm^{-1}. Note that differences in band-intensity ratios are due to random sample orientations. Spectra have normalised intensity and are shown with vertical offset for clarity.

We have subjected Phalaborwa baddeleyite, and a particularly U-rich Brazilian baddeleyite, to a thermal-annealing-and-Raman study. As a reference, pure ZrO_2 was synthesised from synthetic $ZrSiO_4$ following VÁCZI et al. (2009). Annealing for 48 h at 1400 °C resulted in notable decreases of band FWHMs. However, even fully annealed natural samples yielded much broader FWHMs than the chemically pure reference, with FWHMs being correlated with the amounts of non-formula elements. Hence FWHMs are mainly controlled by "chemical broadening" (compare RUSCHEL et al. 2012) whereas the extent of structural disorder in baddeleyite, even after elevated self-irradiation, seems to be rather moderate.

DAVIES, J.H.F.L., STERN, R.A., HEAMAN, L.M., MOSER, D.E., WALTON, E.L., VENNEMANN, T. (2018): Evaluating baddeleyite oxygen isotope analysis by secondary ion mass spectrometry (SIMS). – Chem Geol, 479, 113–122.

LUMPKIN, G.R. (1999): Physical and chemical characteristics of baddeleyite (monoclinic zirconia) in natural environments: an overview and case study. – J Nucl Meth, 274, 206-217.

RUSCHEL, K., NASDALA, L., KRONZ, A., HANCHAR, J.M., TÖBBENS, D.M., ŠKODA, R., FINGER, F., MÖLLER, A. (2012): A Raman spectroscopic study on the structural disorder of monazite–(Ce). – Miner Petrol, 105, 41-55.

VÁCZI, T., NASDALA, L., WIRTH, R., MEHOFER, M., LIBOWITZKY, E., HÄGER, T. (2009): On the breakdown of zircon upon "dry" thermal annealing. – Miner Petrol, 97, 129-138.

Poly-metamorphic evolution and associated magmatic activity in the Inthanon zone, northern Thailand

S. Santitharangkun[1], C. A. Hauzenberger[1], E. Skrzypek, D. Gallhofer.[1]

[1] Department of Earth Sciences - NAWI Graz Geocenter, University of Graz, Graz, Austria
e-mail: srett.santitharangkun@uni-graz.at

The Inthanon core complex, a segment of the western gneissic belt in northern Thailand, records a multifaceted geological history characterized by multiple episodes of metamorphism following a clockwise P–T–t path and granitoid emplacements linked to the Indosinian orogeny, Neo-Tethys subduction, and the India-Eurasia collision. To decipher the complex thermal and deformational history of the Inthanon core complex, we investigated diverse lithologies, including Grt-paragneiss from the western domain and orthogneiss from the eastern domain and granitic bodies. U–Pb monazite dating of Grt-paragneiss reveals a Late Triassic (240–210 Ma) high-temperature, medium-pressure metamorphic event (M1), characterized by conditions of 680–720 °C and 0.55–0.70 GPa. This event, contemporary with the Indosinian orogeny, is also corroborated by zircon and monazite ages from associated orthogneiss and granite. A subsequent phase of thermal activity and metamorphism around 80 Ma (Late Cretaceous) led to a second garnet growth and breakdown (M2) in the paragneiss, commencing under upper amphibolite facies conditions, reaching 620–680 °C and 0.35–0.55 GPa. Evidence for this M2 event is also found in zircons from associated granitic bodies and recrystallized magmatic monazites within the orthogneiss. Furthermore, monazite, partially recrystallized within orthogneiss, is directly associated with localized granitic melts emplaced between 40 and 20 Ma. These results provide crucial evidence for a third high-grade metamorphic event (M3) under P-T conditions of 640–710 °C and 0.60–0.80 GPa. Our findings reveal a multi-stage tectonic evolution: a Late Triassic–Early Jurassic metamorphic event in the western domain, evidenced by Grt-paragneiss formation during crustal thickening and nappe tectonics associated with the Sibumasu-Sukhothai collision, at the same time granite emplacement in occurred in the eastern domain. This was followed by a Late Cretaceous thermal event across both domains, linked to Neo-Tethys subduction. A later Eocene-Miocene metamorphic event, preserved only in orthogneiss in the eastern domain, suggests localized transpressional thickening and subsequent isothermal-decompression melting that generated small granitic bodies and pegmatite veins during the India-Eurasia collision.

Petrography and geochemistry of tholeiitic basalts from Mt. Etna's early eruptive units

P. Schilcher[1], C. A. Hauzenberger[1], F. Casetta[2], G. Lanzafame[3]

[1]Department of Earth Sciences, University of Graz, Graz, Austria,
[2]Department of Lithospheric Research, University of Vienna, Vienna, Austria
[3]Department of Biological, Geological and Environmental Sciences, University of Catania, Catania, Italy
e-mail: p.schilcher@edu.uni-graz.at

The earliest volcanic activity of Mount Etna provides insights into the development of the volcano's magmatic plumbing system and the dynamics of its mantle source. Although the later stages of Etna's alkaline volcanism are well understood, the mechanisms controlling the initial tholeiitic phase and the subsequent transitional to alkaline compositions are unclear.

Here, we present a petrographic and geochemical study of primitive rocks from the Basal Tholeiitic Supersynthem on Mt. Etna's southeastern and southwestern flanks. These early eruptive products exhibit variations in texture, mineral composition and geochemistry.

Samples from the Aci Trezza Synthem, representing Mt. Etna's initial subaqueous stage, were collected from coastal outcrops (Aci Castello, Aci Trezza) and the Cyclopean Islands (Isola Lachea). They display a range of textures from porphyritic with glassy groundmass to fully crystalline and contain varying proportions of olivine, plagioclase, and clinopyroxene phenocrysts. Samples from the coast contain more olivine, whereas samples from the island have a higher pyroxene content and higher whole-rock alkalis. The Adrano Synthem, which corresponds to a later subaerial eruptive phase, includes samples from Motta Sant'Anastasia, Paterno, Adrano and Biancavilla. These samples typically show coarser crystalline textures and phenocryst assemblages that are similar to those in the coastal samples.

For comparison, primitive samples from the alkaline stage, i.e. basalts from Mt. Maletto (eruption 1350±50 AD) have a glassy to microcrystalline groundmass and show relatively low nickel concentrations (~50 ppm), as well as a limited geochemical evolution. Whole-rock compositions suggest relative enrichment in alkalis with respect to tholeiitic basalts.

Electron microprobe analyses across all locations reveal systematic zoning in olivine, pyroxene, and plagioclase. Zoned olivine crystals display Mg# of 60–86 in the Aci Trezza Synthem, 48–83 in the Adrano Synthem. The Mg# of the pyroxenes are 41–85 for the Aci Trezza Synthem, 47–84 for the Adrano Synthem. Mt. Maletto alkali basalts are composed of $Fo_{71–90}$ olivine and clinopyroxene with Mg# = 45–85. Zoned olivines exhibit a decline in NiO (0.005-0.4 wt%) with decreasing Mg# for all locations, while zoned pyroxenes show a corresponding decrease in chromium content. Ni trends are particularly pronounced in samples from Paterno (0.01-0.4 wt%), where olivines exhibit Mg# of 74–83. Additionally, olivines from Motta Sant'Anastasia form two distinct groups with Mg# ranging from 60 to 68 and from 76 to 84, respectively.

Geochemical trends indicate fractional crystallisation for tholeiitic samples, while textural features and a wider Mg# range in the Adrano Synthem suggest more advanced, complex processes during magma evolution.

CASETTA, F., GIACOMONI, P., FERLITO, C., BONADIMAN, C., & COLTORTI, M. (2019). The evolution of the mantle source beneath Mt. Etna (Sicily, Italy): From the 600 ka tholeiites to the recent trachybasaltic magmas. International Geology Review, 62(5–6). https://doi.org/10.1080/00206814.2019.1610979

GIUFFRIDA, M., NICOTRA, E., & VICCARO, M. (2024). How an embryonic magma feeding system evolves: Insights from the primordial pulses of Mt. Etna volcano. Journal of Volcanology and Geothermal Research, 451, 108113. https://doi.org/10.1016/j.jvolgeores.2024.108113

Tracing Neolithic toolstone procurement: Mineralogical and geochemical characterization of amphibole-bearing metabasites in the Jizera Mountains (Bohemian Massif)

I.-L. Schmidt[1,2], M. Brandl[2], M. Gostencnik[1], C. A. Hauzenberger[1]

[1]Department of Earth Sciences, University of Graz, Austria,
[2]Austrian Academy of Sciences, Vienna, Austria,
e-mail: Ischmidt554@gmail.com

Amphibolite lenses from the Jizera Mountains (Northern Bohemia, Czech Republic) represent a significant source of potential raw materials for Neolithic stone tool production due to their favorable physical properties and resistance to weathering. Recent archaeological investigations suggest that these amphibolites were exploited from the early Neolithic period (Linear Pottery Culture, c. 5700/5500–4900 BC) to the Stroke Pottery Culture (c. 4900–4400 BC) and distributed throughout Northern and Central Europe, roughly between Southern Scandinavia and the Eastern Alps. While the general characteristics of the Neolithic communities involved in the use and distribution of artefacts made from this particular lithic raw material are well studied, little is known about the economic background governing this extensive distribution. Lithic economy can be best understood by investigating the underlying resource management strategies employed by the Neolithic agents, which requires the sound determination and fingerprinting of the raw materials to test possibilities of tracing them back to their geological sources.

Therefore, this study aims to geochemically characterize these amphibolite sources and to evaluate their provenance potential based on mineral chemistry and crystallographic features from six localities in the southern Jizera mountains. The amphibolite samples were investigated using X-ray diffraction (XRD) and electron microprobe analysis (EPMA). The regional tectonic setting is characterized by complex Variscan metamorphism within a crystalline basement composed of amphibolites, metagabbros, and gneisses, affected by amphibolite to greenschist facies overprints.

Zoning within amphiboles was consistently observed, primarily in Fe and Ca distributions, indicating successive crystallization under varying PT conditions. The homogenous fine-grained samples include amphibole, feldspar, ilmenite, and quartz. With an average grain size of 0.02 mm. EPMA results show amphiboles of both the calcic group (tremolite, actinolite, hornblende) and the Fe-Mg group (cummingtonite–grunerite series), with the average of X_{Mg} ~0.50 in Fe-Mg group and X_{Mg} ~0.57 in the calcic group. Particularly, cummingtonite and grunerite appear as Fe-rich rims, forming textural intergrowths with hornblende or actinolite. Ca-Mg amphiboles crystallized under amphibolite-facies pressure-temperature conditions, whereas Fe-rich types indicate subsequent recrystallization under lower thermal gradients and reduced Ca activity. These mineralogical differences are related with variations in protolith composition and fluid-rock interaction.

The chemical zoning correlates with distinct unit-cell sizes. Fe-rich amphiboles like grunerite and cummingtonite display slightly smaller unit-cell parameters compared to actinolite, consistent with previous crystallographic models. XRD-derived unit-cell volumes further support this distinction: tremolite and actinolite show larger volumes (~916–920 Å³), whereas grunerite and cummingtonite exhibit smaller volumes (~902–908 Å³), consistent with Fe-for-Mg substitution. XRD results will be linked to EPMA results to enable future chemical interpretation based on unit-cell sizes, as artifact material is too limited for routine microprobe analysis.

A brief Late Cretaceous magmatic pulse based on geochemical data from accessory zircon (Mt. Papuk, Croatia)

P. Schneider[1], D. Gallhofer[2], E. Skrzypek[2], C. A. Hauzenberger[2], D. Balen[1]

[1]Department of Geology, Faculty of Science, University of Zagreb, Zagreb, Croatia,
[2]Department of Earth Sciences, NAWI Graz Geocenter, University of Graz, Graz, Austria,
e-mail: pschneider@geol.pmf.unizg.hr

The Slavonian Mts. (including Mt. Papuk), located in the southwestern part of the Pannonian Basin in Croatia, consist mostly of pre-Alpine igneous and metamorphic rocks, which represent the outcrops of the crystalline basement known as Tisia Mega-Unit (PAMIĆ & LANPHERE 1991; SCHMID et al. 2020). In the northwestern part of Mt. Papuk, however, dyke swarms of younger igneous rocks cut through the migmatitic gneisses and granitoid basement rocks. These younger rocks with varying compositions are classified as basalts, andesites and rhyolites. Their mineral and chemical composition reflect the high-temperature, dry and oxidised nature of magmas typical of divergent settings, with A-type geochemical signature for acidic varieties (SCHNEIDER et al. 2022).

Accessory zircon from four rhyolite and one andesite sample was used to unveil the timing of the magmatic event and constrain the origin of the parental magma. Zircon age dating by LA-ICP-MS reveals a Late Cretaceous (between 81.1±1.1 and 81.5±1.1 Ma) and brief (< 3 million years) magmatic pulse. The geochemical record of zircon (trace elements and Hf isotopes) indicates its magmatic origin and an early crystallisation timing in a deep magma chamber at a relatively high (~850 ºC) and constant temperature. The parental magma was derived from melting of Palaeozoic continental crust with a juvenile mantle component, either directly from mantle-derived melts or remelting of mantle-derived mafic lower crust. The new data from accessory zircon support previous geodynamic models, which propose the formation of deep rifts and melting in a late- or post-orogenic setting following the Late Cretaceous closure of the Neotethys Ocean (BELAK et al. 1998; SCHNEIDER et al. 2022). The magma may have formed by partial melting of mantle material that was located above a subduction zone, interacted to some extent with the overlying, slightly thickened crust (up to 42 km), but was not extensively contaminated by older continental crust, and underwent extensive fractional crystallisation and differentiation during its rapid ascent through the crust.

BELAK, M., HALAMIĆ, J., MARCHIG, V., TIBLJAŠ, D. (1998): Upper Cretaceous–Paleogene tholeiitic basalts of the southern margin of the Pannonian Basin: Požeška gora Mt. (Croatia). – Geol Croat, 51, 163-174.

PAMIĆ, J., LANPHERE, M. (1991): Hercynian granites and metamorphic rocks from the Papuk, Psunj, Krndija and the surrounding basement of the Pannonian Basin (Northern Croatia, Yugoslavia). – Geologija Ljubljana, 34, 81-253.

SCHMID, S.M., FÜGENSCHUH, B., KOUNOV, A., MATENCO, L., NIEVERGELT, P., OBERHÄNSLI, R., PLEUGER, J., SCHEFER, S., SCHUSTER, R., TOMLJENOVIĆ, B., USTASZEWSKI, K., VAN HINSBERGEN, D.J.J. (2020): Tectonic units of the Alpine collision zone between Eastern Alps and western Turkey. – Gondwana Res, 78, 308-374.

SCHNEIDER, P., BALEN, D., OPITZ, J., MASSONNE, H.-J. (2022): Dating and geochemistry of zircon and apatite from rhyolite at the UNESCO geosite Rupnica (Mt. Papuk, northern Croatia) and the relationship to the Sava Zone. – Geol Croat, 75, 249-267.

Chemical characterization of fahlore (tetrahedrite–tennantite solid solution series) from different tectono-stratigraphic units in North Tyrol

E. Schreieck, P. Tropper, C. Patten

Institute of Mineralogy and Petrography, University of Innsbruck, Innsbruck, Tyrol, Austria
e-mail: elias.schreieck@student.uibk.ac.at

Fahlore minerals of the tetrahedrite–tennantite solid solution series are of both scientific and economic relevance, occurring in a wide range of ore deposit types including porphyry-epithermal systems, skarns, orogenic gold deposits, and metamorphosed base metal mineralizations. Their variable chemical composition is controlled by multiple geological factors such as host lithology, fluid chemistry, mineral paragenesis and metamorphic overprint. In North Tyrol, fahlore is abundant and has been extensively mined in the past, yet many fahlore-bearing mineralizations remain underexplored with respect to their geochemical systematics, genesis, and resource potential.

This study presents a comparative geochemical investigation of fahlore from approximately 80 localities across various tectono-stratigraphic units in North Tyrol. These mineralizations are largely associated with regionally metamorphosed units and exhibit diverse genetic backgrounds and mineral associations. In-situ microanalytical techniques (SEM-EDX/WDX, LA-ICP-MS, and μ-XRF mapping) are applied to characterize major and trace element compositions and to assess the influence of geological parameters such as lithology, metamorphic grade and paragenesis on element enrichment and distribution.

A particular focus is placed on elements of the EU Critical Raw Materials list, such as Cu, Sb, Bi, Co, and Ge. Previous work on the chemical composition of Alpine tetrahedrite-tennantite (SCHROLL & AZER IBRAHIM, 1985) is re-evaluated using state-of-the-art methods. By integrating mineral chemistry with regional geological context, this study aims to improve the genetic understanding of Alpine fahlore deposits and assess their potential as future sources of critical metals.

SCHROLL, E., AZER IBRAHIM, N.: Beitrag zur Kenntnis ostalpiner Fahlerze. Teil III. Geochemische Untersuchungen ostalpiner Fahlerze.- TMPM, III.F., 7, (1-2), p. 70-105, Vienna, 1961.

Metallogenesis and sulphide-hosted critical and precious metals in epithermal Au and porphyry Cu deposits of Iran

E. Sist[1], V. Bertrandsson Erlandsson[2], M. Ghasemi Siani[3], A. Dolati[3], F. Melcher[2]

[1]Department of Mathematics, Informatics and Geosciences, University of Trieste, Trieste, Italy,
[2]Department of Applied Geosciences and Geophysics, Technical University of Leoben, Leoben, Austria,
[3]Faculty of Earth Sciences, Kharazmi University, Tehran, Iran,
e-mail: EFREM.SIST@studenti.units.it

The Alpine-Himalayan Tethyan orogenic belt, a major mountain system extending for over 12,000 km from the Alps to Tibet, formed as a result of the Mesozoic-to-Cenozoic closure of the Paleo-Tethys and Neo-Tethys Oceans (ALTENBERGER et al., 2022). Situated in the Alpine-Himalayan belt, Iran experienced several orogenic phases, with the most significant geological and metallogenic evolution occurred during the Alpine-Himalayan orogeny (Late Mesozoic-Cenozoic), driven by the subduction of the Neo-Tethys Ocean.

This period was marked by a complex combination of tectonic, magmatic and metallogenic processes, leading to the formation of a wide range of economically valuable deposits. Among these, porphyry Cu ± Mo ± Au and epithermal Au ± Cu deposits emerged as the dominant types (RICHARDS, 2015). While Iran's surface deposits are relatively well understood due to its mining history, sparse vegetation, and decades of exploration (GHORBANI, 2013), many regions of Iran remain underexplored and are believed to still hold untapped mineral potential.

In this study, we aim to expand the current understanding of magmatic-hydrothermal mineralisation in Iran by analysing major and trace elements in key sulphide minerals (pyrite, chalcopyrite, arsenopyrite, sphalerite, pyrrhotite) using scanning electron microscopy (SEM) and laser ablation inductively coupled plasma mass spectrometry (LA-ICP-MS) techniques. The goal is to constrain the physico-chemical conditions of ore formation and assess the critical and precious metal potential of these underexplored deposits.

Samples were collected from 11 newly discovered mineral deposits and occurrences from different major tectono-magmatic zones across Iran. They include: the Oshvand skarn Fe-Cu deposit and the Hassan Abad, Hossein Abad, and Dare Sari epithermal or orogenic Cu-Au deposits in the Sanandaj–Sirjan Zone; the Shahr-Babak and Maran Qaleh epithermal Au deposits in the Urumieh–Dokhtar Magmatic Arc; the Bazman and Janja epithermal–porphyry systems in the Makran volcanic belt; and the Hired and Godakan deposits in the Lut Block.

The Bazman pyrite exhibits promising contents of precious metals like Au and Ag (median values up to 7.81 ppm and 9.14 ppm, respectively), as well as notable levels of Sb and Te (median values up to 5.40 ppm and 8.43 ppm, respectively). In contrast, it shows limited enrichment in critical metals such as Ni and Co. The Bazman chalcopyrite contains In as the only notable critical metal, with a median concentration up to 9.85 ppm. Ongoing analyses of minerals from other deposits will further clarify metallogenic trends across the region.

ALTENBERGER, F. P., RAITH, J. G., BAKKER, R. J., ZARASVANDI, A. (2022): The Chah-Mesi epithermal Cu-Pb-Zn-(Ag-Au) deposit and its link to the Meiduk porphyry copper deposit, SE Iran: Evidence from sulfosalt chemistry and fluid inclusions. – Ore Geo Rev, 142, 104732.

GHORBANI, M. (2013): The Economic Geology of Iran: Mineral Deposits and Natural Resources. – 569 p., Springer Geology.

RICHARDS, J. P. (2015): Tectonic, magmatic, and metallogenic evolution of the Tethyan orogen: From subduction to collision. – Ore Geo Rev, 70, 323-345.

Carbonate-bearing alkaline syenite magmatism in Quarter eruptive centers of the Eifel

M. A. Sitnikova[1], S. Sindern[2], S. Goldmann[1], G. Jacques[1], U. Kramm[2]

[1]Federal Institute for Geosciences and Natural Resources, BGR, Hannover
[2]RWTH Aachen University, Aachen
e-mail: MariaAlexandrovna.Sitnikova@bgr.de

The Quaternary Rockeskyller Kopf Volcanic Complex (RKVC) of the western Eifel contains a series of plutonic to sub-volcanic xenoliths that correspond to a full sequence of rocks, which are characteristic of alkaline-ultramafic magmatic complexes with carbonatites worldwide. Calcite-bearing foiditic lapilli are abundant in pumice layers of the RKVC. Calcite also forms spherical globules in unhydrated foiditic glass shards and inclusions entrapped in olivine and clinopyroxene phenocrysts of palagonite tuffs from RKVC.

Carbonate-bearing nosean syenites are observed in plutonic to sub-volcanic xenoliths from Laacher See volcano (LSV) as well. They have variable calcite proportion and locally have carbonatitic composition. In both occurrences, the main rock-forming carbonate is calcite. It is associated with apatite, magnetite, phlogopite, and pyrochlore, comprising a typical carbonatite paragenesis worldwide.

The description of major textural characteristics of carbonate-bearing alkaline syenite rocks of RKVC and LSV, their geochemistry, Sr/Nd and C/O isotopic signatures of carbonate fractions and calcite mineral chemistry are presented.

The chondrite-normalized REE patterns for carbonate-bearing nosean syenite, mafic xenoliths, and carbonate-bearing lapilli of RKVC show similarities to each other and to other carbonatites and alkaline syenites worldwide. All samples have smooth chondrite-normalized REE patterns with strong LREE enrichment. The REE patterns of the carbonate-bearing nosean syenites of LSV, on the other hand, show different patterns with a depletion of the heavy REEs and a negative Eu anomaly, which is unusual for such rocks.

Based on petrographic, geochemical and mineral chemical evidence of these rocks, we assume magmatic carbonate formation in a highly fractionated undersaturated silicate magma. The petrographic spectrum of the studied xenoliths allows a comparison with occurrences of older alkaline rocks in which a vertical zoning from ultramafic units at greater depth and increasingly alkaline syenite composition at higher levels is observed. The proportion of carbonatitic rocks also increases at higher levels and is accompanied by an increased proportion of volatiles.

The RKVC and LSV can be considered as volcanic segments of alkaline magmatic systems extending over great depths. The high proportion of ashes and pumice layers, as well as volatile-containing phases of subvolcanic formations, indicate the high proportion of volatiles in this system.

Rotemite (6*R*), $Ca_4Cr_2(OH)_{12}Cl_2 \cdot 4\,H_2O$ – natural Cr-bearing lamellar double hydroxide, Ca_2Cr-LDH

K. Skrzyńska[1,2], H. Müller[2], R. Juroszek[1], B. Krüger[3], G. Cametti[4], A. Pakhomova[2], I. Galuskina[1], Y. Vapnik[5], K. Woźniak[6], E. Galuskin[1]

[1]Faculty of Natural Sciences, University of Silesia in Katowice, Poland
[2]European Synchrotron Radiation Facility, Grenoble, France
[3]Institute of Mineralogy and Petrography, University of Innsbruck, Austria
[4]Institute of Geological Sciences, University of Bern, Switzerland
[5]Department of Geological and Environmental Sciences, Ben-Gurion University of the Negev, Beer-Sheva, Israel
[6]Department of Chemistry, University of Warsaw, Poland
e-mail: katarzyna.skrzynska@us.edu.pl

A new mineral, rotemite, $Ca_4Cr_2(OH)_{12}Cl_2 \cdot 4H_2O$ (IMA 2024-058), represents the first Cr-bearing member of the hydrocalumite group, within the hydrotalcite supergroup, part of a broader family of lamellar/layered double hydroxides (LDH). Recently, LDH compounds including Ca_2Cr-LDH, have attracted considerable attention due to their ion-exchange and catalytic properties (SZABÓ et al. 2025). However, their accurate characterization is scarce, as they are prone to crystallize in a multiphase powder form. Herein, the multi-methodological investigation of a natural sample enabled, for the first time, an unambiguous determination of the physical and optical properties of Ca_2Cr-LDH, including crystal structure and chemical composition. Rotemite was discovered in low-temperature rocks of the Hatrurim Complex, Israel. It occurs as tiny hexagonal platelet-shaped crystals, appearing pale bluish-violet in daylight and pinkish-violet under artificial light. The mineral has a Mohs hardness of 2.5–3. Optically, rotemite is negatively uniaxial with $\omega = 1.565(2)$, $\varepsilon = 1.544(2)$ ($\lambda = 589$ nm). Empirical formula $(Ca_{3.94}Sr_{0.01})_{\sum 3.95}(Cr^{3+}_{1.47}Al_{0.52}Fe^{3+}_{0.05})_{\sum 2.04}(OH)_{12}[Cl_{1.68}(OH)_{0.32}(SO_4)_{0.01}]_{\sum 2.01} \cdot 4H_2O$ was yielded by microprobe analysis. Rotemite exhibits a rare 6-layered LDH polytype structure, with a trigonal symmetry ($R\bar{3}c$) and unit cell parameters: $a = b = 5.7944(2)$ Å, $c = 46.69(4)$Å, $V = 1357.7(10)$Å^3. The main motif of the structure is hydrocalumite-type layers $[Ca_4(Cr,Al)_2(OH)_{12}(H_2O)_4]^+$ with intercalated Cl^- ions. In these layers, Ca^{2+} is sevenfold coordinated by six OH^- groups and one H_2O molecule, where 3^+ cations (Cr, Al) are octahedrally coordinated with six OH^- groups. Raman spectra of rotemite are characterized by a prominent band at ~525 cm^{-1}, typical of LDH compounds. Polarized Raman spectroscopy revealed that signals from O–H stretching vibrations at 3441-3442cm^{-1} and 3609-3612 cm^{-1} strongly depend on the crystal orientation, indicating an ordered arrangement of water molecules and a perpendicular arrangement of O–H bonds within the hydrocalumite layers, respectively.

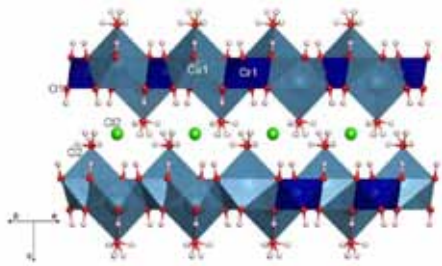

Figure 1: Part of the rotemite structure, with two hydrocalumite-type layers and intercalated Cl^- ions (green). In dark-blue are presented $(Cr,Al)OH_6$ octahedra, pale blue $Ca(OH)_6(OH_2)$ polyhedra, red O atoms and pink H atoms

SZABÓ, V., MÉSZÁROS, R., KUTUS, B., SAMU, G.F., KÓNYA, Z., KUKOVECZ, Á., SIPOS, P., SZABADOS, M. (2025): Sonochemically improved regeneration of mechanically amorphized Ca_2Cr-layered double hydroxides – Synthesis, characterization and photocatalytic lidocaine decomposition. – App. Clay Sci. 265.

Fluid-absent and fluid-present alteration of magmatic monazite in Variscan crystalline rocks from Mt. Papuk (Croatia)

E. Skrzypek[1], D. Gallhofer[1], D. Balen[2], P. Schneider[2], C. A. Hauzenberger[1]

[1]Department of Earth Sciences, NAWI Graz Geocenter, University of Graz, Graz, Austria,
[2]Department of Geology, Faculty of Science, University of Zagreb, Zagreb, Croatia,
e-mail: etienne.skrzypek@uni-graz.at

Monazite is commonly used to date magmatic or metamorphic processes, but is also prone to alteration reactions. These reactions must be understood in order to assess the geochronological robustness of monazite. We present two contrasting monazite alteration textures found in two different lithologies from Mt. Papuk (Slavonian Mts., Croatia). The aim is to understand monazite formation and alteration in order to assess the timing of thermal events in this portion of the European Variscan belt. For a migmatite and peraluminous granite sample, we document the texture and composition of monazite and associated phases (xenotime, actinide-rich phases) and date them by EPMA and/or LA-ICP-MS.

The texture observed in the quartz–feldspar±biotite migmatite shows a replacement of primary magmatic monazite by secondary (Th-poorer and LREE-richer) monazite, xenotime and Th–Si-rich phases, and is locally rimmed by apatite. The re-integrated composition of this texture is compatible with that of (Th- and Y-richer) primary monazite. Primary monazite domains yield a magmatic crystallization age of 351±9 Ma while secondary domains are contaminated by non-radiogenic Pb or give slightly younger Th–U–total Pb and $^{208}Pb/^{232}Th$ dates (~340 Ma). The texture found in the two-mica granite involves replacement by apatite and allanite, with some secondary (Th-poorer) monazite and minute uraninite or Th–Si-rich phases. Relicts of primary monazite grains record magmatic crystallization at 352±9 Ma, like primary xenotime domains. Secondary monazite contains non-radiogenic Pb, secondary xenotime domains yield $^{206}Pb/^{238}U$ dates younger than 338 Ma and uraninite preserves Th–U–total Pb dates averaging at 332 Ma.

The first reaction is a decomposition that involved little to no fluid phase, and efficiently trapped all elements (except Y) at the location of the monazite precursor. It is attributed to monazite re-equilibration (Th and Y+HREE loss) at subsolidus conditions. The second reaction is a replacement by hydrous minerals that needs the presence of fluid, and results in REE mobility at least at the millimetre scale. The contrast between both reactions is ascribed to sample composition, one being an anhydrous migmatite refractory to fluid infiltration and the other already offering all necessary components for the observed reaction. Both alteration reactions are correlated with a late Variscan thermal event at ca. 335 Ma. The latter could also be dated using actinide-rich phases, in which case tiny U-oxides appear more reliable than Th-silicates.

Monazite, garnet, and melt inclusions: Insights into mineral growth and crustal melting during P–T evolution

D. Sorger[1,2], C. A. Hauzenberger[2], F. Finger[3], M. Linner[4]

[1]Geoscience Center, University of Göttingen, Göttingen , Germany
[2]NAWI Graz Geocenter, University of Graz, Graz, Austria
[3]Department of Geography and Geology, University of Salzburg, Salzburg, Austria
[4]Competence Unit Hard Rock Geology, GeoSphere Austria, Vienna, Austria
e-mail: dominik.sorger@uni-goettingen.de

Monazite is a crucial accessory mineral in high-grade metamorphic rocks, acting both as a resilient geochronometer and as a major host for rare earth elements (REE), Th, and U. This study focuses on melt inclusions enclosed within monazite and garnet to unravel crustal melting mechanisms and element partitioning during granulite facies metamorphism in the Bohemian Massif. Raman spectroscopy and electron microscopy reveal that these nanogranitoid inclusions exhibit polycrystalline assemblages of quartz and feldspar polymorphs, micas, and occasionally carbonates. Such inclusions are located within chemically distinct domains of both monazite and garnet, offering critical insights into melt entrapment, mineral growth, and prevailing metamorphic conditions. The garnet shows compositional zoning with variations in major and trace elements, correlating with zoning patterns in monazite, and together they allow a detailed reconstruction of the pressure–temperature (P–T) evolution during high-grade metamorphism. Results indicate two distinct garnet generations, each characterised by unique chemical zoning and associated with monazite inclusions of different ages. Monazite grains dated to ~370 Ma are linked with the first garnet generation (Garnet 1), whereas grains dated to ~340 Ma are related to the second generation (Garnet 2). Both inclusion and matrix monazite grains display contrasting REE and Th/U signatures, reflecting variable growth environments and the influence of garnet breakdown during decompression. A systematic analysis of these inclusions in their textural and chemical context deepens our understanding of monazite stability in melt-bearing systems and its role in capturing the temporal dynamics of crustal melting. This integrative approach establishes a robust basis for deciphering the complex interplay among mineral chemistry, melt inclusions, and P–T evolution, highlighting the importance of accessory minerals like monazite as critical archives of crustal processes.

Primordial monazite formation in Archean metapelites of the Isua Supracrustal Belt, Greenland: New insights from in-situ U-Th-Pb dating

D. Sorger[1], T. Müller[1], A. Webb[2]

[1]Geoscience Center, University of G□ttingen, German,
[2]Institute of Geological Sciences, Freie Universit□t Berlin, Germany,
e-mail: dominik.sorger@uni-goettingen.de

We investigate the origin of some of Earth's earliest monazite discovered within the Isua Supracrustal Belt (ISB). Monazite, a key host for light rare earth elements as well as Th and U, is commonly found in low-Ca granitic rocks and metapelites, with its formation primarily controlled by the Al/Ca ratio of the host rock and potentially preceded by allanite under lower-grade metamorphic conditions. While modern geological environments often include rocks with high Al/Ca ratios favourable for monazite crystallisation, Archean lithologies, dominated by basaltic to ultramafic compositions, typically lack this condition. Nonetheless, crustal differentiation processes occasionally produced suitable protoliths exceeding this threshold, though the mechanisms remain poorly constrained.

Our study provides direct evidence for early monazite formation in the ISB. Examination of a metapelitic rock hosting garnet porphyroblasts reveals two distinct monazite generations: older monazites enclosed in garnet cores dated to ~3.6 Ga, placing them among the oldest recorded monazites, and younger grains in garnet rims and matrix dated to ~2.7 Ga. The absence of other monazite occurrences in Isua, alongside the in situ formation of both generations, supports a metamorphic rather than detrital origin. These rocks, possessing pelitic bulk compositions, represent some of the oldest preserved clastic sediments, derived from ultramafic, mafic, and felsic igneous sources or reflecting metasomatic modification of basaltic precursors. The presence of ~3.6 Ga monazite establishes a minimum age for the high Al/Ca compositions required for monazite growth in Isua's Archean crust, supporting interpretations of late Eoarchean metamorphism.

Metasomatic origin of chemical zoning in crystals of the apatite supergroup minerals from the Shadil Khokh Volcano

D. Środek[1], M. Dulski[2]

[1]Faculty of Natural Sciences, University of Silesia, Katowice, Poland
[2]Faculty of Science and Technology, University of Silesia, Katowice, Poland
e-mail: dorota.srodek@us.edu.pl

The apatite supergroup minerals are characterized by structural flexibility, allowing for extensive chemical substitution at multiple crystallographic sites. These minerals can therefore serve as sensitive recorders of fluid and melt compositions in a wide range of geological environments due to the wide substitution possibilities.

Zoned apatite grains were found within the endocontact zone of a pyrometamorphic carbonate-silicate xenolith (xenolith no. 7) from the ignimbrites of the Upper Chegem Caldera, Northern Caucasus. Interestingly, the zoning pattern reflects substitutions at the Ca site (Sr and REE), tetrahedral sites (mainly As), and within the anion column (F and OH groups). The crystals comprise three distinct zones: fluorapatite (core), fluorcaphite (intermediate zone), and johnbaumite (rim) (Fig. 1). In some cases, a transitional zone was also observed between fluorcaphite and johnbaumite, composed of Sr-rich johnbaumite. Raman spectroscopy revealed a weak band near 1080 cm^{-1} in the fluorapatite and fluorcaphite zones, which may be associated with minor carbonate (CO_3^{2-}) substitution – undetectable by electron microprobe analysis.

Fluorapatite is a common mineral in metamorphic rocks, generally considered to be a remnant of the protolith (HARLOV, 2015). Moreover, volcanic apatites usually lack halogen zoning (PICCOLI & CANDELA, 2002). Together, these observations suggest that the fluorcaphite–johnbaumite rim formed during a subsequent metasomatic event, involving compositionally variable fluids enriched in strontium and arsenic.

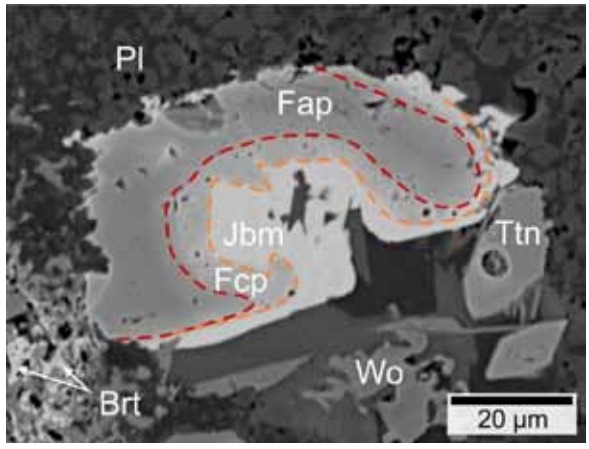

Table 1: Chemical compositions of the apatite suprgroup minerals from the xenolith no. 7

Fluorapatite
$[Ca_{4.92}Na_{0.03}Sr_{0.02}Ce_{0.02}La_{0.01}]_{\Sigma 5.00}[(PO_4)_{2.96}(SiO_4)_{0.02}(AsO_4)_{0.02}]_{\Sigma 3.00}[F_{0.89}(OH)_{0.09}]_{\Sigma 0.98}$

Fluorcaphite
$[Sr_{0.96}Ca_{3.99}Na_{0.02}Ce_{0.02}La_{0.01}]_{\Sigma 5.00}[(PO_4)_{2.83}(AsO_4)_{0.10}(SiO_4)_{0.05}(SO_4)_{0.02}]_{\Sigma 3.00}[F_{0.81}(OH)_{0.17}]_{\Sigma 0.98}$

Sr-rich johnbaumite
$[Ca_{4.17}Sr_{0.03}]_{\Sigma 5.00}[(AsO_4)_{2.49}(SO_4)_{0.22}(SiO_4)_{0.20}(AlO_4)_{0.06}(PO_4)_{0.04}]_{\Sigma 3.00}[(OH)_{0.63}F_{0.36}]_{\Sigma 0.99}$

Johnbaumite
$[Ca_{4.95}Sr_{0.05}]_{\Sigma 5.00}[(AsO_4)_{2.22}(SiO_4)_{0.35}(SO_4)_{0.35}(PO_4)_{0.08}]_{\Sigma 3.00}[(OH)_{0.72}F_{0.28}]_{\Sigma 1.00}$

Figure 1: Back-scattered electron image of the zoned crystal of the apatite supergroup minerals. Mineral abbreviations: Brt - barite, Fap -fluorapatite, Fcp - fluorcaphite, Jbm - johnbaumite, Pl - plagioclase, Ttn - titanite, Wo - wollastonite.

HARLOV, D.E. (2015): Apatite: A fingerprint for metasomatic processes. – Elements, 11, 171-176.
PICOLI, P.M., CANDELA, P.A. (2002): Apatite in Igneous Systems. – Rev Mineral Geochem, 48, 255-292.

Amorphous silica vs short-range ordered hydroxy-aluminosilicate formation

F. M. Stamm[1], A. Baldermann[1], D. A. Frick[2,3], P. J. Frings[2], M. Pettauer[1], H. M. R. Wilkening[4], A. Marko[4], F. von Blanckenburg[2,5], J. Schott[6], M. Dietzel[1]

[1]Institute of Applied Geosciences, Graz University of Technology, Austria
[2]Earth Surface Geochemistry, GFZ German Research Centre for Geosciences, Germany
[3]Institute of Geosciences, Kiel University, Germany
[4]Institute for Chemistry and Technology of Materials, Graz University of Technology, Austria
[5]Department of Earth Sciences, Freie Universität Berlin, Germany
[6]Geosciences Environment Toulouse (GET), Observatoire Midi-Pyrénées, Université de Toulouse, CNRS, IRD, UPS, France
e-mail: fstamm@tugraz.at

Amorphous silica (ASi) and short-range ordered hydroxy-aluminosilicate (SROAS) are highly reactive phases that serve as precursors to opaline silica and various clay minerals. Their silicon isotope signatures preserved in soils and sedimentary deposits are widely applied as environmental indicators to infer formation processes and geochemical pathways. However, the underlying reaction kinetics, mechanisms, and controls on Si isotope fractionation remain incompletely resolved.

In this study, we investigate the environmental factors that control the development of ASi and SROAS phases, and their Si isotopic behavior. Precipitation experiments were conducted at ambient temperature, both in the presence and absence of aluminum, with high temporal resolution to monitor dynamic changes. Results from elemental and Si isotope analyses in both solid and fluid phases revealed that the formation of ASi and SROAS followed different pathways, each with three distinct stages:

- **Stage I**: The slow polymerization of ASi over ~72 hours contrasts with an almost instantaneous (<15 sec) onset of SROAS formation.
- **Stage II**: ASi begins to precipitate following first-order kinetics, while SROAS undergo partial dissolution within a day.
- **Stage III**: ASi transitions into a more mature form, whereas SROAS shows a slower re-precipitation phase.

Aluminum in SROAS occurs in both tetrahedral ([4]) and octahedral ([6]) coordination, with the extent of $Si^{[4]}$ substitution governed by the Al/Si ratio. The data suggest that SROAS formation proceeds via a metastable intermediate involving disordered octahedral sheet clusters, which then undergo Al-for-$Si^{[4]}$ substitution and subsequent polycondensation and (de)polymerization reactions during structural reorganization.

Silicon isotope fractionation is driven primarily by kinetic processes. The largest fractionation observed ($1000\ln(\alpha_{SROAS\text{-}aq}) = -4.55$ ‰) coincides with the onset of isotopic stabilization during Stage III. A clear dependence of Si isotope partitioning on the solid-phase Si/Al ratio was observed. By day 16, the isotopic compositions of both ASi and SROAS approach values characteristic of natural clay minerals and synthetic analogs, implying near-steady-state conditions.

Calcined clays as sustainable precursors in alkali-activated materials

F. R. Steindl[1,2], A. Hassan[1], S. Radinger[1], F. Stainer[3], H. M. R. Wilkening[3], A. Kurka[4], C. Grengg[1]

[1]Christian Doppler Laboratory for Waste-based geopolymer construction materials in the CO_2-neutral circular economy, Institute of Applied Geosciences, Graz University of Technology, Austria,
[2]Institute of Technology and Testing of Building Materials, Graz University of Technology, Austria,
[3]Institute for Chemistry and Technology of Materials, Graz University of Technology, Austria,
[4]Wienerberger AG, Austria
e-mail: florian.steindl@tugraz.at

Alkali-activated materials (AAMs) are produced by mixing (Ca-)Al-Si-rich solids with alkaline substances in the presence of water, initiating hydration and geopolymerisation reactions which result in a concrete-like material. AAMs containing wastes and secondary raw materials (WSRMs) allow reduced CO_2 emissions, resource consumption and waste arisings (e.g. GRENGG et al. 2024), but are often combined with other Al-Si-rich substances to enhance reactivity and ensure adequate strength and durability. High-purity calcined clays, such as high-grade metakaolin, are often used for this purpose but are in short supply and/or expensive due to demand from other industries. Therefore, this study systematically investigates two Austrian mixed clay samples, calcined at 400 to 1000 °C in 100 °C intervals, as possible alternatives.

P-XRD analyses, corroborated by XRF spectroscopy, revealed that the initial clays differ in particular in their sheet silicate contents: clay A is dominated by chlorite and muscovite and/or illite, while clay B contains significant amounts of kaolinite and traces of muscovite/illite. During calcination, kaolinite, chlorite and muscovite/illite are gradually transformed into their amorphous metaclay analogues at around 500-600, 500-800, and 700-900 °C, respectively. FTIR and ^{27}Al MAS-NMR confirmed the transformations to be driven by dehydroxylation reactions and octahedral to tetrahedral Al coordination changes. In addition, traces of carbonates such as calcite and dolomite are decomposed at >700 °C, while newly-formed mullite and gehlenite are observed after calcination at >900 °C.

Subsequently, the calcined clay powders were utilised in AAM pastes with granulated blast-furnace slag, coal fly ash and various mineral WSRMs. The resulting paste specimens exhibited adequate compressive strengths, e.g. up to 75 MPa for a blast-furnace-slag – clay B mixture after 7 days of reaction. Optimal compressive strengths were reached with clay A calcined at 700-800 °C and clay B calcined at 600-700 °C, with significantly higher compressive strengths observed for clay B, demonstrating the superior reactivity and lower required calcination temperatures of metakaolinite in comparison to other metaclays. AAM pastes containing clay B calcined at 700 °C and various mineral by-products exhibited 7-day compressive strengths of up to 40 MPa, verifying the feasibility of low-grade kaolinitic clays as corrective substances for waste-based AAMs.

This contribution demonstrates the possibilities offered by the usage of mixed calcined clays as Al-Si-rich precursor components in AAMs. We gratefully acknowledge the contributions of Leila Legat and Lisa Schuller regarding the characterisation and AAM mixing tasks. The study was carried out in the course of the GECCO$_2$ Christian Doppler Laboratory. The financial support by the Austrian Federal Ministry of Labour and Economy, the Christian Doppler Research Association and several industry partners is gratefully acknowledged.

GRENGG, C., RUDIC, O., SAADE, M., STEINDL, F., WILKENING, M., JODLBAUER, A., ZOEGL, I., WOHLMUTH, D., MITTERMAYR, F. (2024): Alkali activated steel slag – oil composites: Towards resource efficiency and CO_2 neutrality. – Cem Con Res, 186, 107678.

From drill cores to photons: New perspectives from high-resolution core scanning and direct spectrum filtering

M. Strasser[1], A. Ramisch[1], G. J. Weltje[2], L. Schley[1], R. Tjallingii[3]

[1]Institute of Geology, University of Innsbruck, Innsbruck, Austria
[2]Department of Earth and Environmental Sciences, KU Leuven, Leuven, Belgium
[3]Helmholtz Centre Potsdam - German Research Centre for Geosciences GFZ, Postdam, Germany
e-mail: michael.strasser@uibk.ac.at

The Austrian Core Facility for Scientific Core Analyses at the University of Innsbruck (ACFI) is Austria's first dedicated research facility utilizing and providing state-of-the-art laboratory infrastructure for logging and scanning of cores obtained by drilling and coring. Making use of non-destructive analyses with a multi-sensor physical core logger (MSCL; including gamma-attenuation density, p-wave velocity, magnetic susceptibility, and visible light photospectroscopy sensors), an X-ray Fluorescence Core Scanner (XRF-CS), and a new custom-built Hyperspectral Imaging Core Scanner (HSI-CS), we aim at acquiring and analysing data from a broad range of the electromagnetic wave spectrum. This includes coherent spectroscopy raw data processing, noise reduction, and data analysis techniques to obtain high-resolution optical, physical-property, element chemical, and mineralogical data from advanced scientific core analysis across different geoscientific research fields.

In this presentation, we present the results of a recent benchmarking study redefining the limits of XRF-CS with "Direct Spectrum Filtering (DSF)". DSF is an invention jointly conceived by Arne Ramisch and Gert Jan Weltje and reduces shot noise in spectral data. Benchmarked against both XRF line-scan and imaging, results document DSF´s transformative potential by increasing both the precision (10 to 100-fold) and speed (1.000 to 10.000-fold) of non-destructive elemental analysis. Furthermore, it maintains detection accuracy for light and trace elements typically not quantified with XRF-CS even at drastically shortened acquisition times. This study highlights our ongoing research now focusing on extending DSF to a wider range of photon-detecting systems, aiming to enable ultra-fast, high-precision, and low-count detection for defining new frontiers in geological sensing.

The Martian 'low-humidity kieserite' – what is it indeed?

D. Talla[1], M. Wildner[1]

[1]Institut für Mineralogie und Kristallographie, Universität Wien, Vienna, Austria
e-mail: dominik.talla@univie.ac.at

While the presence of hydrous sulphates on the surface of Mars – being part of the water budget mainly at equatorial latitudes – is firmly established (e.g. NOEL et al. 2015), some ambiguity still exists concerning the character of the monohydrated Mg-sulfate, formerly presumed to be kieserite, i.e. monoclinic $MgSO_4 \cdot H_2O$. In dehydration experiments revising the behaviour of Mars-related hydrated Mg-sulphates, WANG et al. (2009) obtained a so-called 'low-humidity' ('lh') kieserite, spectroscopically largely similar to 'classic' kieserite *sensu stricto* (s.s.). However, in powder X-ray diffraction, this new 'polytype' shows a second strong Bragg reflection not seen in kieserite (s.s.). Furthermore, some authors previously disputed the stability of kieserite (s.s.) on Mars in respect to the prevailing surface conditions (CHIPERA & VANIMAN, 2006).

In our studies, however, we noticed a striking resemblance between this enigmatic 'lh'-kieserite and the tetragonal Mg-sulfate caminite, $MgSO_4 \cdot \frac{1}{3}Mg(OH)_2 \cdot \frac{1}{3}H_2O$ (HOCHELLA et al. 1983), found on Earth in deep-sea hydrothermal vents. Caminite crystallizes in space group $I4_1/amd$, and a whole series of such compounds with inverse solubility, varying $Mg \leftrightarrow 2H^+$ ratios, and variable lattice parameters was already presumed to exist (HOCHELLA et al., 1983). Using the inverse solubility and specialized hydrothermal autoclaves allowing to vent the solvent at maximum temperature conditions (mostly 270 °C) to preserve the high-temperature product, we were indeed able to obtain single crystals of an entire series of these 'MHSH' (Mg-Hydroxide-Sulfate-Hydrate) phases with *c* lattice parameters ranging between 12.97 and 13.19 Å (cf. caminite, 12.99 Å). In many of our samples the *c* axis lengths scatter around 13.1 Å, which corresponds well to cell parameters of 'lh-kieserite' obtained by WANG et al. (2009) in their dehydration experiments. Furthermore, the MHSH compound group is nearly entirely resistant to rehydration even under Earth's ambient conditions, in difference to kieserite (s.s.), which rehydrates to hexahydrite in a matter of weeks. This enhanced stability also emphasizes its presence on Mars.

Although the structures of kieserite and MHSH contain the same structural motive (most probably being responsible for the similarity of their vibrational spectra), MHSH does apparently not, in difference to kieserite (s.s.), incorporate divalent transition metals except for Zn^{2+}. This might be related to the more rigid three-dimensional octahedral framework of MHSH, which can accommodate only divalent cations of the same size as Mg^{2+}, in difference to kieserite, where discrete octahedral chains allow for much more structural flexibility.

CHIPERA, S.J., VANIMAN, D.T. (2006): Experimental stability of magnesium sulphate hydrates that may be present on Mars. – Geochim Cosmochim Acta, 71, 241-250.

HOCHELLA, M.F., KEEFER, K.D., deJONG, B.H.W.S. (1983): The crystal chemistry of a naturally occurring magnesium hydroxide sulfate hydrate, a precipitate of heated seawater. – Geochim Cosmochim Acta, 47, 2053-2058.

NOEL, A., BISHOP, J.L., AL-SAMIR, M., GROSS, C., FLAHAUT, J., McGUIRE, P.C., WEITZ, C.M., SEELOS, F., MURCHIE, S. (2015): Mineralogy, morphology and stratigraphy of the light-toned interior layered deposits at Juventae Chasma – Icarus, 251, 315-331.

WANG, A., FREEMAN, J.J., JOLLIFF, B.L. (2009): Phase transition pathways of the hydrates of Mg sulfate in the temperature range 50°C to 5°C: Implication for sulphates on Mars. – J Geophys Res, 114, E04010.

Quantitative mineralogical characterization of Triassic karst bauxites from the Adriatic Region (Croatia)

E. Topalović[1], S. Jelavić[2], N. Tomašić[1]

[1]Department of Geology, University of Zagreb, Zagreb, Croatia,
[2]University Grenoble Alpes, University Savoie Mont Blanc, CNRS, IRD, University Gustave Eiffel, ISTerre, Grenoble, France,
e-mail: ena.topalovic@geol.pmf.unizg.hr

Bauxite is the principal ore of aluminium, a metal essential to industries such as transportation, energy, construction, and packaging. With increasing demand for sustainable materials and green technologies, bauxite deposits are gaining strategic importance—not only as sources of aluminium but also as potential resources for rare earth elements (REE), particularly when considering by-products such as red muds. This study presents a quantitative mineralogical characterization of Triassic bauxite samples from Croatia. A total of 20 samples were collected from the Rudopolje and Vrace bauxite deposits in Zadar County, along the Adriatic coast. These karst-type bauxites, described as bauxitic clays with kaolinitic interbeds, overlie Anisian limestones and dolomites and are overlain by Carnian conglomerates (MARKOVIĆ, 2002). Quantitative mineralogical analyses were conducted using powder X-ray diffraction (XRD) with Rietveld refinement. The results show that kaolinite and böhmite are the dominant aluminosilicate phases. Kaolinite contents range from 17 to 84 wt.%, showing a clear inverse correlation with böhmite, which reaches up to 51 wt.% where kaolinite is least abundant. Conversely, in kaolinite-rich samples (up to 84 wt.%), böhmite is nearly absent (<1 wt.%). Diaspore is present in only two samples (20 and 40 wt.%), associated with intermediate kaolinite contents (60 and 39 wt.%, respectively), while böhmite remains below 1 wt.% in these cases. The absence of gibbsite and dominance of böhmite, with diaspore present in only two samples, suggests formation under intermediate to elevated temperatures and/or low water activity. This mineralogical assemblage likely reflects post-depositional diagenesis, mild hydrothermal alteration, or burial history within a karst environment (BÁRDOSSY, 1982). All samples exhibit structurally disordered kaolinite, as indicated by low Hinckley Index values (<0.90; HINCKLEY, 1962; APARICIO et al. 2006), supporting low-temperature formation and post-depositional kaolinization, potentially driven by silica-rich fluids in the karstic system. Hematite is the dominant Fe oxide phase (8–20 wt.%), with minor goethite detected in only two samples (<2 wt.%). Quartz is consistently present in amounts <1 wt.%. Anatase is the primary Ti-bearing phase (1.5–3 wt.%), with minor rutile (0.5–0.9 wt.%). Accessory REE-bearing florencite–group minerals were identified in two samples (~0.5 wt.%). The dominance of disordered kaolinite, along with variable proportions of böhmite and diaspore, suggests a multiphase evolution influenced by weathering intensity, fluid interactions, and possible diagenetic overprint in a karstic setting. These findings contribute to a better understanding of the genesis and post-formational history of karst bauxites and establish a foundation for future geochemical and provenance investigations, particularly in the context of critical raw material potential.

APARICIO, P., GALA, E., FERRELL, R.E. (2006): A new kaolinite order index based on XRD profile fitting. – Clay Miner, 41, 811-817.

BÁRDOSSY, G. (1982): Karst bauxites: bauxite deposits on carbonate rocks. – 441p., Elsevier, Budapest.

HINCKLEY, D. N. (1962): Variability in cristallinity values among the kaolin deposits of the coastal plain of Georgia and South Carolina. – Clays Clay Miner, 11, 229-235.

MARKOVIĆ, S. (2002): Hrvatske mineralne sirovine. – 543p., Inst Geol Istr, Zagreb.

Tl(I) retention under acidic, sulphate-rich conditions: synthesis and structural insights in the Tl(I)–Al(III)–S(VI)–H_2O system

K. Vacek[1], M. Hagn[1], M. Danzinger[1], Lj. Karanović[2], T. Đorđević[1,3]

[1]Department of Mineralogy and Crystallography, University of Vienna, Vienna, Austria
[2]Laboratory of Crystallography, Faculty of Mining and Geology, University of Belgrade, Belgrade, Serbia
[3]E057-02 USTEM, TU Wien, Vienna, Austria
e-mail: tamara.djordjevic@univie.ac.at

Thallium (Tl) is a highly toxic metal commonly found in sulfides associated with low-temperature hydrothermal mineralization, as well as in mining-impacted environments. Weathering and oxidation of these sulfides produce acid drainage enriched in Tl, posing a significant environmental risk. Thallium can also be incorporated into secondary sulfate minerals, such as those of the jarosite and alunite groups, which may serve as temporary storage phases. However, the interactions between Tl and these sulfates remain poorly understood.

We performed experiments in the Tl(I)–Al(III)–S(VI)–H_2O system using hydrothermal synthesis (stainless steel autoclaves, autogenous pressure, T_(max) = 170 °C). The main product obtained was good-quality single crystals of $TlAl(SO_4)_2 \cdot 12H_2O$, a synthetic analogue of the mineral lanmuchangite and the Tl analogue of the mineral alunite. This mineral has only been reported once before, from the type locality the Lanmuchang Hg-Tl deposit in China (CHEN et al., 2001). Due to its poor crystallinity, its structural and compositional characteristics have only been partially understood. Therefore, we performed single-crystal X-ray diffraction experiments to learn more about its crystal structure. The synthetic lanmuchangite crystal structure was refined using single-crystal data (MoKα radiation, CCD area detector) to a conventional $R1$ factor of 0.0279 for 652 unique reflections with $I > 2\sigma(I)$ and 0.0525 for all 947 reflections. Hydrogen atoms were located using difference Fourier maps and refined isotropically with the constrains on O—H bond-length and O—H···O angles. The structure is cubic, space group Pa-3 (No. 205), a = 12.2727(14) Å, V = 1848.5(6) Å^3 and Z = 4. The structure was found to be isomorphous with β-alum, $CsAl(SO_4)_2 \cdot 12H_2O$. It contains $[Al(H_2O)_6]^{3+}$ octahedra, SO_4^{2-} tetrahedra and interstitial water molecules that are weakly bonded to the Tl^+ cations.

Our work provides the first detailed structural characterization of the β-polymorph of Tl-alum, expanding our understanding of Tl incorporation in secondary sulfate phases, which sheds valuable light on the mineralogical behavior of Tl in mining-impacted environments.

Financial support of the Austrian Science Fund (FWF) [P 36828-N] to T. Đorđević is gratefully acknowledged.

CHEN, D., WANG, G., ZOU, Z., CHEN, Y.M. (2001): A new mineral - Lanmuchangite. – Acta Mineral Sinica, 21, 271–277. (in Chinese with English abstract)

CROMER, D.T., KAY, M.I., LARSON, A.C. (1966): Refinement of the alum structures. I. X-ray and neutron diffraction study of $CsAl(SO_4)_2 \cdot 12H_2O$, a β-alum. – Acta Crystallogr, 21, 383-389.

Sub-zero carbonates – An experimental approach

L. Werber[1], M. Pettauer[1], T. Tsiotsias[1], D. Hippler[1]

[1]Institute of Applied Geosciences, Graz University of Technology, Austria
e-mail: lena.werber@student.tu-graz.at

Calcium carbonates ($CaCO_3$) form in a variety of natural environments, including low-temperature settings around or just below the freezing point of water, such as ikaite crystals in Arctic and Antarctic sea ice, cryogenic cave carbonates, and subglacial precipitates. These 'sub-zero' calcium carbonates typically form through processes linked to the freezing of an aqueous solution. In contrast, the direct precipitation of $CaCO_3$ minerals from liquid water at sub-zero temperatures under non-freezing conditions remains undocumented.

This study therefore aimed to establish a method for synthesizing $CaCO_3$ minerals at temperatures below 0°C without inducing freezing. To achieve this, precipitation experiments were conducted at -10°C ± 1°C in hypersaline solutions that remained liquid under these conditions. The evolution of the reactive solution was monitored via pH measurements and in-situ Raman spectroscopy, while the resulting precipitates were characterized using Fast-Fourier infrared spectroscopy (ATR-FTIR) and scanning electron microscopy (SEM).

The experiments yielded several key findings: (i) both, calcite and vaterite were successfully synthesized, (ii) evidence for the precipitation of amorphous calcium carbonate (ACC) was observed through pH evolution monitoring and ATR-FTIR analyses, although ACC could not be confirmed via SEM, (iii) the initial solution pH influenced the precipitation pathway, with lower pH values (6.5-7.5) promoting multistage transitions (e.g., vaterite to calcite), whereas higher pH values (>7.5) favored the direct precipitation of calcite, and (iv) the Raman laser appeared to reduce the induction time, suggesting that localized energy supply accelerates the nucleation of $CaCO_3$ minerals.

Our 'sub-zero' carbonate experimental setup provides a new approach and insights for exploring $CaCO_3$ nucleation and crystallization dynamics, including Ostwald's rule of stages and ripening processes under conditions, where $CaCO_3$ precipitation is strongly delayed. Furthermore, calcium carbonates synthesized under such extreme conditions may contribute to calibrating the clumped isotope thermometer (Δ_{47}) at very low temperatures. The approach also offers a promising analog for investigating carbonate mineral formation in extreme terrestrial or extraterrestrial environments.

Element fluxes in surface sediments across the Yangtze River Estuary – East China Sea shelf transect

X. Xu[1,2], A. Baldermann[2], D. Cai[1], J. Guo[1], X. Wu[1], Y. Shouye[1]

[1]State Key Laboratory of Marine Geology, Tongji University, China
[1]Institute of Applied Geosciences, Graz University of Technology, Austria
e-mail: syyang@tongji.edu.cnt

Estuarine sediments play a critical role in controlling land-ocean element fluxes through salinity-driven ion exchange reactions. Globally, these processes can affect riverine inputs: Amazon studies show that Na^+ adsorption by clay-rich sediments reduces the dissolved Na^+ flux by 20–30%, while releasing Ca^{2+} (+5–10%), thus altering continental dissolved inputs to the ocean (CERLING et al., 1989; SAYLES & MANGELSDORF, 1979). For trace metals, Ganges-Brahmaputra systems contribute ~40% of the global dissolved Ni flux via salinity-triggered desorption (SAMANTA & DALAI, 2018). Exchangeable fractions can also serve as environmental proxies, for example, Sr/Ba ratios were used to trace sedimentary provenance and paleoenvironments (WANG et al., 2021). The Yangtze River Estuary–East China Sea shelf transect, receiving the world's third-largest sediment load, exhibits complex ion exchange dynamics: prior work documents Ca^{2+} release (9.3×10^{-2} meq/g) and Na^+ adsorption (19.6×10^{-2} meq/g) in suspended particulate matter during seaward transport, alongside non-conservative Zn/Cu behaviors modulated by dissolved organic carbon content and particle size (FENG et al., 2017). However, systematic investigations regarding exchangeable fraction variations in surface sediments across this critical region remain absent.

In this study, surface sediments from 17 stations along an east-west transect spanning estuary, mud belt, and outer shelf environments were analyzed. Beyond compositional variations in exchangeable fractions, their correlations with mineralogical attributes and grain size distributions are systematically examined. Grain size distributions indicate the sediments are mixtures of mud to sandy mud. XRD data analysis shows illite, chlorite, kaolinite, quartz, feldspar and carbonates are primary contributors to the sediments, which in turn control the ion exchange dynamics at the sediment-(sea)water interface. Our results reveal that ion exchange processes in seabed surface sediments, distinct from suspended particulate matter, exhibit spatial elemental patterns modulated by resuspension history and early diagenesis.

CERLING, T.E., PEDERSON, B.L., VON DAMM, K.L.（1989): Sodium-calcium ion exchange in the weathering of shales: Implications for global weathering budgets. – Geology, 17(6), 552-554.

FENG, C. (2017): Heavy metal partitioning of suspended particulate matter–water and sediment–water in the Yangtze Estuary. – Chemosphere, 185, 717-725.

SAMANTA, S., DALAI, T.K. (2018): Massive production of heavy metals in the Ganga (Hooghly) River estuary, India: Global importance of solute-particle interaction and enhanced metal fluxes to the oceans. – Geochim Cosmochim Acta, 228, 243-258.

SAYLES, F.L., MANGELSDORF, P.C. (1979): Cation-exchange characteristics of Amazon River suspended sediment and its reaction with seawater. – Geochim Cosmochim Acta, 43(5), 767-779.

WANG, A., WANG, Z., LIU, J., XU, N., LI, H. (2021): The Sr/Ba ratio response to salinity in clastic sediments of the Yangtze River Delta. – Chem Geol, 559, 119923.

Mineralogy and petrology of epidote-group minerals

L.-J. Zaminer[1], Ch. A. Hauzenberger[1], D. Gallhofer[1], S. Hänsel[1]

[1]University of Graz, Department of Earth Sciences
e-mail: laura.zaminer@edu.uni-graz.at

Epidote-group minerals are common constituents of a wide range of metamorphic, hydrothermal and magmatic rocks and serve as useful indicators of magmatic and metamorphic conditions as well as fluid compositions. The research at hand focuses on the chemical classification of epidote-group in metamorphic rocks. Major element- and REE-compositions were determined using Electron Probe Micro-Analysis (EPMA) and Laser Ablation-Inductively Coupled Plasma-Mass Spectrometry (LA-ICP-MS). This study aims to classify epidote-group minerals based on the structural and chemical criteria of ARMBRUSTER et al. (2006), emphasizing Fe^{3+}–Al ordering and trace element incorporation. Gem-quality zoisite was included to examine gemological features, composition, and trace-element behavior.

(1) The Knappenwand samples are characterized by typically high Fe^{3+} contents ranging from 0.544–0.966 apfu. Although most samples exhibit typical Fe^{3+} contents ranging from 0.805 to 0.966 apfu, some show overgrowths of clinozoisite with Fe^{3+} contents between 0.544 and 0.798 apfu. The REE patterns display a flat profile. (2) Epidote from Elba Island exhibits pronounced zoning with Fe^{3+} contents from 0.666 to 1.026 apfu and REE patterns marked by a positive Eu anomaly and moderate HREE enrichment. (3) Gem-quality epidote from Pakistan shows low to average Fe^{3+} contents (0.385–0.400 apfu) and exhibits extensive clinozoisite overgrowths. The REE patterns reveal a positive Eu anomaly alongside moderate to strong HREE enrichment. High chromium contents (147-640 ppm) attribute to the extensive green colouration. (4) In contrast, clinozoisite from the eclogite-facies Saualpe samples shows minimal Fe^{3+} substitution (0.000–0.131 apfu) and strong HREE depletion, consistent with garnet sequestration of heavy REEs. Notably, two distinct generations of clinozoisite are discernible based on compositional and textural differences. (5) In the Tien-Shan ultra-high-pressure rocks, epidote contains intermediate Fe^{3+} levels (0.402–0.609 apfu) with limited zoning and a REE pattern similarly depleted in HREEs, again attributable to garnet-rich assemblages. (6) Zoisite from Merelani, Tanzania appears to be compositionally pure, with Fe^{3+} contents ranging from 0.000 to 0.004 apfu. The REE patterns exhibit distinct features: most samples are marked by a negative Eu anomaly and HREE depletion, consistent with feldspar- and garnet-rich assemblages. However, a few samples show slight HREE enrichment and, in some cases, even a positive Eu anomaly. The tanzanite studied exhibits high vanadium contents (828–2178 ppm), which are responsible for the violet-blue coloration (LIEBSCHER & FRANZ, 2004).

The presented metamorphic epidotes exhibit Fe^{3+}–Al cation ordering, diverse zoning patterns, and distinct REE signatures. In contrast, the zoisite from Merelani shows minimal to no Fe^{3+}–Al substitution. The observed coloration of tanzanite corresponds to the chromophore behavior of vanadium. The results are consistent with the mineral assemblages, which reflect the evolving pressure–temperature conditions from greenschist- to eclogite facies.

ARMBRUSTER, T., BONAZZI, P., AKASAKA, M., BERMANEC, V., CHOPIN, C., GIERE, R., HEUSS-ASSBICHLER, S., LIEBSCHER, A., MENCHETTI, S., PAN, Y., & PASERO, M. (2006): Recommended nomenclature of epidote-group minerals. Eur. J. Mineral., 18, 551–567.

LIEBSCHER, A., & FRANZ, G. (2004). Physical and optical properties of the epidote minerals. Rev. Mineral. Geochem., 56, 1–82.

Fertility evaluation of intrusive bodies in the southern part of the Kerman magmatic belt, Iran: using geochemical studies

A. Zarasvandi[1], J. G. Raith[2], A. Soltani,[3], M. Rezaei[4], N. Taghipour[5]

[1,3,4]Department of Geology, Faculty of Earth Sciences, Shahid Chamran University of Ahvaz, Ahvaz, Iran
[2]Department of Applied Geosciences and Geophysics, Technical University of Leoben, Leoben, Austria
[5]School of Earth Sciences, Damghan University, Damghan, Iran
e-mail: zarasvandi_a@scu.ac.ir; taghipour@du.ac.ir

The Kerman Cenozoic magmatic belt (KCMA), a segment of the Urumieh-Dokhtar magmatic arc (UDMA), hosts significant porphyry Cu, Mo, and Au deposits. While the central and northern parts of the belt are recognized as fertile zones, its southern segment remains relatively understudied and is generally considered to have lower mineralization potential (Zarasvandi et al. 2018). This study investigates the quartz diorite intrusive bodies at the Kuh-e-Esfand prospect, located at the southern edge of the KCMA, using whole-rock ICP-MS data to assess their mineralization potential; there Oligocene to Miocene granitoids of the Jebal-e-Barez type intruded into older volcanic and sedimentary rocks and are associated with porphyry copper mineralization. The present study tries to demonstrate that this segment also represents a zone with significant mineralization potential by identifying previously unrecognized fertile intrusions based on detailed geochemical analyses. Hydrothermal alteration in the area includes deep zones characterized by quartz + sericite + K-feldspar + chlorite ± anhydrite, along with potassic, phyllic, argillic, and propylitic alteration assemblages. Geochemically, the intrusive rocks belong to the calc-alkaline to high-K calc-alkaline series, consistent with formation in an active continental margin setting. In the Sr/Y vs. Y diagram (Fig. 1 a; Defant and Drummond, 1993), the quartz diorite samples display a typical andesitic trend at shallow levels and evolve towards an adakite-like signature at depth. This trend likely reflects crustal contamination and/or hydrothermal alteration processes. To evaluate the fertility of the intrusions, the Cu vs. Y and Cu vs. Yb diagrams (Fig. 1 b, c; Atapour and Aftabi, 2021) were applied for differentiating fertile granitoids from barren or weakly mineralized ones. Most of the Kuh-e-Esfand samples plot within the productive field, particularly in zones exhibiting Cu enrichment together with lower Y and Yb values. These geochemical patterns indicate that intrusions previously thought to be barren may, in fact, host economically significant porphyry-type mineralization.

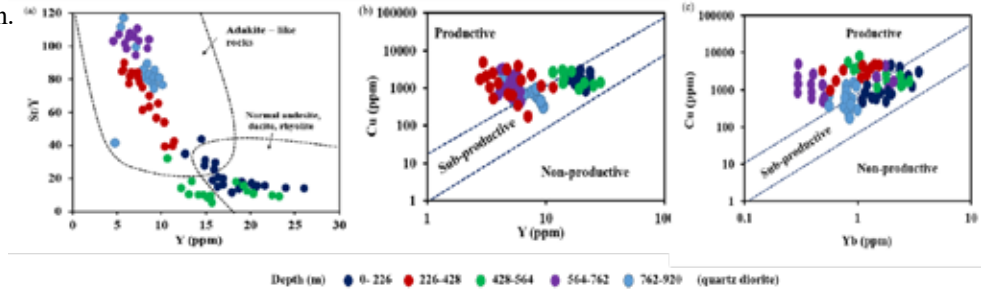

Figure 1. (a) Sr/Y vs. Y diagram (Drummond and Defant, 1993); (b, c) Cu vs. Yb and Cu vs. Y plots distinguishing fertile and barren granitoids (Atapour and Aftabi, 2021).

ATAPOUR, H., AFTABI, A. (2021): Petrogeochemical evolution of calc-alkaline, shoshonitic, and adakitic magmatism associated with Kerman Cenozoic arc porphyry copper mineralization, southeastern Iran: A review. – Lithos, 398, 106261.

DEFANT, M. J., DRUMMOND, M. S. (1993): Mount St. Helens: Potential example of the partial melting of the subducted lithosphere in a volcanic arc. – Geology, 21, 547.

ZARASVANDI, A., REZAEI, M., RAITH, J.G., POURKASEB, H., ASADI, S., SAED, M., LENTZ, D.R. (2018): Metal endowment reflected in chemical composition of silicates and sulfides of mineralized porphyry copper systems, Urumieh-Dokhtar magmatic arc, Iran. – Geochimica et Cosmochimica Acta, 223, 36–59.